THE ROLES OF ORPHAN NUCLEAR RECEPTORS, SHP AND FXR, AND THEIR COFACTORS IN BILE ACID SIGNALING

BY

SUNGSOON FANG

B.S., Seoul National University, 1999
M.S., University of Illinois at Urbana-Champaign, 2005

DISSERTATION

Submitted in partial fulfillment of the requirements
for the degree of Doctor of Philosophy in Molecular & Integrative Physiology
in the Graduate College of the
University of Illinois at Urbana-Champaign, 2008

Urbana, Illinois

Doctoral Committee:

Associate Professor Kim Jongsook Kemper, Chair
Professor Ann W. Nardulli
Professor Benita S. Katzenellenbogen
Professor Byron W. Kemper
Professor Milan K. Bagchi
Assistant Professor Craig A. Mizzen

Abstract

Bile acids, the end-product of cholesterol catabolism, are important for absorption and solubilization of lipids in the intestine because of their detergent properties. In addition to their roles as detergents, previous studies have revealed that bile acids function as signaling molecules in metabolic pathways such as glucose and fatty acid metabolism as well as cholesterol/bile acid homeostasis. Furthermore, many reports have shown that bile acid signaling finely regulates numerous metabolically relevant genes at the level of their transcription. However, the molecular mechanisms of bile acid signaling to control transcription of genes are poorly understood.

In recent years, two orphan nuclear receptors, farnesoid X receptor (FXR) and small heterodimer partner (SHP), have been identified as key regulators in bile acid signaling. FXR was revealed as the first *in vivo* bile acid biosensor and was shown to regulate cholesterol/bile acid homeostasis by suppressing the transcription of cholesterol 7-α hydroxylase (CYP7A1), the first and rate-limiting enzyme in bile acid biosynthesis. The discovery of the bile acid receptor FXR provided a better understanding of the potential roles of orphan nuclear receptors in transcriptional regulation by bile acids. Consecutive reports showed that bile acid-activated FXR suppressed CYP7A1 gene transcription by inducing another orphan nuclear receptor, small heterodimer partner (SHP), that plays a key role in the negative feedback regulation of bile acid synthesis. Later then, our group showed that bile acid-induced SHP actively recruits the mSin3A/HDAC corepressors and the Swi/SNF chromatin remodeling complex, containing Brm as a central ATPase, to the promoter and suppresses the transcription of the CYP7A1 gene.

In order to delineate the repression mechanism of CYP7A1 mediated by SHP, I examined whether histone modifications are also involved in CYP7A1 repression by SHP and whether a functional interplay between chromatin modifying enzymes occurs during the repression of the CYP7A1 gene. Recently, I reported that histone methyltransferase G9a is present in a SHP complex and enhances SHP inhibitory activity to suppress CYP7A1 expression.

Besides cholesterol/bile acid homeostasis, FXR and SHP are involved in other metabolic pathways such as glucose homeostasis and fatty acid metabolism through bile acid signaling. Interestingly, it has been reported that the expression level of SHP was strikingly elevated in the liver of obese mice compared to normal mice. Also, it was reported that SHP-transgenic mice have significant features of fatty liver, such as lipid accumulation and elevated levels of hepatic triglycerides. These findings led me to ask how FXR enhances the level of SHP in the liver of obese mice without bile acid signaling. My recent findings suggest that histone acetyltransferase p300 is a critical FXR coactivator for SHP induction by acetylating core histones in response to bile acid treatment in normal mice. However, even without bile acid treatment, p300 can acetylate FXR, as well as core histones, at the native SHP promoter in obese mice, resulting in constitutively and highly elevated expression of SHP.

These combined studies should lead to a better understanding how bile acid-responsive genes are regulated by the orphan nuclear receptors SHP and FXR and their cofactors in health and disease states.

To my Lord, Eunjung, and Luke

Acknowledgements

My studies would not have been possible without the support of many people. I would like to express deepest appreciation to my advisors, Dr. Kim Jongsook and Byron W. Kemper for the support and guidance throughout my graduate studies at University of Illinois at Urbana-Champaign. Also thanks to my committee members, Dr. Ann M. Nardulli, Dr. Benita S. Katzenellenbogen, Dr. Craig A. Mizzen, and Dr. Milan K. Bagchi for their time and support for my works. Finally, I thank all my lab members I've met over many years at University of Illinois at Urbana-Champaign, especially Dr. Yangjin Bae, Dr. Jun Xia, Ji Miao, Lingjin Xiang, Bhaskar Ponugoti, Deepthi Kanamaluru, Stephanie Tsang, Jiyoung Lee, Hyeryoung Yoon and Ryan Jones. Without the generous help of these individuals, my work would not have been possible.

Table of Contents

Chapter One

Introduction

Bile acids, end-products of cholesterol catabolism, are signaling molecules

In mammalian cells, cholesterol plays an important role in many biological activities as a structural component of the cell membrane and as a precursor for steroid hormones, lipid soluble vitamins, and bile acids. Despite its essential role, excessive cholesterol causes toxic precipitates in blood vessels and leads to atherosclerotic heart disease and gallstone formation. Thus cholesterol levels in the body must be tightly regulated. The amount of cholesterol in the body is increased by *de novo* synthesis from acetyl-coA and by daily dietary intake, and is decreased by conversion into bile acids (73).

Cholesterol catabolism, conversion of cholesterol into bile acids, is the main pathway for the elimination of cholesterol from the body (16, 75, 76). Bile acids, the end-product of cholesterol catabolism, are important for absorption and solubilization of lipids in the intestine. Also, bile acids play important roles as signaling molecules in a wide range of metabolic pathways, such as lipid and glucose metabolism and energy homeostasis (18). However, the detergent properties of bile acids are toxic to the cells. Therefore, it is also important that the levels of cholesterol and bile acids must be coordinately regulated in the body. Cholesterol is converted to primary bile acids, such as cholic acid (CA) and chenodeoxycholic acid (CDCA), in the liver (16, 75). These newly synthesized primary bile acids are then secreted into the lumen of the small intestine where they emulsify lipids, cholesterol, and fat-soluble vitamins. In the small intestine, some of the primary bile acids are further converted to secondary bile acids,

such as lithocholic acid (LCA) and deoxycholic acid (DCA) by intestinal bacteria (4, 18, 32, 82). These bile acids are efficiently absorbed from the intestine by both the ileal bile acid transporter (IBAT) and the ileal bile acid binding protein (IBABP) and transported back to the liver via enterohepatic circulation. About 95% of bile acids are recycled by this route; the remaining 5% are excreted from the body through the stool. The excreted bile acids are replaced by the bile acids newly synthesized from cholesterol in the liver.

The conversion of cholesterol to bile acids occurs by two major bile acid biosynthetic pathways: the alternative and classic pathways (16, 18, 75). The main bile acid biosynthetic pathway is the classic pathway (neutral) which produces two major primary bile acids, CA and CDCA, in roughly equal amounts in humans (16, 18, 22, 67, 75). The classic pathway is initiated by cholesterol 7α-hydroxylase (CYP7A1) which is exclusively expressed in liver (67). The alternative pathway is initiated by sterol 27-hydroxylase (CYP27A1), and also named the "acidic" pathway because of the acidic properties of the intermediates. The alternative pathway contributes less than 18% of total bile acid synthesis in humans (24).

CYP7A1 is a member of the cytochrome P450 superfamily, and a key hepatic microsomal enzyme for the maintenance of cholesterol level

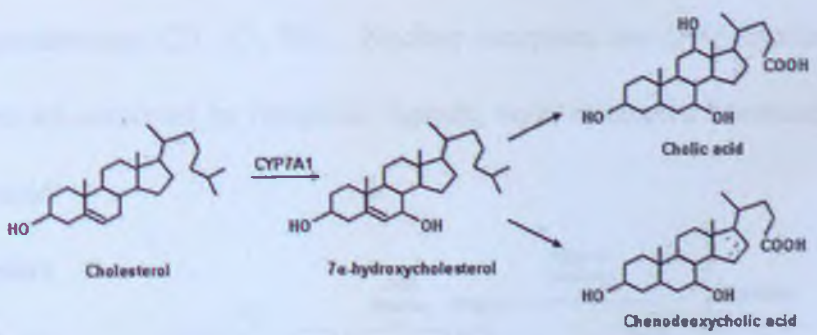

Figure 1. The conversion of cholesterol into bile acids

since it catalyzes the first and rate-limiting step in the conversion of cholesterol into bile acids (67). CYP7A1 incorporates a hydroxyl group at the 7α-position of the cholesterol. The hydroxylation at 7α initiates subsequent hydroxylation in the side chain of cholesterol by a number of enzymes, resulting in oxidation-dependent cleavage of side chains to convert cholesterol into bile acids (Fig.1).

Orphan nuclear receptors are involved in cholesterol/bile acid homeostasis

The bioactivity of CYP7A1 is regulated at the level of transcription by a number of effectors, such as insulin, steroid/thyroid hormones, cytokines, cholesterol, and bile acids, and also exhibits diurnal rhythm (17, 22, 58). Among these effectors, bile acids strongly inhibit the transcription of CYP7A1 by a negative feedback regulatory pathway. Recent studies have revealed that negative feedback regulation of CYP7A1 transcription by bile acids is mediated by the interplay of orphan nuclear receptors (16-18, 22, 73, 75, 76). Orphan nuclear receptors belong to the nuclear receptor superfamily and lack identified ligands when they were initially identified. However, recent advances in the orphan nuclear receptor field revealed that these receptors play critical roles in the regulation of glucose, lipid and drug metabolism (27, 47, 80). Nuclear receptors are DNA-binding transcriptional factors that are activated by lipophilic ligands, such as steroid hormones, vitamin D, and thyroid hormone. Nuclear receptors consist of six domains (A–F) based on regions of conserved sequence and

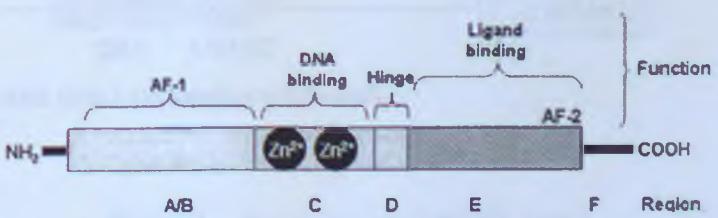

Figure 2. The structure of nuclear receptors

function (Fig.2). They typically have a highly conserved DNA-binding domain in the N-terminal region and a moderately conserved ligand-binding domain in the C-terminal region. Ligand-independent activation function-1 (AF-1) and ligand-dependent activation function-2 (AF-2) are located in the N-terminal and C-terminal regions, respectively. Two cysteine-Zn^{2+} finger motifs located in the DNA-binding domain are directly involved in DNA binding and dimerization. The ligand-binding domain is also involved in dimerization and in interaction with coregulators. Upon activation by their ligands, nuclear receptors directly bind to specific DNA sequences in the regulatory regions of their target genes and usually activate gene transcription.

From promoter deletion analysis, a bile acid response element (BARE) region was identified in the native CYP7A1 promoter (20, 85). Numerous studies have reported that orphan nuclear receptors, such as hepatic nuclear factor-4 (HNF-4), liver receptor homolog-1 (LRH-1), small heterodimer partner (SHP), and farnesoid X receptor (FXR), participate in the negative feedback regulation of CYP7A1 transcription by bile acids (14, 19, 30, 59, 68). The BARE region contains a DR-1 motif, TGGACT_t_AGTTCA (-144 to -132) that binds HNF-4 (Fig.3) (16). HNF-4 is the most abundant orphan nuclear receptor expressed in the liver. HNF-4 homodimers bind to the DR-1 motif in the BARE region and constitutively activate CYP7A1 without ligand binding. Mutation of the HNF-4 binding site

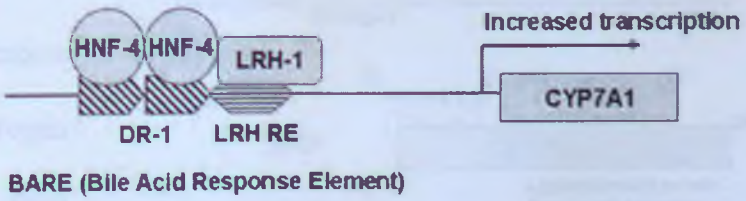

Figure 3. The structure of BARE region

substantially reduced the promoter activity of CYP7A1, indicating that HNF-4 is crucial for CYP7A1 gene expression (84).

In addition to HNF-4, the BARE region also contains a binding site for LRH-1 that is required for the expression of CYP7A1 (68). LRH-1 is expressed in liver, intestine, and pancreas (50). The LRH-1 binding site, TCAAGGCCA (-134 to -126), overlaps with the HNF-4 binding site by three nucleotides in the BARE region (68). Whether these two orphan nuclear receptors, HNF-4 and LRH-1, bind at the same time or whether they compete with each other for binding at the BARE region is not well understood. LRH-1 is also required for the expression of SHP (56, 70). It was shown that SHP and transcriptional corepressors to bind to LRH-1 at the BARE region, resulting in repression of CYP7A1 gene expression (30, 59). Thus, LRH-1 plays an important role for both activation and repression of CYP7A1 transcription.

SHP is an unusual orphan nuclear receptor that contains putative ligand-binding and dimerization domains, but lacks a conventional DNA binding domain (Fig.4) (77). Studies from SHP-null mice showed that SHP is a metabolic regulator and plays a key role in cholesterol/bile acid and energy homeostasis (8). Previous studies showed that SHP interacts with numerous nuclear receptors, such as LRH-1, constitutive androstane receptor (CAR), HNF-4, and estrogen receptor (ER) and inhibits their activities in diverse biological pathways (3, 41, 54, 55).

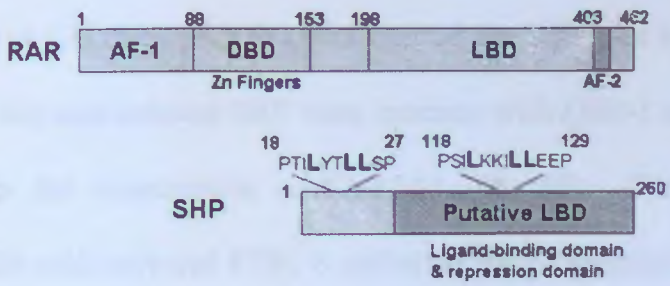

Figure 4. The comparison of domain structure of SHP with RAR, the typical nuclear receptor

Previous *in vitro* and transfection studies suggested that SHP inhibits nuclear receptor activity by two potential inhibitory mechanisms. First, SHP contains two nuclear receptor interacting LXXLL-related motifs, called NR boxes (40). Thus, SHP may compete with p160 coactivators for binding to various nuclear receptors in the regulation of target gene transcription. Second, since SHP contains an intrinsic repression domain in its C-terminus, SHP may inhibit transcription by recruiting corepressor complexes (54). Since the orphan nuclear receptors, HNF-4 and LRH-1, are transcriptional activators of CYP7A1, inhibition by forming heterodimer with SHP may be a general mechanism for repression at the BARE region. However, whether SHP inhibits transcription of its target genes in a chromatin context by these proposed mechanisms was not demonstrated.

In addition to HNF-4, LRH-1, and SHP, FXR has been implicated in bile acid-mediated inhibition of CYP7A1 transcription (30, 59). The nuclear bile acid receptor, FXR is a biosensor for a wide variety of endogenous bile acids and primarily expressed in the liver, kidney, and intestine (53, 61). Previous studies have established that FXR indirectly inhibits CYP7A1 transcription by induction of SHP gene expression (30, 78). Upon activation by physiological concentration of bile acids, FXR heterodimerizes with retinoid X receptor (RXR) and binds to a IR-1 motif in the promoter of the SHP gene to activate the transcription (30, 49). Bile acid-induced SHP, then, interacts with LRH-1 at the CYP7A1 promoter and inhibits the transcription of CYP7A1 (30, 59). This inhibitory mechanism, initiated by bile acid-activated FXR, is called the SHP-dependent repression pathway. However, molecular mechanisms by which bile acid-induced SHP inhibits CYP7A1 transcription were not delineated.

Modifications of chromatin structure are important for gene expression

Chromatin structure plays a fundamental role in the regulation of eukaryotic gene function. In the chromatin of eukaryotic cells, the basic unit of organization is the nucleosome. One nucleosome consists of about 146 base pairs of DNA wrapped around a core histone octamer, which contains two copies each of histones H2A, H2B, H3 and H4. Structural changes of chromatin play a fundamental role in eukaryotic gene regulation by altering the accessibility of DNA-bound factors and the basal transcriptional machinery to the gene (39, 83).

There are two types of chromatin-modifying complexes that are involved in modifying histone residues and nucleosome conformation, thereby leading to transcriptional activation or repression of genes. The first class contains ATP-dependent remodeling complexes such as, the Swi/Snf complex. These complexes modify chromatin structure in a non-covalent manner and the modification results in a disrupted or altered nucleosomal structure (91). Brm and Brg-1 are central ATPases for the Swi/Snf chromatin remodeling complexes. The second class includes histone acetyltransferases (HATs), histone deacetylases (HDACs), and histone methyltransferases (HMTs), which covalently modify core histones (39, 83). The core histones, particularly H3 and H4, can be acetylated at lysine residues in the N-terminal tails. The acetylation of histones mediated by HATs causes a reduction in the affinity of histones for DNA and results in unpacking of the nucleosome, which leads to increased access of transcriptional factors to DNA. The deacetylation of histones mediated by HDACs causes opposite effects on chromatin structure (39, 83). Transcription correlates with the degree of histone acetylation, with hyperacetylated regions more actively transcribed

than hypoacetylated regions (39, 83). Likewise, histone methylation also plays an essential role in regulating gene transcription (48, 52, 98). In general, histone methylation occurs on lysine and arginine residues of histones. Methylation of K4, 36, and 79, and R17 and 23 of histone H3 and R3 of histone H4 have been associated with transcriptional activation, whereas methylation K9 and 27 of histone H3 and K20 of histone H4 have been correlated with gene silencing (6).

Although the detailed molecular mechanisms of CYP7A1 repression by bile acids are not well understood, the SHP-dependent repression pathway in response to bile acids is likely to converge on chromatin structural changes at the CYP7A1 promoter. Our lab recently found that bile acid-induced SHP was involved in *in vivo* chromatin remodeling at the human CYP7A1 promoter (45). Restriction endonuclease accessibility assays demonstrated that the accessibility of the core nucleosomes to restriction enzymes was substantially decreased after bile acid treatment, implying that the CYP7A1 promoter was remodeled into a more closed configuration. Biochemical studies indicated that SHP directly interacted with Brm and mSin3A through its repression domain in a mSin3A/Swi/Snf-Brm complex. Transcriptional assays in cultured cells showed that expression of Brm, but not a Brm ATPase mutant, inhibited CYP7A1 promoter activity and further enhanced SHP-mediated repression. Moreover, in the chromatin immunoprecipitation assays, mSin3A and the Swi/Snf-Brm complex were recruited to the CYP7A1 promoter in a SHP-dependent manner. This recruitment was associated with chromatin remodeling after bile acid treatment. Thus, our studies suggested that SHP mediates recruitment of the mSin3A/Swi/Snf-Brm chromatin remodeling complex to the CYP7A1 promoter, resulting in chromatin remodeling and

gene repression. This study established the first link between the mSin3A/Swi/Snf-Brm chromatin remodeling complex and regulation of cholesterol metabolism (Fig.5) (45). However, the question of how the chromatin modifying enzymes, such as HDACs, HMTs, and the ATP-dependent chromatin-remodeling complexes, may act in concert with SHP to regulate CYP7A1 transcription still remain unknown.

Histone methyltransferase G9a is responsible for mono- and dimethylation of H3K9 in euchromatin, and is critically involved in transcriptional silencing (87, 88). Recently, it was reported that SHP directly interacts with G9a and potentiates SHP-mediated suppression in *in vitro* studies (9). However, the role of G9a in the regulation of the CYP7A1 transcription has not been studied. Thus, it prompted me to examine the roles of G9a in the repressive action of SHP. Recently, I found that G9a is a critical cofactor that is present in the inhibitory SHP complex which regulates the transcription of CYP7A1 in response to bile acids. This study was recently published in *Molecular and Cellular Biology* (26).

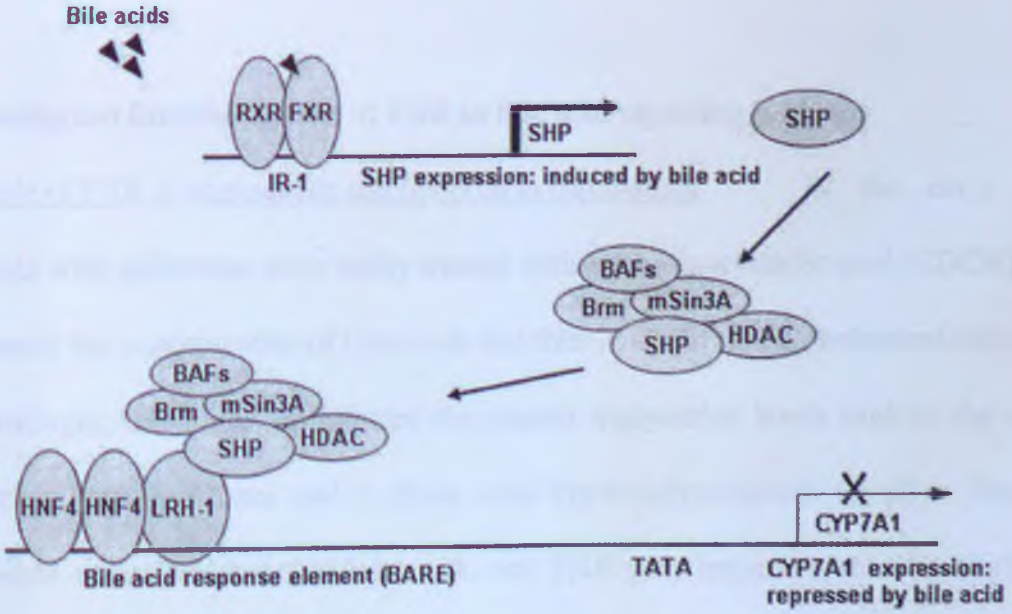

Figure 5. Bile Acids negative feedback CYP7A1 regulation by SHP

The nuclear receptor FXR is a bile acid biosensor

FXR, a member of the nuclear hormone receptor superfamily, has been identified as a bile acid biosensor (61). FXR is mainly expressed in liver and intestine, but also at lower levels in the adrenal gland and kidney (53). Like many other hormone nuclear receptors, FXR binds to specific DNA response elements to activate the transcription of bile acid-responsive genes by forming a heterodimeric complex with the retinoid X receptor (RXR) (7, 53, 64, 66). The FXR response element (FXRE) is composed of an inverted repeat of 2 AGGTCA half-sites separated by 1 nucleotide (IR-1) (49). Besides the IR-1 motif, the FXR/RXR heterodimer can also bind to direct repeat (DR) elements including DR4 and DR5 *in vitro* (49). Physiological concentrations of endogenous bile acids activate FXR which then induces expression of a number of bile acid-responsive FXR target genes and regulates bile acid signaling pathways that control various metabolic processes, such as HDL, triglyceride, and glucose metabolism (51, 53, 60, 62, 92, 94), as well as cholesterol/bile acid homeostasis.

Physiological functional roles of FXR in bile acid signaling pathway

A. Role of FXR in triglyceride and lipoprotein metabolism In the early 1970s, patients with gallstones were orally treated with chenodeoxycholic acid (CDCA) which enhanced the concentration of bile acids and thus solubilized the cholesterol-rich stones. Interestingly, this treatment reduced the plasma triglyceride levels both in the patients suffering from gallstones and in those with hypertriglyceridemia (5, 65). Studies in FXR-null mice indicated that bile acids and FXR play important roles in triglyceride metabolism. The levels of HDL-cholesterol are elevated in FXR-null mice, which

results in hypercholesterolemia (78). Notably, administration of FXR agonists to normal rats and mice reduced plasma triglyceride levels (44, 63).

Recently, FXR has been suggested to promote the hepatic clearance of lipoproteins and reduce plasma cholesterol levels. It was shown that bile acid-activated FXR induces its target gene SHP which correlates with decreased expression of the master lipogenic regulator sterol regulatory element binding protein (SREBP)-1c, providing a potential mechanism for the triglyceride-lowering effect of bile acids (92). FXR activation with natural and synthetic agonists induces ApoCII which activates LPL, a key enzyme involved in lipoprotein lipolysis, and suppresses ApoCIII, an inhibitor of LPL activity (21, 44, 53). Consistent with this finding, FXR induces the expression of the phospholipid transfer protein (PLTP), an enzyme which transfers phospholipid groups from triglyceride-rich lipoproteins to HDL (90). Moreover, activated FXR induces the expression of the very-low-density lipoprotein receptor (VLDL Rc) which plays a key role in the metabolism of lipoproteins by enhancing LPL-mediated triglyceride hydrolysis (79). Thus, FXR controls important genes involved in triglyceride and lipoprotein metabolism.

B. Role of FXR in glucose metabolism Recently, in *in vitro* and *in vivo* studies it was shown that bile acids modulate gluconeogenesis by regulating the expression of the rate-limiting enzyme, phosphoenolpyruvate carboxykinase (PEPCK), as well as glucose-6-phosphatase (G6Pase). The expression of PEPCK and G6Pase genes are negatively regulated by bile acid treatment *in vivo* (94). This study showed that the negative regulation of PEPCK and G6Pase resulted from the induction of SHP (94). In addition,

it has been shown in FXR-null mice that circulating free fatty acids were increased, which was associated with elevated plasma glucose and impaired glucose and insulin tolerance (11). Activation of FXR in wild type or diabetic mice promoted hypoglycemia and increased insulin sensitivity (11, 97).

C. Other physiological functions of FXR in response to bile acids FXR also plays a critical role in protecting the liver from toxic bile acids (53). Like CYP7A1 inhibition, the FXR/SHP pathway is also involved in repression of Na^+-taurocholate contransporting polypeptide (NTCP), a hepatic bile acid import transporter that mediates the entry of intestinal bile acids into hepatocytes (23). When hepatic bile acid levels are elevated, FXR induces SHP and thereby represses CYP7A1 and NTCP, resulting in inhibition of both bile acid biosynthesis and uptake of intestinal bile acids, respectively. Thus, the FXR/SHP pathway can prevent excess accumulation of bile acids in the liver. Besides NTCP, bile acid-activated FXR also protects the liver from elevated toxic bile acids by increasing the export of hepatic bile acids to the gall bladder. Bile salt export pump (BSEP) is a major bile acid transporter that mediates the transport of bile acids across the canalicular membrane into the bile duct and its expression is induced by FXR. Bile acid-activated FXR induces the expression of BSEP and reduce accumulation of hepatic bile acids to protect the liver from elevated hepatic bile acids (1). Therefore, FXR plays a critical role in protecting the liver from elevated hepatic bile acids via inhibition of bile acid synthesis and bile acid import from the intestine, and induction of excess bile acid export from the liver to the gall bladder.

FXR is also important in the liver regeneration process (37). Treatment of mice with cholic acid resulted in accelerated liver regeneration, and this effect was markedly reduced in FXR-null mice (37). Therefore, it has been proposed that FXR regulates the size or regeneration of the liver in response to the levels of bile acids. In addition, FXR protects the intestine from the bacterial growth. CYP27-null mice have impaired bile acid synthesis which results in decreased FXR activation and FXR target gene induction (38). Treatment of CYP27-null mice with a FXR agonist, GW4064, repressed mucosal injury in the intestine due to attenuated intestinal bacterial overgrowth, whereas FXR-null mice did not have any beneficial effect (38). Thus, it has been suggested that FXR-mediated transactivation provides protection from bacterial overgrowth. Although such important physiological roles of FXR have been revealed, the molecular mechanisms by which FXR mediates such diverse metabolic pathways in response to bile acids are not known.

Modulation of FXR activity by transcriptional cofactors

Nuclear receptors collaborate with a number of transcriptional cofactors, such as coactivators and corepressors, to regulate expression of their target genes. Ligand binding induces conformational changes in nuclear receptors and promotes their association with a diverse group of nuclear proteins, such as SRC-1/p160, SRC-2/TIF-2/GRIP-1, SRC-3/AIB1 and CBP/p300 which function as coactivators of transcription (12, 28, 33, 71, 86). In the absence of ligand, several nuclear receptors, such as TR, LXR, and PXR, associate with corepressors, such as HDAC, SMRT, and NcoR-1, and maintain target genes in a repressed state (15, 34, 35, 42, 89, 93). Previous *in vitro* and

functional reporter studies suggested that several transcriptional cofactors may collaborate with FXR to modulate its target genes. The histone arginine methyltransferase, CARM1, methylates histones at the promoter of the BSEP gene and increase the activity of FXR (2). Another arginine methyltransferase, PRMT1, methylates histones at the SHP and BSEP promoters and enhances transactivation by FXR (74). A transcriptional cofactor and mediator, DRIP205, was also shown to interact with FXR in vitro and enhanced transcriptional activation by FXR in reporter assays (72). A metabolic coactivator PGC-1α and GRIP-1, a p160 coactivator, have been shown to directly interact with FXR in vitro and increase FXR transactivation in reporter assays (43, 96). However, whether these cofactors modulate FXR transactivation in response to bile acids in vivo has not been delineated.

p300 is a transcriptional coactivator that is involved in the regulation of various DNA-binding transcriptional factors (29). p300 was initially identified in protein interaction assays by its interaction with the adenoviral-transforming protein E1A (25) and identified as a histone acetyltransferase (69). The correlation between histone acetylation and gene activation has been documented (6, 39), therefore, the finding that p300 was a histone acetyltransferase indicated that p300 functions as a transcriptional coactivator by modulating the covalent modifications of chromatin. Acetylation by p300 was shown to regulate the transcriptional functions of non-histone proteins as well (31). Several transcriptional regulators were shown to be acetylated, including ER, HNF-4, EKLF, GATA-1, p53, NF-Y, and ACTR (10, 13, 31, 46, 57, 81, 95). Acetylation of these proteins by p300 affects their transcriptional activity by altering DNA binding, cofactor interaction, stability, and subcellular localization.

Although the essential biological roles of FXR have been determined, how FXR modulates the transcription of the target genes is poorly understood. Therefore, to broaden my interests and understanding of bile acid signaling pathway in the liver, I have been investigating whether p300 can modulate FXR activity for regulation of the transcription of the target genes, including SHP, a well known FXR target gene in bile acid signaling. Previous study showed that SHP-transgenic mice have a fatty liver-phenotype (8). Consistent with these data, a recent study showed that SHP expression was abnormally elevated in obese mice, suggesting that dysregulation of SHP expression may lead to hepatic metabolic disease (36). Thus, I also have investigated the role of FXR and p300 in dysregulated SHP expression in obese mice.

Recently, I found that p300 plays a critical role in FXR transactivation in the induction of the expression of SHP through bile acid signaling. Moreover, p300 can constitutively acetylate FXR, as well as core histones, in obese mice in the absence of bile acid signaling, resulting in dysregulated hepatic SHP expression in the liver.

SHP and FXR play key roles in glucose and triglyceride metabolism, as well as in cholesterol/bile acid homeostasis. The physiological roles of SHP and FXR have been exclusively studied, however, the molecular mechanisms and the pathways by which they regulate the expression of target genes involved in hepatic metabolism have not been explored in detail. Thus, my study will provide information about the regulation of the expression of these genes that may help in developing novel therapeutic agents to treat metabolic disorders, such as, hyperlipidemia and atherosclerosis.

References

1. **Ananthanarayanan, M., N. Balasubramanian, M. Makishima, D. J. Mangelsdorf, and F. J. Suchy.** 2001. Human bile salt export pump promoter is transactivated by the farnesoid X receptor/bile acid receptor. J Biol Chem **276:**28857-65.

2. **Ananthanarayanan, M., S. Li, N. Balasubramaniyan, F. J. Suchy, and M. J. Walsh.** 2004. Ligand-dependent activation of the farnesoid X-receptor directs arginine methylation of histone H3 by CARM1. J Biol Chem **279:**54348-57.

3. **Bae, Y., J. K. Kemper, and B. Kemper.** 2004. Repression of CAR-mediated transactivation of CYP2B genes by the orphan nuclear receptor, short heterodimer partner (SHP). DNA Cell Biol **23:**81-91.

4. **Baron, S. F., C. V. Franklund, and P. B. Hylemon.** 1991. Cloning, sequencing, and expression of the gene coding for bile acid 7 alpha-hydroxysteroid dehydrogenase from Eubacterium sp. strain VPI 12708. J Bacteriol **173:**4558-69.

5. **Bell, G. D., B. Lewis, A. Petrie, and R. H. Dowling.** 1973. Serum lipids in cholelithiasis: effect of chenodeoxycholic acid therapy. Br Med J **3:**520-3.

6. **Berger, S. L.** 2007. The complex language of chromatin regulation during transcription. Nature **447:**407-12.

7. **Blumberg, B., and R. M. Evans.** 1998. Orphan nuclear receptors--new ligands and new possibilities. Genes Dev **12:**3149-55.

8. **Boulias, K., N. Katrakili, K. Bamberg, P. Underhill, A. Greenfield, and I. Talianidis.** 2005. Regulation of hepatic metabolic pathways by the orphan nuclear receptor SHP. Embo J **24:**2624-33.

9. **Boulias, K., and I. Talianidis.** 2004. Functional role of G9a-induced histone methylation in small heterodimer partner-mediated transcriptional repression. Nucleic Acids Res **32:**6096-103.

10. **Boyes, J., P. Byfield, Y. Nakatani, and V. Ogryzko.** 1998. Regulation of activity of the transcription factor GATA-1 by acetylation. Nature **396:**594-8.

11. **Cariou, B., K. van Harmelen, D. Duran-Sandoval, T. H. van Dijk, A. Grefhorst, M. Abdelkarim, S. Caron, G. Torpier, J. C. Fruchart, F. J. Gonzalez, F. Kuipers, and B. Staels.** 2006. The farnesoid X receptor modulates adiposity and peripheral insulin sensitivity in mice. J Biol Chem **281:**11039-49.

12. **Chakravarti, D., V. J. LaMorte, M. C. Nelson, T. Nakajima, I. G. Schulman, H. Juguilon, M. Montminy, and R. M. Evans.** 1996. Role of CBP/P300 in nuclear receptor signalling. Nature **383:**99-103.

13. **Chen, H., R. J. Lin, W. Xie, D. Wilpitz, and R. M. Evans.** 1999. Regulation of hormone-induced histone hyperacetylation and gene activation via acetylation of an acetylase. Cell **98:**675-86.

14. **Chen, J., A. D. Cooper, and B. Levy-Wilson.** 1999. Hepatocyte nuclear factor 1 binds to and transactivates the human but not the rat CYP7A1 promoter. Biochem Biophys Res Commun **260:**829-34.

15. **Chen, J. D., and R. M. Evans.** 1995. A transcriptional co-repressor that interacts with nuclear hormone receptors. Nature **377:**454-7.

16. **Chiang, J. Y.** 2002. Bile acid regulation of gene expression: roles of nuclear hormone receptors. Endocr Rev **23:**443-63.

17. **Chiang, J. Y.** 1998. Regulation of bile acid synthesis. Front Biosci **3:**d176-93.

18. **Chiang, J. Y.** 2004. Regulation of bile acid synthesis: pathways, nuclear receptors, and mechanisms. J Hepatol **40:**539-51.

19. **Chiang, J. Y., R. Kimmel, C. Weinberger, and D. Stroup.** 2000. Farnesoid X receptor responds to bile acids and represses cholesterol 7alpha-hydroxylase gene (CYP7A1) transcription. J Biol Chem **275:**10918-24.

20. **Chiang, J. Y., and D. Stroup.** 1994. Identification and characterization of a putative bile acid-responsive element in cholesterol 7 alpha-hydroxylase gene promoter. J Biol Chem **269:**17502-7.

21. **Claudel, T., Y. Inoue, O. Barbier, D. Duran-Sandoval, V. Kosykh, J. Fruchart, J. C. Fruchart, F. J. Gonzalez, and B. Staels.** 2003. Farnesoid X receptor agonists suppress hepatic apolipoprotein CIII expression. Gastroenterology **125:**544-55.

22. **Davis, R. A., J. H. Miyake, T. Y. Hui, and N. J. Spann.** 2002. Regulation of cholesterol-7alpha-hydroxylase: BAREly missing a SHP. J Lipid Res **43:**533-43.

23. **Denson, L. A., E. Sturm, W. Echevarria, T. L. Zimmerman, M. Makishima, D. J. Mangelsdorf, and S. J. Karpen.** 2001. The orphan nuclear receptor, shp, mediates bile acid-induced inhibition of the rat bile acid transporter, ntcp. Gastroenterology **121:**140-7.

24. **Duane, W. C., and N. B. Javitt.** 1999. 27-hydroxycholesterol: production rates in normal human subjects. J Lipid Res **40:**1194-9.

25. **Eckner, R., M. E. Ewen, D. Newsome, M. Gerdes, J. A. DeCaprio, J. B. Lawrence, and D. M. Livingston.** 1994. Molecular cloning and functional analysis of the adenovirus E1A-associated 300-kD protein (p300) reveals a protein with properties of a transcriptional adaptor. Genes Dev **8:**869-84.

26. **Fang, S., J. Miao, L. Xiang, B. Ponugoti, E. Treuter, and J. K. Kemper.** 2007. Coordinated recruitment of histone methyltransferase G9a and other chromatin-modifying enzymes in SHP-mediated regulation of hepatic bile acid metabolism. Mol Cell Biol **27:**1407-24.

27. **Giguere, V.** 1999. Orphan nuclear receptors: from gene to function. Endocr Rev **20:**689-725.

28. **Glass, C. K., D. W. Rose, and M. G. Rosenfeld.** 1997. Nuclear receptor coactivators. Curr Opin Cell Biol **9:**222-32.

29. **Goodman, R. H., and S. Smolik.** 2000. CBP/p300 in cell growth, transformation, and development. Genes Dev **14**:1553-77.

30. **Goodwin, B., S. A. Jones, R. R. Price, M. A. Watson, D. D. McKee, L. B. Moore, C. Galardi, J. G. Wilson, M. C. Lewis, M. E. Roth, P. R. Maloney, T. M. Willson, and S. A. Kliewer.** 2000. A regulatory cascade of the nuclear receptors FXR, SHP-1, and LRH-1 represses bile acid biosynthesis. Mol Cell **6**:517-26.

31. **Gu, W., and R. G. Roeder.** 1997. Activation of p53 sequence-specific DNA binding by acetylation of the p53 C-terminal domain. Cell **90**:595-606.

32. **Hofmann, A. F.** 1976. The enterohepatic circulation of bile acids in man. Adv Intern Med **21**:501-34.

33. **Hong, H., K. Kohli, A. Trivedi, D. L. Johnson, and M. R. Stallcup.** 1996. GRIP1, a novel mouse protein that serves as a transcriptional coactivator in yeast for the hormone binding domains of steroid receptors. Proc Natl Acad Sci U S A **93**:4948-52.

34. **Horlein, A. J., A. M. Naar, T. Heinzel, J. Torchia, B. Gloss, R. Kurokawa, A. Ryan, Y. Kamei, M. Soderstrom, C. K. Glass, and et al.** 1995. Ligand-independent repression by the thyroid hormone receptor mediated by a nuclear receptor co-repressor. Nature **377**:397-404.

35. **Hu, X., S. Li, J. Wu, C. Xia, and D. S. Lala.** 2003. Liver X receptors interact with corepressors to regulate gene expression. Mol Endocrinol **17**:1019-26.

36. **Huang, J., J. Iqbal, P. K. Saha, J. Liu, L. Chan, M. M. Hussain, D. D. Moore, and L. Wang.** 2007. Molecular characterization of the role of orphan receptor small heterodimer partner in development of fatty liver. Hepatology **46**:147-57.

37. **Huang, W., K. Ma, J. Zhang, M. Qatanani, J. Cuvillier, J. Liu, B. Dong, X. Huang, and D. D. Moore.** 2006. Nuclear receptor-dependent bile acid signaling is required for normal liver regeneration. Science **312**:233-6.

38. **Inagaki, T., A. Moschetta, Y. K. Lee, L. Peng, G. Zhao, M. Downes, R. T. Yu, J. M. Shelton, J. A. Richardson, J. J. Repa, D. J. Mangelsdorf, and S. A. Kliewer.** 2006. Regulation of antibacterial defense in the small intestine by the nuclear bile acid receptor. Proc Natl Acad Sci U S A **103:**3920-5.

39. **Jenuwein, T., and C. D. Allis.** 2001. Translating the histone code. Science **293:**1074-80.

40. **Johansson, L., A. Bavner, J. S. Thomsen, M. Farnegardh, J. A. Gustafsson, and E. Treuter.** 2000. The orphan nuclear receptor SHP utilizes conserved LXXLL-related motifs for interactions with ligand-activated estrogen receptors. Mol Cell Biol **20:**1124-33.

41. **Johansson, L., J. S. Thomsen, A. E. Damdimopoulos, G. Spyrou, J. A. Gustafsson, and E. Treuter.** 1999. The orphan nuclear receptor SHP inhibits agonist-dependent transcriptional activity of estrogen receptors ERalpha and ERbeta. J Biol Chem **274:**345-53.

42. **Johnson, D. R., C. W. Li, L. Y. Chen, J. C. Ghosh, and J. D. Chen.** 2006. Regulation and binding of pregnane X receptor by nuclear receptor corepressor silencing mediator of retinoid and thyroid hormone receptors (SMRT). Mol Pharmacol **69:**99-108.

43. **Kanaya, E., T. Shiraki, and H. Jingami.** 2004. The nuclear bile acid receptor FXR is activated by PGC-1alpha in a ligand-dependent manner. Biochem J **382:**913-21.

44. **Kast, H. R., C. M. Nguyen, C. J. Sinal, S. A. Jones, B. A. Laffitte, K. Reue, F. J. Gonzalez, T. M. Willson, and P. A. Edwards.** 2001. Farnesoid X-activated receptor induces apolipoprotein C-II transcription: a molecular mechanism linking plasma triglyceride levels to bile acids. Mol Endocrinol **15:**1720-8.

45. **Kemper, J. K., H. Kim, J. Miao, S. Bhalla, and Y. Bae.** 2004. Role of an mSin3A-Swi/Snf chromatin remodeling complex in the feedback repression of bile acid biosynthesis by SHP. Mol Cell Biol **24:**7707-19.

46. **Kim, M. Y., E. M. Woo, Y. T. Chong, D. R. Homenko, and W. L. Kraus.** 2006. Acetylation of estrogen receptor alpha by p300 at lysines 266 and 268 enhances the deoxyribonucleic acid binding and transactivation activities of the receptor. Mol Endocrinol **20:**1479-93.

47. **Kliewer, S. A., J. M. Lehmann, and T. M. Willson.** 1999. Orphan nuclear receptors: shifting endocrinology into reverse. Science **284:**757-60.

48. **Kouzarides, T.** 2002. Histone methylation in transcriptional control. Curr Opin Genet Dev **12:**198-209.

49. **Laffitte, B. A., H. R. Kast, C. M. Nguyen, A. M. Zavacki, D. D. Moore, and P. A. Edwards.** 2000. Identification of the DNA binding specificity and potential target genes for the farnesoid X-activated receptor. J Biol Chem **275:**10638-47.

50. **Lala, D. S., P. M. Syka, S. B. Lazarchik, D. J. Mangelsdorf, K. L. Parker, and R. A. Heyman.** 1997. Activation of the orphan nuclear receptor steroidogenic factor 1 by oxysterols. Proc Natl Acad Sci U S A **94:**4895-900.

51. **Lambert, G., M. J. Amar, G. Guo, H. B. Brewer, Jr., F. J. Gonzalez, and C. J. Sinal.** 2003. The farnesoid X-receptor is an essential regulator of cholesterol homeostasis. J Biol Chem **278:**2563-70.

52. **Lee, D. Y., C. Teyssier, B. D. Strahl, and M. R. Stallcup.** 2005. Role of protein methylation in regulation of transcription. Endocr Rev **26:**147-70.

53. **Lee, F. Y., H. Lee, M. L. Hubbert, P. A. Edwards, and Y. Zhang.** 2006. FXR, a multipurpose nuclear receptor. Trends Biochem Sci **31:**572-80.

54. **Lee, Y. K., H. Dell, D. H. Dowhan, M. Hadzopoulou-Cladaras, and D. D. Moore.** 2000. The orphan nuclear receptor SHP inhibits hepatocyte nuclear factor 4 and retinoid X receptor transactivation: two mechanisms for repression. Mol Cell Biol **20:**187-95.

55. **Lee, Y. K., and D. D. Moore.** 2002. Dual mechanisms for repression of the monomeric orphan receptor liver receptor homologous protein-1 by the orphan small heterodimer partner. J Biol Chem **277:**2463-7.

56. **Lee, Y. K., K. L. Parker, H. S. Choi, and D. D. Moore.** 1999. Activation of the promoter of the orphan receptor SHP by orphan receptors that bind DNA as monomers. J Biol Chem **274:**20869-73.

57. **Li, Q., M. Herrler, N. Landsberger, N. Kaludov, V. V. Ogryzko, Y. Nakatani, and A. P. Wolffe.** 1998. Xenopus NF-Y pre-sets chromatin to potentiate p300 and acetylation-responsive transcription from the Xenopus hsp70 promoter in vivo. Embo J **17:**6300-15.

58. **Li, T., X. Kong, E. Owsley, E. Ellis, S. Strom, and J. Y. Chiang.** 2006. Insulin regulation of cholesterol 7alpha-hydroxylase expression in human hepatocytes: roles of forkhead box O1 and sterol regulatory element-binding protein 1c. J Biol Chem **281:**28745-54.

59. **Lu, T. T., M. Makishima, J. J. Repa, K. Schoonjans, T. A. Kerr, J. Auwerx, and D. J. Mangelsdorf.** 2000. Molecular basis for feedback regulation of bile acid synthesis by nuclear receptors. Mol Cell **6:**507-15.

60. **Ma, K., P. K. Saha, L. Chan, and D. D. Moore.** 2006. Farnesoid X receptor is essential for normal glucose homeostasis. J Clin Invest **116:**1102-9.

61. **Makishima, M., A. Y. Okamoto, J. J. Repa, H. Tu, R. M. Learned, A. Luk, M. V. Hull, K. D. Lustig, D. J. Mangelsdorf, and B. Shan.** 1999. Identification of a nuclear receptor for bile acids. Science **284:**1362-5.

62. **Malerod, L., M. Sporstol, L. K. Juvet, S. A. Mousavi, T. Gjoen, T. Berg, N. Roos, and W. Eskild.** 2005. Bile acids reduce SR-BI expression in hepatocytes by a pathway involving FXR/RXR, SHP, and LRH-1. Biochem Biophys Res Commun **336:**1096-105.

63. **Maloney, P. R., D. J. Parks, C. D. Haffner, A. M. Fivush, G. Chandra, K. D. Plunket, K. L. Creech, L. B. Moore, J. G. Wilson, M. C. Lewis, S. A. Jones, and T. M. Willson.** 2000. Identification of a chemical tool for the orphan nuclear receptor FXR. J Med Chem **43**:2971-4.

64. **Mangelsdorf, D. J., and R. M. Evans.** 1995. The RXR heterodimers and orphan receptors. Cell **83**:841-50.

65. **Miller, N. E., and P. J. Nestel.** 1974. Triglyceride-lowering effect of chenodeoxycholic acid in patients with endogenous hypertriglyceridaemia. Lancet **2**:929-31.

66. **Mohan, R., and R. A. Heyman.** 2003. Orphan nuclear receptor modulators. Curr Top Med Chem **3**:1637-47.

67. **Myant, N. B., and K. A. Mitropoulos.** 1977. Cholesterol 7 alpha-hydroxylase. J Lipid Res **18**:135-53.

68. **Nitta, M., S. Ku, C. Brown, A. Y. Okamoto, and B. Shan.** 1999. CPF: an orphan nuclear receptor that regulates liver-specific expression of the human cholesterol 7alpha-hydroxylase gene. Proc Natl Acad Sci U S A **96**:6660-5.

69. **Ogryzko, V. V., R. L. Schiltz, V. Russanova, B. H. Howard, and Y. Nakatani.** 1996. The transcriptional coactivators p300 and CBP are histone acetyltransferases. Cell **87**:953-9.

70. **Oiwa, A., T. Kakizawa, T. Miyamoto, K. Yamashita, W. Jiang, T. Takeda, S. Suzuki, and K. Hashizume.** 2007. Synergistic regulation of the mouse orphan nuclear receptor SHP gene promoter by CLOCK-BMAL1 and LRH-1. Biochem Biophys Res Commun **353**:895-901.

71. **Onate, S. A., S. Y. Tsai, M. J. Tsai, and B. W. O'Malley.** 1995. Sequence and characterization of a coactivator for the steroid hormone receptor superfamily. Science **270**:1354-7.

72. **Pineda Torra, I., L. P. Freedman, and M. J. Garabedian.** 2004. Identification of DRIP205 as a coactivator for the Farnesoid X receptor. J Biol Chem **279:**36184-91.

73. **Repa, J. J., and D. J. Mangelsdorf.** 2000. The role of orphan nuclear receptors in the regulation of cholesterol homeostasis. Annu Rev Cell Dev Biol **16:**459-81.

74. **Rizzo, G., B. Renga, E. Antonelli, D. Passeri, R. Pellicciari, and S. Fiorucci.** 2005. The methyl transferase PRMT1 functions as co-activator of farnesoid X receptor (FXR)/9-cis retinoid X receptor and regulates transcription of FXR responsive genes. Mol Pharmacol **68:**551-8.

75. **Russell, D. W.** 2003. The enzymes, regulation, and genetics of bile acid synthesis. Annu Rev Biochem **72:**137-74.

76. **Russell, D. W.** 1999. Nuclear orphan receptors control cholesterol catabolism. Cell **97:**539-42.

77. **Seol, W., H. S. Choi, and D. D. Moore.** 1996. An orphan nuclear hormone receptor that lacks a DNA binding domain and heterodimerizes with other receptors. Science **272:**1336-9.

78. **Sinal, C. J., M. Tohkin, M. Miyata, J. M. Ward, G. Lambert, and F. J. Gonzalez.** 2000. Targeted disruption of the nuclear receptor FXR/BAR impairs bile acid and lipid homeostasis. Cell **102:**731-44.

79. **Sirvent, A., T. Claudel, G. Martin, J. Brozek, V. Kosykh, R. Darteil, D. W. Hum, J. C. Fruchart, and B. Staels.** 2004. The farnesoid X receptor induces very low density lipoprotein receptor gene expression. FEBS Lett **566:**173-7.

80. **Sladek, R., and V. Giguere.** 2000. Orphan nuclear receptors: an emerging family of metabolic regulators. Adv Pharmacol **47:**23-87.

81. **Soutoglou, E., N. Katrakili, and I. Talianidis.** 2000. Acetylation regulates transcription factor activity at multiple levels. Mol Cell **5:**745-51.

82. **Stellwag, E. J., and P. B. Hylemon.** 1976. Purification and characterization of bile salt hydrolase from Bacteroides fragilis subsp. fragilis. Biochim Biophys Acta **452:**165-76.

83. **Strahl, B. D., and C. D. Allis.** 2000. The language of covalent histone modifications. Nature **403:**41-5.

84. **Stroup, D., and J. Y. Chiang.** 2000. HNF4 and COUP-TFII interact to modulate transcription of the cholesterol 7alpha-hydroxylase gene (CYP7A1). J Lipid Res **41:**1-11.

85. **Stroup, D., M. Crestani, and J. Y. Chiang.** 1997. Identification of a bile acid response element in the cholesterol 7 alpha-hydroxylase gene CYP7A. Am J Physiol **273:**G508-17.

86. **Suen, C. S., T. J. Berrodin, R. Mastroeni, B. J. Cheskis, C. R. Lyttle, and D. E. Frail.** 1998. A transcriptional coactivator, steroid receptor coactivator-3, selectively augments steroid receptor transcriptional activity. J Biol Chem **273:**27645-53.

87. **Tachibana, M., K. Sugimoto, T. Fukushima, and Y. Shinkai.** 2001. Set domain-containing protein, G9a, is a novel lysine-preferring mammalian histone methyltransferase with hyperactivity and specific selectivity to lysines 9 and 27 of histone H3. J Biol Chem **276:**25309-17.

88. **Tachibana, M., K. Sugimoto, M. Nozaki, J. Ueda, T. Ohta, M. Ohki, M. Fukuda, N. Takeda, H. Niida, H. Kato, and Y. Shinkai.** 2002. G9a histone methyltransferase plays a dominant role in euchromatic histone H3 lysine 9 methylation and is essential for early embryogenesis. Genes Dev **16:**1779-91.

89. **Tagami, T., L. D. Madison, T. Nagaya, and J. L. Jameson.** 1997. Nuclear receptor corepressors activate rather than suppress basal transcription of genes that are negatively regulated by thyroid hormone. Mol Cell Biol **17:**2642-8.

90. **Urizar, N. L., D. H. Dowhan, and D. D. Moore.** 2000. The farnesoid X-activated receptor mediates bile acid activation of phospholipid transfer protein gene expression. J Biol Chem **275:**39313-7.

91. **Vignali, M., A. H. Hassan, K. E. Neely, and J. L. Workman.** 2000. ATP-dependent chromatin-remodeling complexes. Mol Cell Biol **20:**1899-910..

92. **Watanabe, M., S. M. Houten, L. Wang, A. Moschetta, D. J. Mangelsdorf, R. A. Heyman, D. D. Moore, and J. Auwerx.** 2004. Bile acids lower triglyceride levels via a pathway involving FXR, SHP, and SREBP-1c. J Clin Invest **113:**1408-18.

93. **Wong, J., D. Patterton, A. Imhof, D. Guschin, Y. B. Shi, and A. P. Wolffe.** 1998. Distinct requirements for chromatin assembly in transcriptional repression by thyroid hormone receptor and histone deacetylase. Embo J **17:**520-34.

94. **Yamagata, K., H. Daitoku, Y. Shimamoto, H. Matsuzaki, K. Hirota, J. Ishida, and A. Fukamizu.** 2004. Bile acids regulate gluconeogenic gene expression via small heterodimer partner-mediated repression of hepatocyte nuclear factor 4 and Foxo1. J Biol Chem **279:**23158-65.

95. **Zhang, W., and J. J. Bieker.** 1998. Acetylation and modulation of erythroid Kruppel-like factor (EKLF) activity by interaction with histone acetyltransferases. Proc Natl Acad Sci U S A **95:**9855-60.

96. **Zhang, Y., L. W. Castellani, C. J. Sinal, F. J. Gonzalez, and P. A. Edwards.** 2004. Peroxisome proliferator-activated receptor-gamma coactivator 1alpha (PGC-1alpha) regulates triglyceride metabolism by activation of the nuclear receptor FXR. Genes Dev **18:**157-69.

97. **Zhang, Y., F. Y. Lee, G. Barrera, H. Lee, C. Vales, F. J. Gonzalez, T. M. Willson, and P. A. Edwards.** 2006. Activation of the nuclear receptor FXR improves hyperglycemia and hyperlipidemia in diabetic mice. Proc Natl Acad Sci U S A **103:**1006-11.

98. **Zhang, Y., and D. Reinberg.** 2001. Transcription regulation by histone methylation: interplay between different covalent modifications of the core histone tails. Genes Dev **15**:2343-60.

Chapter Two

Roles of the key metabolic regulator SHP and its cofactor, histone methyltransferase G9a in the regulation of bile acid biosynthesis

Abstract

SHP has been implicated as a pleiotropic regulator of diverse biological functions by its ability to inhibit numerous nuclear receptors. Recently, we reported that SHP inhibits transcription of CYP7A1, a key gene in bile acid biosynthesis, by recruiting HDACs and a Swi/Snf-Brm complex. To further delineate the mechanism of this inhibition, we have examined whether methylation of histones is also involved and whether a functional interplay between chromatin modifying enzymes occurs. Histone methyltransferase, G9a was colocalized with SHP and directly interacted with SHP *in vitro*. G9a, that was coimmunopreciptated with hepatic SHP, methylated lys-9 of histone 3 (H3K9) *in vitro*. Expression of G9a enhanced inhibition of CYP7A1 transcription by SHP, while a catalytically inactive G9a dominant negative (DN) mutant reversed the SHP inhibition. G9a was recruited to and H3K9 was methylated at the CYP7A1 promoter in a SHP-dependent manner in bile acid-treated HepG2 cells. Expression of the G9a-DN mutant inhibited H3K9 methylation, blocked the recruitment of the Brm complex, and partially reversed the CYP7A1 inhibition by bile acids. Inhibition of HDAC activity with trichostatin A (TSA) blocked deacetylation and methylation of H3K9 at the promoter, and conversely, inhibition of H3K9 methylation by G9a-DN partially blocked deacetylation. Hepatic expression of G9a-DN in mice fed cholic acid disrupted bile acid homeostasis, resulting in increased bile acid pools and partial de-repression of Cyp7a1

and Cyp8b1. Our studies establish a role for G9a methyltransferase, histone deacetylases, and the Swi/Snf-Brm complex in the SHP-mediated inhibition of bile acid synthesis via coordinated chromatin modification at target genes.

Introduction

The small heterodimer partner (SHP, NR0B2), an unusual orphan nuclear receptor which lacks a DNA binding domain but contains a putative ligand binding domain, interacts with a number of nuclear receptors including LRH-1, HNF-4, ERR, CAR, LXR, GR, and ER, and inhibits their transcriptional activities (1, 4, 7, 30, 39, 40). Thus, SHP acts as a pleiotropic transcriptional repressor affecting diverse biological functions, including cholesterol and glucose metabolic pathways, energy homeostasis, and reproductive biology (2). SHP has been shown to be a key regulator in the negative feedback regulation of bile acid biosynthesis from cholesterol in the liver (15, 25, 31, 48). Bile acid-activated FXR, upon heterodimerization with RXR, binds to the promoter of the SHP gene and increases transcription (15, 31). The bile acid-induced SHP then suppresses transcription of CYP7A1 and CYP8B1, key hepatic genes involved in the neutral pathway of bile acid biosynthesis, by interacting with LRH-1 and/or HNF-4, which are bound to the promoters of the genes. In addition to regulation of bile acid biosynthesis by SHP, recent studies show that bile acid-induced SHP also inhibits expression of hepatic bile acid transporters, such as, NTCP and BSEP (5, 11, 13). Bile acid homeostasis was disrupted in SHP-null mice, establishing an *in vivo* physiological role of SHP in the regulation of cholesterol/bile acid metabolism (25, 48).

Previous studies showed that SHP interacts with the AF-2 domain of nuclear receptors through the LXXLL motifs in SHP and subsequently inhibits the activity of nuclear receptors by competing with coactivators (20, 21, 29). In addition to this coactivator competition model, it was also proposed that SHP could directly repress the activities of nuclear receptors via its C-terminal intrinsic repression domain, presumably by recruiting corepressors (29, 30). However, the molecular mechanisms underlying the direct suppression of transcription by SHP have not been well defined and the mechanisms of SHP action at target genes in a natural chromatin context are largely unexplored. Recently, we reported that SHP mediates repression by recruiting chromatin modifying enzymes including the mSin3A/HDAC1/2 corepressor and Swi/Snf-Brm chromatin remodeling complexes to the CYP7A1 promoter in HepG2 cells after bile acid treatment, which results in histone deacetylation and chromatin remodeling (24).

Chromatin structure plays a fundamental role in the regulation of eukaryotic gene activity (23, 26, 50). Primary structural units of chromatin are nucleosomes, which suppress transcription by imposing a barrier for access of transcription factors and basal transcriptional machinery to DNA. ATP-dependent chromatin remodeling complexes, such as Swi/Snf, weaken DNA/histone contacts in the core nucleosome, which may disrupt or alter nucleosomal conformation (23, 50). The Swi/Snf complexes contain either of two ATPases, Brm or Brg-1, and variable subunits of Brm or Brg-1 associated factors (BAFs). Brm and Brg-1 preferentially interact with different types of transcription factors and target promoters (22). Recent studies, including ours, show that these Swi/Snf complexes are involved in gene repression as well as activation (24,

51). A second class of chromatin modifying complexes includes enzymes that are involved in covalent modification of core histone tails, such as, acetylation and methylation of lysine (19, 44). While histone acetylation generally correlates with transcriptional activation (19), histone methylation has either negative or positive effects on transcription, depending on the residue methylated and the type of modification (19, 27, 38). Methylation at lys-9 of histone 3 (H3K9) has been correlated with transcriptional silencing in most cases, whereas methylation at lys-4 of histone 3 (H3K4) is associated with gene activation. The mammalian histone methyltransferase, G9a, is responsible for mono- and di-methylation of H3K9 in euchromatin (45). Studies in G9a-null mice showed that euchromatic H3K9 methylation by G9a is essential in early embryogenesis and is critically involved in transcriptional silencing of developmentally regulated genes (46). In contrast, SUV39H1, a heterochromatic histone lysine methyltransferase, directs trimethylation of H3K9 in pericentric heterochromatin and this modification creates a binding motif for the HP1 protein that is directly associated with DNA methylation and gene silencing (27, 43).

Our previous study showed that SHP interacts with HDAC-1, HDAC-2, and mSin3A corepressors and recruits these factors to the CYP7A1 promoter in response to bile acid treatment (24). We further observed that acetylation of histones H3 and H4 in the CYP7A1 promoter was markedly decreased in a SHP-dependent manner after bile acid treatment. Consistent with our observations are recent reports that SHP interacts with HDACs and that its repressive effects are mediated through recruitment of HDACs (14). It was also shown from a recent interesting study that SHP functionally interacts with HDAC-1 and with G9a in cells (6), but a role for G9a in SHP-mediated suppression

of genes involved in hepatic bile acid metabolism has not been demonstrated. Since CYP7A1 and CYP8B1, two key genes in hepatic bile acid biosynthesis, are well-known SHP target genes, we explored whether H3K9 methylation catalyzed by G9a at the promoters of the endogenous CYP7A1 and CYP8B1 genes is critical for SHP-mediated feedback inhibition of the expression of these genes by bile acids. Since HDACs and Brm have been shown to be involved in gene repression by SHP (24), another important question is whether coordinated enzymatic modification of histones by G9a and HDACs and ATP-dependent remodeling by the Swi/Snf-Brm complex at the CYP7A1 promoter are critical for transcriptional silencing mediated by bile acid-induced SHP. We found that H3K9 methylation by G9a and H3K9 deacetylation by HDACs are interdependent and necessary for the recruitment of the Swi/Snf-Brm complex, which is essential for SHP-mediated transcriptional silencing of the CYP7A1 gene. Interestingly, inhibition of hepatic G9a activity in mice by expression of a dominant negative mutant of G9a partially de-repressed Cyp7a1 and Cyp8b1, and resulted in elevated bile acid pools in mice fed cholic acid. Our studies establish a critical role for these chromatin modifying enzymes in the suppression of SHP target genes involved in hepatic bile acid metabolism.

Materials and Methods

Cell culture and HepG2 stable cells

Human hepatoma HepG2 cells (ATCC HB8065) were grown in phenol red-free Dulbecco's modified Eagle's medium/F12 (1:1). Cos-1 and human embryonic cells-derived Ad-293 cells (Cell Biolabs, Inc) were maintained in DMEM media. Media were supplemented with 100 units/ml penicillin G-streptomycin sulfate and 10% heat

inactivated fetal bovine serum. For ChIP and RTPCR experiments, HepG2 cells were seeded, and incubated and treated with 25-50 μM CDCA (Sigma) for 6 hr to18 hr in serum-free media. Because we observed that the response of the HepG2 cells to bile acids was often diminished after long-term culture, new cultures were established every 6-8 weeks from frozen aliquots of our original HepG2 cell culture. In addition, the effect of CDCA on CYP7A1 and SHP mRNA levels was regularly assessed to ensure that the response of the cells to CDCA had not been changed. To construct a HepG2 cell line with the CYP7A1-luc reporter stably incorporated into the genome, a DNA fragment containing human -1887 CYP7A1-luc (8), was inserted into pcDNA3 in which the CMV promoter had been removed. HepG2 cells were transfected with the pcDNA3-CYP7A1-luc plasmid and selected with 800μg/ml of G418 for 2-3 weeks. Drug-resistant colonies were pooled and expanded, and subjected to luciferase assays to ensure that the CYP7A1-luc plasmid was stably incorporated into genome.

Transfection reporter assays

For transient transfections, HepG2 or Cos-1 cells were cotransfected with DNA of the -1887 human CYP7A1-luc reporter (8), Gal4-TATA-luc reporter (29), G4DBD, G4DBD-HNF-4 (130-368) (28), pcDNA3-PGC-1α (3), pcDNA3-SHP (24), pCMV-HNF-4, pcDNA3.1-G9a (16), pEGFP-G9a (36), pcDNA3.1 G9a-DN (16), or pcDNA3.1-HA-SUV39H1 (34) as indicated in the figure legends. Empty vector DNA was added as needed so that the same amounts of CMV expression vector DNA were present in each transfection. Transfection was carried out using lipofectamine 2000 in 24-well plates. Twenty-four hr after transfection, cells were collected and luciferase and ß-galactosidase

activities were determined. Firefly luciferase activities were divided by ß-galactosidase activities to normalize for transfection efficiency. Consistent results were observed in 2-4 independent triplicate transfection assays in each experiment.

Construction of plasmids and adenoviral vectors

Plasmid pGEX4T1-SHP region 1 (amino acids 1-92) was constructed by PCR amplification of mouse SHP using forward and reverse primers which contained BamH1 and Xho1 sites, respectively. The PCR product was digested with BamH1 and Xho1 and inserted into pGEX4T-1 digested with the same enzymes. Recombinant adenoviruses, Ad-si human SHP and Ad-G9a-DN, were constructed with the Ad-Easy system (18) in which the recombinant adenoviruses also express GFP. For the construction of Ad-G9a-DN virus, a Hind III/EcoRV fragment encoding G9a-DN from pcDNA3.1G9a-DN (16) was inserted into Ad-Track CMV shuttle vector. For the construction of Ad-human SHP siRNA, the pSUPER vector containing the siRNA for human SHP (+76 to +94) (24) was digested with EcoR1 and filled-in with the Klenow fragment of *E.coli* DNA polymerase, and further digested with Hind III, and cloned between the EcoRV and Hind III sites of the Ad-Track vector (18). *E. coli* BJ5183 cells, that contain the AdEasy backbone vector, were transformed with the Ad-Track vector DNA that was linearized by Pme1 digestion. Homologous recombination via adenoviral sequences in the shuttle vector and backbone vector in these cells yielded the recombinant adenoviral vectors. The recombinant viral vectors were characterized by Pac1 digestion to ensure that no rearrangement had occurred. Ad-293 cells were transfected with the recombinant adenoviral DNA, and the recombinant virus was then

amplified by several rounds of infection of the Ad-293 cells. The viruses were isolated by $CsCl_2$ step gradient centrifugation as described (18) and dialyzed in PBS/10% Glycerol. Total viral particles were determined by absorbance at A_{260} (1 A_{260} unit is approximately 1 x 10^{12} particles) and the number of active viral particles were determined by measurement of cells expressing GFP by confocal microscopy.

***In vivo* experiments**

BALB/c male mice (8-12 weeks old) were maintained on a 12 hr light and 12 hr dark cycle. For ChIP assays, mice were randomly divided into groups that were fed normal chow or normal chow supplemented with 0.5% cholic acid for indicated times (5 hr to 24 hr). For *in vivo* G9a-DN experiments, mice were injected with about 1 x 10^9 active viral particles in 500µl PBS via the tail vein, and 3 days after infection, the mice were briefly fasted for 5 hr to synchronize feeding and then fed normal or the 0.5% cholic acid-containing chow for 5 hr or 24 hr. Feeding with cholic acid-containing diets was always started at 5:00 P.M. The liver, gall bladder, and entire small intestine were collected for further analyses.

Measurement of total bile acid pool size

Bile acid pools were colorimetrically measured using a diagnostic bile acid analysis kit (Trinity Biotech) as described (48). Briefly, gall bladder, parts of liver directly surrounding the gall bladder, and the entire small intestine were collected for measuring the total pool of bile acids. Samples were homogenized, and bile acids were extracted

in 75% ethanol at 50°C for 2 hr, followed by centrifugation. The bile acid pool size was calculated as μmoles of bile acid per gram of body weight.

Real time RTPCR

Total RNA was isolated from mouse liver or HepG2 cells using Trizol reagent and cDNA was synthesized using a reverse transcriptase kit (Promega Inc.). Real-time RTPCR was performed with an iCycler iQ (Biorad, Inc) following the manufacturer's instructions. The amount of PCR product for each mRNA was normalized by dividing by the amount of ß-actin or 36B4 PCR product. Each real time RTPCR was repeated at least three times with similar reproducible results.

Colocalization study

Cos-1 cells were seeded on cover slips in 6-well plates and cotransfected with expression plasmid DNA for GFP-SHP, G9a, or SUV39H1. Twenty-four hr after transfection, cells were fixed with 2.5% paraformaldehyde and permeabilized with 0.1% Triton X-100. Samples were blocked with 3% BSA for 30 min, incubated with rabbit G9a antibody (1:50) or HA rat monoclonal antibody (Roche Inc., 1:25) for 30 min, washed, and then incubated with Rhodamine-conjugated secondary antibody (1:200) for 30 min. Mounting medium was added and green fluorescence and red immunfluorescence were detected with a Zeiss LSM confocal microscope as before (3, 33).

Coimmunoprecipitation (CoIP) assay

CoIP assays were performed as described with minor modifications (3, 24). Cell extracts or nuclear extracts from HepG2 cells or mouse liver were incubated in lysis buffer (20 mM KOH-Hepes, pH 8.0, 0.2 mM EDTA, 5% glycerol, 250 mM NaCl, 0.5% NP40, 0.25% sodium deoxycholate, 1 mM DTT, and protease inhibitors) with antibodies against G9a or SHP or rabbit IgG at 4° C for 4 hr to overnight and the immune complex was collected by incubation with 30 µl of a 25% slurry of protein A or G agarose for 2 hr. Immunoprecipitates were washed four times with lysis buffer supplemented with NaCl to 400 mM and subjected to western blotting or used in *in vitro* HMT assays.

GST pull down assay

GST-SHP fusion proteins (7) and GST-G9a (621-1000) (45) were expressed in *E. coli* BL21/DE3/RIL (Stratagene, Inc.) and purified by binding to glutathione-Sepharose (Pharmacia, Inc.). ^{35}S-labeled SHP or G9a was synthesized by the *in vitro* TNT system (Promega, Inc.). GST pull down assays were performed as described (3, 24). Briefly, one µg of the GST fusion proteins was incubated with ^{35}S-labeled proteins in incubation buffer (20 mM KOH-Hepes, pH 7.8, 0.1 mM EDTA, 10% glycerol, 100 mM KCl, 0.5% NP40, protease inhibitors, 1 mM DTT) at 4°C for 2 hr. After washing 5 times with incubation buffer, proteins associated with GST fusion proteins were analyzed by SDS-PAGE. Five µg of GST-SHP or GST was incubated with 0.5 mg or 1.4 mg protein of HepG2 and mouse liver nuclear extracts, respectively, in incubation buffer at 4°C for 2 hr. After washing 4 times with incubation buffer (supplemented to 400 mM NaCl and

0.5% NP40), proteins associated with GST-SHP or GST were subjected to western blotting or HMT assays.

Histone methyltansferase (HMT) assays

HMT assays were performed as described with minor modifications (12, 16, 36, 43). Briefly, anti-SHP immunoprecipitates or GST-SHP protein complexes were washed with 1X HMT buffer (50 mM Tris-HCl, pH 8.0) twice and incubated with 2 μg of core histones isolated from HeLa cells or 2 μg of bacterially expressed and purified GST-H3 (1-84) or GST-H3R9 as histone substrates in HMT buffer containing 0.25 μCi of S-adenosyl methyl ^{3}H-methionine at 30°C for 1 hr with occasional gentle mixing. Proteins were separated by SDS-PAGE and visualized by Coomassie blue staining and radioactivity was detected by autoradiography.

Chromatin immunoprecipitation (ChIP) assays in mouse liver and HepG2 cells

ChIP assays in HepG2 cells and in mouse liver were carried out essentially as described (3, 24, 32). Briefly, livers were finely minced and incubated in PBS containing 1% formaldehyde at room temperature for 10 min, and glycine was added to stop the reaction. Cells were resuspended in hypotonic buffer (10 mM KOH-Hepes, pH 7.9, 1.5 mM $MgCl_2$, 10 mM KCl, 0.2% NP40, 0.15 mM spermine, 0.5 mM spermidine, 1 mM EDTA, 5% sucrose) and lysed by homogenization. Nuclei were pelleted and resuspended in sonication buffer (50 mM Tris-HCl, pH 8.0, 2 mM EDTA, 0.85% SDS). The samples were sonicated to reduce DNA length to between 200-1,000 bp. After centrifugation, the chromatin sample was pre-cleared and further immunoprecipitated

with 1-3 μg of antisera at 4°C for overnight. G9a antibody was kindly provided by Y. Nakatani (37, 41) and SHP antibody was described previously (7, 21). Antibodies against acetylated histone H3, diacetylated H3K9/K14, dimethylated H3K9, and HDAC-1 were purchased from Upstate Biotech and antibodies against Brm, BAF170, mSin3A, HDAC-2, HDAC-3, and NcoR1, were purchased from Santa Cruz Biotech. The immune complex was collected and the beads were extensively washed and the bound chromatin was eluted as described (3, 24, 32). Genomic DNA was purified by organic extraction and used as a template for semi-quantitative PCR. The linearity of the PCR reactions was established using different number of cycles and different amounts of template.

For cells infected with adenoviral vectors before ChIP assays in HepG2 cells, confluent cells in 15 cm plates (2×10^7) were infected at a MOI of 10 with adenoviruses, and 24 hr after infection, cells were treated with CDCA or vehicle for indicated times before collection of cells for ChIP assays. For TSA experiments, HepG2 cells were pretreated with 100 nM of TSA for 1 hr before 25 μM of CDCA treatment for 7 hr and cells were then collected for either real time RTPCR or ChIP assay.

Results

G9a is associated with SHP in mouse liver and HepG2 cells

SHP recruited HDAC-containing corepressor complexes to the native CYP7A1 promoter, which resulted in histone deacetylation and transcriptional repression after bile acid treatment (24). Since histone methylation as well as deacetylation are functionally correlated with gene repression (19, 27, 44), we examined if G9a and SUV39H1,

euchromatic and heterochromatic histone lysine methyltransferases, respectively (27), colocalize with SHP in the nucleus. Cos-1 cells were cotransfected with expression plasmid DNA for either G9a or SUV39H1 and GFP-SHP. SHP was detected by GFP fluorescence and G9a or SUV39H1 was detected by immunofluorescence in cells imaged by confocal microscopy. Staining of G9a (Fig. 1A) and SUV39H1 (Fig. 1B) was localized diffusely in the nucleus with patches of higher intensity. SHP was present in both the cytoplasm and nucleus with bright punctuated fluorescence as well as more diffuse patches of increased fluorescence. In 80% of the cells observed, the positions of the brighter patches of fluorescence of GFP-SHP overlapped patches of increased staining of G9a, but not that of SUV39H1, consistent with colocalization of SHP and G9a in the nucleus.

Next, we examined if G9a associates with SHP in mouse hepatocytes *in vivo* and human hepatoma HepG2 cells. Nuclear extracts from mouse liver and HepG2 cells were incubated with either GST-SHP or GST bound to glutathione-Sepharose. After washing the beads, the bound proteins were analyzed by western blotting. G9a was pulled-down from both extracts by GST-SHP, but not by GST (Fig.1C). In addition, interaction between endogenous SHP and G9a in HepG2 cells was examined by co-immunoprecipitation. HepG2 nuclear extracts were immunoprecipitated with antisera against SHP, G9a, or control IgG, and the immunoprecipitates were analyzed by western blotting. G9a was detected in the anti-SHP immunoprecipitates and conversely, SHP was detected in the anti-G9a immunopreciptiates (Fig. 1D). These results indicate that endogenous SHP interacts directly, or indirectly within a complex, with endogenous G9a in hepatic cells.

To test if G9a can directly interact with SHP, GST fusions with SHP or fragments of SHP (Fig.1E) that had been bound to glutathione-Sepharose were incubated with ^{35}S-labeled G9a. G9a bound to SHP or SHP mutants containing the N-terminal domain (1-92 amino acids), whereas no binding was detected with SHP mutants lacking this region (Fig.1F). In parallel experiments (not shown), the C-terminal domain (amino acids160-260) of SHP was required for its interaction with mSin3A and Brm as previously reported (24). To examine if the C-terminal catalytic SET (Su (*var*), Enhancer of *Zeste*, Trithorax) domain of G9a was sufficient for interaction with SHP, a GST-G9a C-terminal fragment containing amino acids 621-1000 (Fig.1G) was bound to the glutathionine-Sepharose and incubated with ^{35}S-labeled SHP. The GST-G9a C-terminal fragment efficiently interacted with SHP (Fig. 1H). These results indicate that the N-terminus of SHP is required for direct interaction with G9a and that the C-terminal SET domain of G9a is sufficient for direct interaction with SHP *in vitro*.

G9a coimmunoprecitated with SHP methylates H3K9 *in vitro*

If the G9a associated with SHP is functionally active, then, histone methyltransferase activity (HMT) should be detected in the protein complex immunoprecipitated by SHP antisera. SHP-containing protein complexes from mouse liver or HepG2 nuclear extracts were obtained by immunoprecipitation with SHP antibody or by binding to GST-SHP and used in *in vitro* HMT assays. Histone H3 was methylated in reactions containing proteins pulled down by GST-SHP from nuclear extracts of mouse liver or HepG2 cells while proteins pulled down by GST did not exhibit HMT activity (Fig. 2A). Further, western blotting with antibody specific for dimethyl H3K9 revealed that the

methylation of histone H3 in the HMT reaction included methylation at K9 (Fig. 2B). Histone H3 was also methylated in reactions containing anti-SHP immunopreciptiates from HepG2 nuclear extracts, but not in reactions containing immunoprecipitates with control IgG (Fig. 2C). Since G9a is pulled down by GST-SHP (Fig. 1) and specifically catalyzes K9 methylation of histone H3 (45), these results are consistent with the conclusion that the H3K9 methylation was catalyzed by G9a. To directly determine whether the G9a in the SHP complex catalyzes H3K9 methylation, we utilized a catalytically inactive G9a dominant negative mutant (G9a-DN) in HepG2 cells. The G9a-DN contains two amino acid substitutions within the catalytic SET domain and efficiently blocked activity of wild type G9a in the PRD-BF1-mediated inhibition of the interferon ß gene (16). The G9a-DN interacted as efficiently as wild type with the N-terminus of GST-SHP in GST pull down assays (not shown). HepG2 cells were infected with adenoviral vector encoding G9a-DN (Ad-G9a-DN) or control empty vector (Ad-empty) and the cells were further subjected to real-time RTPCR, western blotting, or coimmunoprecipitation followed by *in vitro* HMT assays (Fig. 2D). The adenoviral vectors express green fluorescence protein (GFP) and GFP fluorescence was detected in over 90% of cells by confocal microscopy (not shown).

RTPCR and western blotting revealed that mRNA and protein levels of total G9a (endogenous G9a and G9a-DN) were substantially increased in HepG2 cells infected with Ad-G9a-DN (Fig. 2E). HMT activity in anti-SHP or control IgG immunoprecipitates of extracts from the HepG2 cells infected with Ad-empty or Ad-G9a-DN was analyzed using purified GST-H3 (1-84) as the substrate. Methylation of GST-H3 was observed with the anti-SHP immunoprecipitates of extracts from cells infected

with Ad-empty. However, methylation of GST-H3 was not observed in the anti-SHP immunoprecipitates from cells infected with Ad-G9a-DN (Fig. 2F), which indicates that G9a is responsible for the observed methylation of GST-H3. To provide further evidence that the residue methylated was Lys-9, purified GST-H3R9, in which Lys-9 is mutated to Arg, was added as substrate in the reactions. GST-H3R9 was not methylated in reactions containing anti-SHP immunoprecipitates from cells infected with either Ad-empty or Ad-G9a-DN (Fig. 2F). Control IgG immunoprecipitates did not show any HMT activity (Fig. 2F). These results provide evidence that G9a is present in a hepatic SHP complex and is catalytically active for methylation of H3K9.

G9a increases inhibition of CYP7A1 transcription by SHP

HNF-4 and its coactivator PGC-1α transactivate the CYP7A1 promoter and are well-known targets of SHP inhibition (4, 10, 24, 29, 42). Therefore, we determined whether exogenously expressed G9a increases the inhibition of HNF-4/ PGC-1α activation by SHP using a Gal4 reporter system in transfected Cos-1 cells. Expression of PGC-1α dramatically increased HNF-4 transactivation and increasing amounts of SHP progressively suppressed the HNF-4/PGC-1α activation (Fig. 3A, lanes 4-7). Transfection of increasing amounts G9a expression plasmid with a constant amount of SHP plasmid increased inhibition of the HNF-4/ PGC-1α activation in a dose-dependent manner (Fig. 3A, lanes 8-11, Fig. 3B, lanes 3,4). In contrast, expression of the heterochromatic histone methyltransferase, SUV39H1, did not enhance SHP-mediated inhibition, but slightly increased transcription (Fig. 3B, lanes 5, 6). These results are

consistent with our observations that G9a, but not SUV39H1, colocalized with SHP in Cos-1 cells and that G9a is present in SHP-containing complexes (Fig. 1).

To test if G9a inhibition of HNF-4/PGC-1α activation is dependent on SHP, G9a was expressed in transfected Cos-1 cells with or without expression of SHP. In the absence of exogenous SHP, G9a had little effect on the HNF-4/PGC-1α transactivation (Fig. 3C, lanes 6-8) while increasing inhibition was observed with SHP (lanes 3-5), suggesting that SHP is required for the inhibitory effect of G9a. We also tested if G9a enhances SHP inhibition of HNF-4-mediated transactivation of the natural CYP7A1 promoter rather than the Gal4 reporter used above. Exogenous expression of SHP inhibited HNF-4 transactivation of CYP7A1 promoter activity and cotransfection of increasing amounts of G9a vector potentiated the SHP inhibition in a dose-dependent manner in Cos-1 cells while expression of G9a in the absence of SHP had much lesser effects (Fig. 3D). Transfection of increasing amounts of G9a also potentiated the inhibition of CYP7A1 promoter activity by exogenously expressed SHP in HepG2 cells (not shown). These functional reporter studies suggest that G9a cooperatively enhances inhibition of CYP7A1 transcription with SHP.

Overexpression of G9a-DN reverses CYP7A1 inhibition in bile acid-treated HepG2 cells

It has been shown that bile acid treatment results in the induction of SHP, which inhibits expression of CYP7A1 in HepG2 cells and in animals *in vivo* (8, 9, 15, 24, 31). To evaluate the role of G9a in the suppression of the CYP7A1 promoter activity mediated by bile acid-induced SHP, HepG2 cells, in which CYP7A1 promoter-luciferase reporter plasmid DNA is stably incorporated into the genome, were infected with either Ad-empty

or Ad-G9a-DN and 2 days later, cells were treated with 25 or 50 μM of a primary bile acid, chenodeoxycholic acid (CDCA) and reporter activity was measured. Luciferase activity was inhibited about 30% and 40% by 25 and 50 μM CDCA treatment, respectively, (Fig. 3E, lanes, 1, 2, 5) and infection with the increasing amounts of Ad-G9a-DN completely reversed the inhibition (lanes, 3, 4, 6, 7). We further tested if expression of G9a-DN reversed the SHP-mediated inhibition of endogenous CYP7A1 gene expression after bile acid treatment. HepG2 cells were infected with Ad-empty or Ad-G9a-DN, and 2 days after infection, cells were treated with 25 μM of CDCA. Levels of the endogenous CYP7A1 mRNA in HepG2 cells were measured by quantitative real time RTPCR. After CDCA treatment, CYP7A1 mRNA levels were decreased about 50% and infection of HepG2 cells with Ad-G9a-DN completely reversed the decrease (Fig. 3F). These results indicate that G9a is involved in SHP-mediated suppression of endogenous CYP7A1 expression, most likely, by catalyzing H3K9 methylation at the native promoter in bile acid-treated HepG2 cells.

G9a is recruited to the endogenous CYP7A1 and CYP8B1 promoters and H3K9 is methylated in mice fed cholic acid and in bile acid-treated HepG2 cells

If the interaction of G9a with SHP is physiologically relevant for bile acid metabolism, then G9a should be recruited to the transcriptionally suppressed promoters of the SHP target genes, Cyp7a1 and Cyp8b1, in mice fed cholic acid. In mice fed chow containing 0.5% cholic acid for 24 hr, SHP mRNA levels were increased, whereas Cyp7a1 and Cyp8b1 mRNA levels were substantially decreased as determined by real time RTPCR (Fig. 4A). In mice fed cholic acid, increased association of SHP with the promoters of

the hepatic Cyp7a1 and Cyp8b1 genes was detected by chromatin immunoprecipitation (ChIP) assays compared to mice fed normal chow (Fig. 4B, C). In addition, increased association of G9a was observed in these mice (Fig. 4B, C). These results indicate that both SHP and G9a are recruited to these promoters in response to increased bile acid levels which is consistent with a functional interaction between SHP and G9a.

We previously reported that bile acid treatment resulted in a decrease in the acetylation of H3 and H4 at the human CYP7A1 promoter in HepG2 cells but did not determine whether H3K9 was the modified residue (24). Further, since the recruitment of G9a to the Cyp7a1 and Cyp8b1 promoters was increased after bile acid treatment and methylation of H3K9 has been inversely correlated with acetylation at H3K9 and H3K14 (27, 41, 43), it seemed likely that methylation of H3K9 should also increase. Therefore, these histone modifications were examined by ChIP assay using antisera specific for either dimethyl H3K9 or diacetyl H3K9/K14. In mice fed cholic acid, Cyp7a1 and Cyp8b1 promoter sequences precipitated by antisera against diacetyl H3 K9/K14 were substantially decreased, while the promoter sequences precipitated by antisera against dimethyl H3K9 were markedly increased (Fig. 4B, C). The control GAPDH coding region was not precipitated by any of the antisera. These results indicate that H3K9 at the Cyp7a1 and Cyp8b1 promoters is deacetylated and then methylated in livers of mice fed cholic acid.

We also examined the effects of treatment of HepG2 cells with CDCA. CDCA treatment markedly increased SHP mRNA levels and decreased CYP7A1 mRNA levels in HepG2 cells (Fig. 4D). ChIP assays showed that CDCA treatment increased recruitment of SHP and G9a, decreased H3K9 acetylation, and increased H3K9

methylation at the promoters of CYP7A1 and CYP8B1 (Fig. 4E, F), which is consistent with the studies above on mice fed cholic acid (Fig. 4B, C). These studies in vivo in mice fed cholic acid and in bile acid-treated HepG2 cells establish that endogenous SHP and G9a are recruited to the transcriptionally repressed native CYP7A1 and CYP8B1 promoters. Consistent with this recruitment, and that of HDACs observed previously (24), H3K9 at the native CYP7A1 and CYP8B1 promoters is deacetylated and methylated.

G9a recruitment and subsequent H3K9 methylation after bile acid treatment is dependent on SHP expression

To determine if SHP is directly involved in the recruitment of G9a and subsequent H3K9 methylation at the native CYP7A1 promoter after bile acid treatment, HepG2 cells were either transiently transfected with pSuper-siSHP (24) or infected with adenoviral vector encoding human SHP siRNA (Ad-siSHP). Treatment of HepG2 cells with CDCA increased and decreased mRNA levels of SHP and CYP7A1, respectively (Fig. 5A). Transient transfection of SHP siRNA vectors significantly reversed the changes in mRNA for SHP and CYP7A1 after CDCA treatment which is consistent with previous studies (24).

As determined by ChIP assay, SHP was recruited to the native CYP7A1 promoter by CDCA treatment but the recruitment was decreased in cells transiently transfected with pSuper-siSHP or infected with Ad-siSHP and association of G9a with the promoter was also reduced in these cells (Fig. 5B, C). The state of histone methylation and acetylation was examined in the adenoviral infected cells. The

decrease in histone acetylation and increase in methylation at H3K9 observed after bile acid treatment were markedly reversed in the cells infected with Ad-siSHP (Fig. 5C). These results suggest that recruitment of G9a to the native CYP7A1 promoter and subsequent H3K9 methylation are contingent on expression of bile acid-induced SHP. These results, together with in vitro protein interaction studies (Fig. 1), suggest that G9a is recruited by SHP to CYP7A1 promoter after bile acid treatment, probably by direct interaction with SHP.

Blocking the H3K9 methylation by G9a-DN partially inhibits histone deacetylation at the CYP7A1 promoter chromatin

Methylated H3K9 by G9a could serve as a binding platform to recruit SHP-associated chromatin modifying complexes for transcriptional silencing. For example, it has been suggested that H3K9 methylation affects deacetylation by enhancing recruitment and/or activity of HDACs and by inhibiting the association and/or the activity of HATs (41, 43, 44). Therefore, to test if inhibition of H3K9 methylation at the CYP7A1 promoter affects deacetylation at H3K9, HepG2 cells were infected with either Ad-G9a-DN or Ad-empty, treated with CDCA, and analyzed by ChIP assays using antibodies against either dimethylated H3K9 or diacetylated H3K9/K14. In addition, the infected cells were subjected to real time RTPCR to analyze effects of G9a-DN on CYP7A1 expression. After CDCA treatment, CYP7A1 mRNA levels were decreased about 70% and infection of HepG2 cells with Ad-G9a-DN partially but significantly reversed the decrease (Fig. 6A).

CYP7A1 promoter chromatin precipitated with the dimethylated H3K9 antibody was increased after CDCA treatment in cells infected with Ad-empty (Fig. 6B,

C), as expected from ChIP studies with uninfected cells (Fig. 4, 5). However, in CDCA-treated HepG2 cells infected with Ad-G9a-DN, methylation was reduced about 50% (Fig. 6B, C). The control GAPDH coding region was not precipitated by any of the antisera (not shown). These results indicate that increased dimethylation of H3K9 at the native CYP7A1 promoter after CDCA treatment is dependent on G9a activity.

CYP7A1 promoter sequence precipitated with diacetylated H3K9/K14 antibody was reduced about 80% after CDCA treatment in cells infected with Ad-empty (Fig. 6B, C) as expected from studies with uninfected cells (Fig. 4, 5). However, the amount of precipitated promoter DNA was markedly increased about 2-fold in CDCA-treated cells infected with Ad-G9a-DN compared to cells infected with Ad-empty although this increase was just short of statistical significance (Fig. 6B, C). These results indicate that inhibition of the endogenous G9a by G9a-DN inhibited H3K9 methylation as expected, but also partially blocked diacetylation of H3K9. These results are consistent with the idea that acetylation of H3K9 is decreased after CDCA treatment even if methylation is blocked by recruitment of HDACs and possibly dissociation of HATs. Methylation by G9a may block re-acetylation of H3K9, resulting in nearly complete deacetylation.

In bile acid-treated HepG2 cells, Ad-G9a-DN blocks recruitment of the Swi/Snf-Brm complex, but not of HDAC-containing corepressor complexes, to the CYP7A1 promoter

Since blocking methylation partially reversed deacetylation, it is possible that methylation is required for recruitment of chromatin modifying complexes, such as

HDAC corepressor and the Swi/Snf-Brm chromatin remodeling complexes to the native CYP7A1 promoter. To examine this question, HepG2 cells were infected with either Ad-G9a-DN or Ad-empty, treated with CDCA, and subjected to ChIP assays using antibodies against mSin3A, HDAC-1, HDAC-2, NcoR1, HDAC-3, BAF170, or Brm. CYP7A1 promoter sequences precipitated with antibodies against all these cofactors were increased in HepG2 cells infected with Ad-empty after CDCA treatment, indicating that corepressor mSin3A/HDAC-1/2, corepressor NcoR1/HDAC3, and the Swi/Snf-Brm remodeling complexes are recruited after CDCA treatment (Fig. 6D, E) as previously shown (24). CYP7A1 promoter sequences precipitated with antibodies against mSin3A, HDAC-1, HDAC-2, NcoR1, or HDAC-3, were not reduced in HepG2 cells infected with Ad-G9a-DN, suggesting that recruitment of these corepressor complexes is not dependent on dimethylation at H3K9 even though deacetylation is partially blocked. The amounts of the CYP7A1 promoter sequence precipitated with antibodies against Brm or BAF 170 were reduced about 50% in cells infected with Ad-G9a-DN (Fig. 6D, E). These results suggest that G9a is critical for the inhibitory SHP action by catalyzing dimethylation of H3K9, which prevents reversible acetylation thereby "locking" H3K9 in a deacetylated state and is prerequisite for recruitment of the Brm complex, which in turn catalyzes chromatin remodeling, ultimately resulting in transcriptional silencing of the CYP7A1 gene.

Inhibition of HDAC activity by TSA blocks H3K9 methylation but not recruitment of G9a to the CYP7A1 promoter

Histone deacetylation and methylation are coordinated events and are functionally associated with gene silencing (19, 27). H3K9 deacetylation is required in order for methylation to occur at H3K9, but it is not clear whether deacetylation is required for the recruitment of the G9a methyltransferase. To examine this question, the effect of TSA, an inhibitor of HDAC activity, on bile acid-induced chromatin modification and G9a recruitment in HepG2 cells was examined. First, to examine the functional correlation between histone deacetylation and methylation, Cos-1 cells were cotransfected with a Gal4-TATA-luc reporter and expression plasmids for Gal4DBD-HNF-4, PGC-1α, SHP, and G9a and the transfected cells were treated with increasing amounts of TSA. Expression of SHP reduced transactivation mediated by HNF-4/ PGC-1α and coexpression of G9a further enhanced the SHP inhibitory activity (Fig. 7A, lanes, 1-3). Increasing amounts of TSA completely reversed the inhibitory effects of SHP and G9a on the reporter activity in a dose-dependent manner (lanes, 4-7).

To assess the effects of TSA on bile acid regulation of endogenous CYP7A1 expression, cells were pretreated with TSA and then additionally treated with CDCA. Treatment with CDCA suppressed CYP7A1 mRNA levels by about 50% (Fig. 7B). Treatment with TSA resulted in a complete reversal of the decreased in CYP7A1 mRNA levels, indicating that histone deacetylation is important for the suppression of CYP7A1 expression by bile acids.

In ChIP assays under the same experimental conditions described in Fig. 7B, addition of TSA reversed the decrease in diacetylation and the increase in dimethylation

at H3K9 after bile acid treatment (Fig. 7C, D). Interestingly, TSA treatment did not reduce the amount of CYP7A1 promoter sequence precipitated by G9a antibody in the bile acid-treated cells, indicating that G9a recruitment to the promoter was not dependent on deacetylation (Fig. 7C, D). In contrast, the control GAPDH coding region was not precipitated by any of the antisera (not shown). This result is consistent with the studies above indicating that both HDACs and G9a are recruited to the CYP7A1 promoter by bile acid-induced SHP.

Results from ChIP assays and these functional reporter assays suggest that histone deacetylation by HDACs at H3K9 is required for dimethylation by G9a and conversely, dimethylation by G9a is important in HDAC-mediated deacetylation and transcription suppression. These results further suggest that recruitment and activity of chromatin modifying cofactors including G9a and HDACs are coordinated and inter-dependent events in the transcriptional silencing of CYP7A1 mediated by bile acid-induced SHP.

Acute liver-specific inhibition of G9a disrupts bile acid homeostasis and partially reverses suppression of Cyp7a1 and Cyp8b1 genes in mice in vivo

To determine the *in vivo* significance of G9a in the SHP-mediated negative feedback inhibition of hepatic bile acid metabolism, the activity of G9a in mouse liver was inhibited by the expression of G9a-DN. Mice were injected with Ad-G9a-DN or Ad-empty virus via the tail vein. Three days later, mice were fed either normal or 0.5% cholic acid-supplemented chow for 5 hr or 24 hr and then the liver, gall bladder, and small intestine were collected for further analyses. Expression of G9a-DN in the liver was

confirmed by western blotting and similar infection efficiencies of over 80% between experimental groups were observed based on GFP expression (not shown).

First, to ensure that G9a-DN expressed in mouse liver blocked endogenous G9a activity, liver extracts were prepared from mice infected with Ad-G9a-DN or Ad-empty virus and immunoprecipitated with SHP antibody or control IgG. Then, the immunoprecipitates were incubated with purified GST-H3 (1-84) or GST-H3R9 mutant as histone substrates in an *in vitro* HMT assay. The control IgG immunoprecipitates did not show any HMT activity (Fig. 8A). In contrast, hepatic SHP complex immunoprecipitated from mice infected with Ad-empty methylated GST-H3 (1-84), whereas the complex from mice infected with Ad-G9aDN did not methylate GST-H3 (1-84) (Fig. 8A) consistent with the results obtained with HepG2 cells (Fig. 2F). These results indicate that overexpression of G9a-DN inhibited H3K9 methylation by blocking endogenous G9a activity present in the hepatic SHP complex.

To determine if blocking hepatic G9a activity by G9a-DN affects bile acid homeostasis, we measured the total bile acid pool size in mice infected with either Ad-empty or Ad-G9a-DN. Bile acid pools in these two groups were similar when fed with normal chow (Fig. 8B). In contrast, the total bile acid pools were slightly elevated in mice fed cholic acid for 5 hr and significantly increased by 2-fold after 24 hr in mice infected with Ad-G9a-DN compared to those infected with Ad-empty (Fig. 8B).

To better understand the molecular basis of elevated bile acid pools in mice expressing G9a-DN, we examined effects of G9a-DN on the mRNA levels of the SHP target genes in bile acid biosynthesis, Cyp7a1 and Cyp8b1. As expected, in uninfected mice fed 0.5% cholic acid-supplemented chow, the levels of mRNA for Cyp7a1 and

Cyp8b1 were decreased about 50% after 5 hr of feeding (Fig. 8C) and about 80% after 24 hr of feeding (Fig. 8D). In mice infected with Ad-empty, similar effects were observed although the inhibition at 5 hr was greater than in the uninfected controls (Fig. 8C, D). Interestingly, at 5 hr, suppression of Cyp7a1 in the Ad-G9a-DN mice fed cholic acid was significantly reversed compared to the Ad-empty group, while at 24 hr of cholic acid feeding, a modest nonsignificant reversal was observed (Fig. 8C, D). Compared to regulation of Cyp7a1, suppression of Cyp8b1 was modestly, but significantly, reversed in the Ad-G9a-DN mice after 5 hr of feeding, although the difference was not significant at 24 hr (Fig. 8C, D). SHP mRNA levels, as expected, were increased after bile acid feeding in all groups at 5 hr and more dramatically at 24 hr (Fig. 8C, D). Compared to the Ad-empty mice, SHP mRNA levels in the Ad-G9a-DN mice after cholic acid feeding was slightly reduced, but the changes were not statistically significant. These results indicate that inhibition of endogenous G9a activity by G9a-DN elevated the total bile acid pool size which in part may be caused by transient reversal of suppression of Cyp7a1 and Cyp8b1 expression by bile acid feeding.

These *in vivo* animal studies, along with the studies in HepG2 cells and *in vitro* mechanistic studies, establish a physiological role of G9a as a key downstream cofactor of the bile acid-activated SHP pathway resulting in acute transcriptional suppression of Cyp7a1 and Cyp8b1 genes.

Discussion

In this paper we present evidence that G9a plays a critical role in the SHP-mediated suppression of hepatic bile acid biosynthesis, by catalyzing H3K9 methylation at the

CYP7A1 and CYP8B1 promoters which is required for recruiting the Swi/Snf-Brm complex and transcriptional silencing. Our major findings to support this conclusion are as follows: endogenous G9a was associated with SHP in mouse liver and HepG2 cells, and G9a in hepatic SHP complexes methylated H3K9 *in vitro*. SHP and G9a were recruited to the native CYP7A1 and CYP8B1 promoters after bile acid treatment and recruitment of G9a and subsequent H3K9 methylation were impaired if SHP expression was reduced by siRNA, indicating that SHP is required for G9a recruitment. G9a expression enhanced the inhibition of CYP7A1 transcription by SHP which was correlated with the methylation of H3K9 by G9a. Inhibition of G9a activity by expression of G9a-DN in HepG2 cells inhibited H3K9 methylation after bile acid treatment and partially reversed bile acid-mediated suppression of the endogenous CYP7A1 gene expression. Interestingly, expression of G9a-DN also partially reversed deacetylation of H3K9 and blocked recruitment of the Brm complex to the promoter, indicating that deacetylation and methylation were required for recruitment of the Brm complex and ultimately for transcriptional silencing. Acute liver-specific inhibition of G9a by G9a-DN elevated the total bile acid pool size in mice fed cholic acid and partially de-repressed Cyp7a1 and Cyp8b1, indicating bile acid homeostasis was disrupted. These results establish a critical role for G9a in the SHP-mediated suppression of Cyp7a1 and Cyp8b1 in cholesterol/bile acid metabolism.

From chromatin immunoprecipitation studies in mouse liver and in HepG2 cells, we observed that SHP was recruited to the native CYP7A1 promoter in mice fed cholic acid and CDCA-treated HepG2 cells (Fig. 4). Acetylation of histones H3 and H4 and specific acetylation of H3K9 were markedly decreased and H3K9 methylation was

substantially increased after feeding mice cholic acid or treating HepG2 cells with bile acids, consistent with recruitment of HDACs and G9a. Consistent with our observations, a recent study showed that SHP was detected at the Cyp7a1, as well as Cyp8b1, promoter in transgenic mice expressing SHP in the liver at levels equivalent to those observed after feeding cholic acid (5). Interestingly, chromatin changes at these two promoters differed in that study. In contrast to our observations, HDACs and changes in histone acetylation and methylation were not detected at the Cyp7a1 promoter in the transgenic mice, while in parallel to our studies, histone acetylation was decreased and H3K9 methylation was increased at the Cyp8b1 promoter. This discrepancy for Cyp7a1 may result from the length of time that SHP was elevated in the two systems. Our studies were done in a transient acute setting to assess direct effect of bile acids on the association of regulatory proteins with the native promoters, whereas in the transgenic animal model, high levels of SHP were sustained continuously in the liver, which may lead to secondary effects that affect regulation of Cyp7a1 expression, but not that of Cyp8b1. Differential responses to different lengths of cholic acid feeding were also observed in our *in vivo* study. Suppression of Cyp7a1 was substantially reversed in the Ad-G9a-DN mice after 5 hr of cholic acid feeding compared to the control Ad-empty mice, while the reversal was very modest at 24 hr. Suppression of Cyp8b1 was only modestly reversed at both time points suggesting that regulation of these two genes is not identical which has also been observed with long cholic acid feeding times in SHP-null mice (47). These results imply that at longer times of cholic acid feeding, the influence of the FXR/SHP pathway on Cyp7a1 regulation may decrease and SHP-independent pathways may become predominant. This interpretation is consistent with the trends

observed in previous SHP-null mice studies in which Cyp7a1 was still mostly repressed after 1 week of cholic acid feeding, whereas it was almost completely reversed 1 day after cholic acid feeding. These studies were interpreted to suggest that the FXR/SHP pathway was more important acutely after cholic acid feeding (25, 47-49). In our studies, however, at 24 hr after cholic acid feeding, the reversal of Cyp7a1 expression was already largely lost. One interpretation of this result is that the role of G9a is even more transient than that of SHP/FXR in the suppression of Cyp7a1. A second is that inactivation of G9a will have effects on the activity of multiple transcription factors, in addition to SHP, which might have indirect effects on Cyp7a1 expression not observed in the SHP-null mice. Nevertheless these data are consistent with an important role for G9a in the acute regulation of Cyp7a1 *in vivo*. This is consistent with an increase in bile acid pools although other factors probably also contribute to the increased pool size.

H3K9 methyltransferase enzymes can be recruited to the target promoters by direct interaction with gene-specific DNA binding proteins or with non-DNA binding corepressors. For instance, G9a has been shown to interact with PRD-BF1, CtBP, CDP/cut, Gfi1, and SHP and is mainly responsible for silencing of target genes in the euchromatin region (6, 12, 16, 36, 43). SHP was also shown to be localized exclusively with nuclease-sensitive euchromatin and not with the heterochromatic DNA binding protein HP1 (6). Consistent with these findings, we observed that SHP and the euchromatic methyltransferase, G9a, but not the heterochromatic methyltransferase, SUV39H1, were colocalized in the nucleus (Fig. 1). Further, inhibition of CYP7A1 transcription by SHP was increased by expression of G9a, but not by expression of SUV39H1 (Fig. 3). Interestingly, SHP, like other inhibitory factors, interacts with G9a

and corepressor HDACs through distinct domains, its N-terminal and C-terminal domains, respectively (6, 24). These results suggest that SHP could recruit both HDAC-containing corepressor complexes and G9a to the native CYP7A1 promoter simultaneously.

Although the role of H3K9 methylation by G9a has been established in epigenetic gene silencing, little is known about how this enzyme is recruited and coordinately works with other chromatin modifying cofactors at the native target promoters. Inhibition of SHP expression by siRNA in HepG2 cells demonstrated that G9a recruitment to the CYP7A1 promoter and subsequent H3K9 methylation is contingent on SHP expression (Fig. 5). Since we, and others (6), have shown that SHP can interact with G9a, the simplest conclusion from these SHP siRNA studies is that G9a recruitment is mediated by a direct interaction with SHP. The siRNA data, however, do not eliminate the possibility that G9a is recruited indirectly by another SHP-dependent protein. Inhibition of H3K9 deacetylation by a specific HDAC inhibitor, TSA, inhibited the H3K9 methylation at the promoter chromatin, but interestingly, did not inhibit recruitment of G9a (Fig. 7). The recruitment of G9a alone, therefore, was not sufficient for methylation at H3K9 but required previous deacetylation at H3K9. Functional reporter assays showed that G9a increased SHP inhibition of transactivation mediated by HNF-4/PGC-1α, but these effects were blocked by TSA. These results suggest a central role of histone deacetylation in mediating the transcriptional repression either directly, or indirectly, by permitting G9a-mediated methylation. Coordinated sequential modification of deacetylation and methylation of H3K9 have been shown in other systems as well, for example, the CtBP corepressor complex in oncogenesis (41), Gfi1 in

the regulation of development and oncogenesis (12), PRDI-BF1 in interferon ß gene transcription (16), and HP1 recruitment for gene silencing (34, 43).

Conversely, H3K9 deacetylation at the CYP7A1 promoter after bile acid treatment was markedly affected by inhibition of H3K9 methylation by G9a-DN, whereas the recruitment of HDACs-containing corepressor complexes was not affected (Fig. 7). Methylation appears to be required to "lock" the H3K9 in a deacetylated state and prevent reversible acetylation rather than for recruitment of HDACs. Interestingly, deacetylation and methylation at H3K9 are required for recruitment of the Brm remodeling complex during transcriptional silencing of CYP7A1 (Fig. 6). Therefore, these results collectively suggest that recruitment and activity of chromatin modifying cofactors are temporally coordinated sequential events in SHP-mediated repression of CYP7A1.

Based on the *in vitro*, *in vivo* and cell culture results, we propose a model for SHP-mediated active suppression of CYP7A1 transcription (Fig. 9). As proposed earlier (20, 21, 29), bile acid-induced SHP may compete with coactivator HATs, including p300, CBP, and SRC-1, for binding at the target promoters initially. SHP then directly interacts with HDAC-containing mSin3A and NcoR1 corepressor complexes and G9a methyltransferase through its C-and N-terminus, respectively, recruiting these factors to the promoter, which results in deacetylation and subsequent dimethylation. Deacetylation of H3K9 is required for methylation and conversely, methylation of H3K9 is also required to prevent reversal of the deacetylation. H3K9 methylation and deacetylation create a binding surface for the Swi/Snf-Brm complex which allows the SHP-dependent recruitment of this remodeling complex to the CYP7A1 promoter. The

Swi/Snf complex then catalyzes the ATP-dependent remodeling of the promoter chromatin as demonstrated previously (24), which establishes a transcriptionally suppressed chromatin structure. These coordinated biochemical and enzymatic events at the native CYP7A1 promoter help convert the chromatin from an active to a repressed state which underlies the feedback inhibition of bile acid synthesis by SHP.

In the present and previous studies, we demonstrated that chromatin modifying enzymes, such as histone deacetylases, G9a histone methyltransferase, and Swi/Snf-Brm, are critical downstream cofactors in mediating SHP activity in the regulation of hepatic cholesterol/bile acid metabolism (24). Abnormal SHP function has been implicated in metabolic disorders such as hypercholesterolemia, cholestasis, obesity, and diabetes (2). Interestingly, heterozygous mutations of the SHP gene in humans are associated with a predisposition for moderate obesity and diabetes (35). Therefore, it will be interesting to test whether these naturally occurring SHP mutants show an impaired ability to recruit these chromatin modifying enzymes to target genes. Aberrant regulation of histone methylation and deacetylation is now emerging as a major contributor to carcinogenesis, and molecules that affect epigenetic regulation, such as HDAC inhibitors, are now actively being tested as therapeutic agents (17). In this regard, modulation of SHP function by targeting these chromatin modifying enzymes may help lead to new pharmacological agents for metabolic disorders.

Acknowledgments

We are grateful to Drs. Y. Nakatani and B. Vogelstein for generously providing the G9a antibody and Ad-Easy system, respectively. We thank Drs. K. Wright, C. Mizzen, M.

Horwitz, M. Walsh, J. Chiang, Yoon-Kwang Lee, M. Ananthanarayanan, M. Evans, Y. Shinkai, J. Auwerx, T. Kuzarides, and I. Talianidis for kindly providing plasmids and reagents for this study.

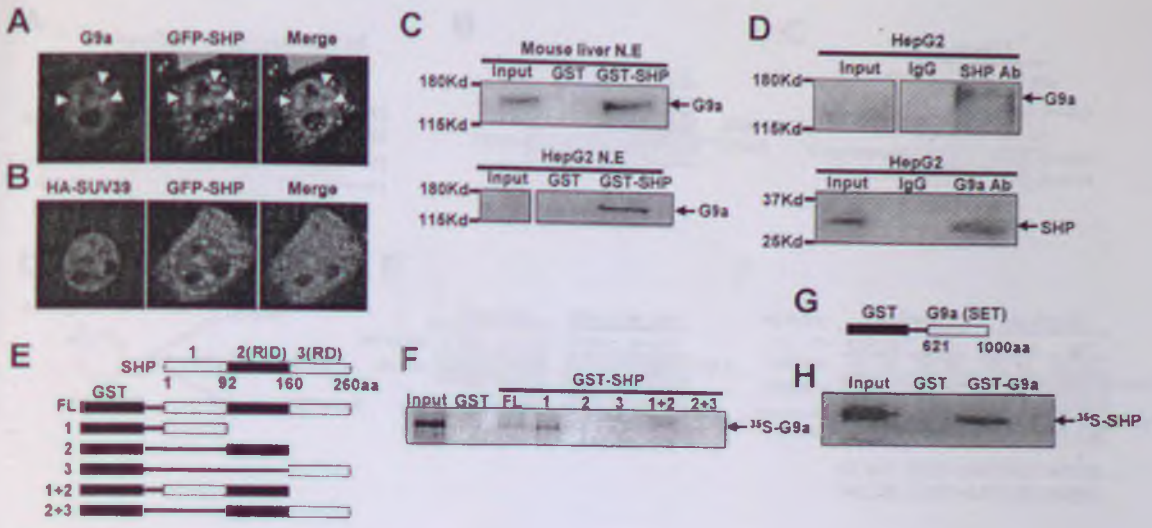

Fig. 1. G9a associates with SHP in mouse liver and HepG2 cells. (A, B) SHP and G9a (A), but not SUV39H1 (B), colocalize in the nucleus. Cos-1 cells were cotransfected with expression plasmid DNA for GFP-SHP and either G9a or HA-SUV39H1. SHP was detected by GFP fluorescence (green) and G9a and SUV39H1 were detected by immunofluorescence using Rhodamine-conjugated secondary Ab (red) as described in Materials and Methods. Representative confocal microscopic images for G9a or SUV39H1 immunofluorescence (left), green fluorescent images for GFP-SHP (center), and merged images (right) are shown. The yellow regions in the merged images indicate colocalization of G9a and SHP. (C) Nuclear extracts were prepared from mouse liver or HepG2 cells and incubated with GST or GST-SHP. The GST proteins were bound to glutathionine-Sepharose, and after washing, proteins associated with the GST proteins were detected by SDS-PAGE and western blotting using G9a antibody. The position of G9a is indicated and positions of molecular weight markers are indicated at the left. The input contains 10% of the amount of extract used in the binding reactions. (D). Nuclear extracts prepared from HepG2 cells were immunoprecipitated using IgG as a control or with antibody against SHP or G9a and association of endogenous G9a or SHP in the immunoprecipitates was detected by SDS-PAGE and western blotting using G9a or SHP antibodies, respectively. The diffuse bands for G9a compared to those in (C) result from the large amount of protein from the precipitating antibody in the sample which reduces the resolution of the bands. (E). Schematic diagrams of SHP and full length (FL) GST-SHP, and GST-SHP deletion mutants. RID and RD refer to receptor interacting and intrinsic repression domains, respectively. (F). ^{35}S-G9a was synthesized in vitro, and GST pull down assays were performed as described in Materials and Methods. The input represents 20% of the ^{35}S-labeled G9a used in the binding reactions. The position of G9a is indicated. (G). A schematic diagram of the GST-G9a deletion mutant (621-1000). SET indicates a domain common to Su (*var*), Enhancer of *Zeste*, and Trithorax. (H). ^{35}S-SHP was synthesized and GST pull down assays were performed as described in F. The input represents 20% of the ^{35}S-labeled SHP used in the reactions.

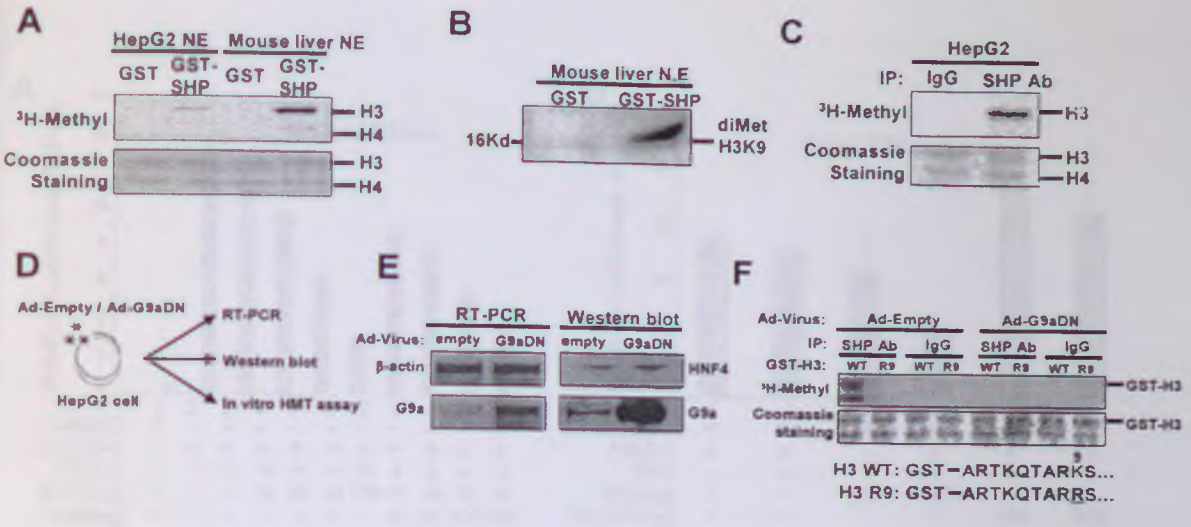

Fig. 2. G9a in SHP-containing complexes methylates H3K9 in vitro. (A). Nuclear extracts from HepG2 cells or mouse liver were incubated with bacterially expressed, purified GST-SHP or GST that had been bound to glutathione-Sepharose. The proteins associated with GST-SHP or GST were used as the source of enzyme in in vitro HMT assays. Proteins were separated by SDS-PAGE, followed by Coomassie staining (lower panel) of the gels and autoradiography (upper panel). The positions of histones H3 and H4 are indicated. (B). Mouse liver nuclear extracts were incubated with bacterially expressed, purified GST-SHP or GST that had been bound to glutathione-Sepharose. The proteins associated with the Sepharose beads were used as the source of enzyme in HMT assays. After the reaction, proteins were separated by SDS-PAGE and dimethylated H3K9 histones were detected by western blotting using dimethylated H3K9 antibody. The position of a molecular weight marker is shown at the left. The position of H3 (dimethyl H3K9) is indicated at the right. (C). HepG2 nuclear extracts were immunprecipitated with either SHP antibody or control IgG and the immunoprecipitates were used as the source of enzyme in HMT assays. The proteins were separated by SDS-PAGE and then by Coomassie staining of the gels to detect the amounts of core histone substrate used in the assay (lower panel), followed by autoradiography to detect ^{3}H-labeled histones (upper panel). The position of histones H3 and H4 are indicated. (D-F). (D). Experimental outlines: HepG2 cells were infected with control empty adenoviral vector (Ad-empty) or adenoviral vector encoding G9a-DN (Ad-G9a-DN) and 36 hr later, the infected cells were subjected to semi-quantitative RTPCR, western blotting (E) or immunoprecipitation followed by in vitro HMT assays (F). (E). Cell extracts were subjected to western blotting using G9a antibody and HNF-4 antibody as a control. (F). Cell extracts were immunoprecipitated with SHP antibody or control IgG, and the immunopreciptates were used as the source of enzyme in in vitro HMT assays. Bacterially-expressed and purified GST-H3 (1-84) (WT) or a GST-H3 mutant (H3R9) in which K9 is mutated to Arg as shown was used as histone substrates. The HMT reaction samples were analyzed as described in A.

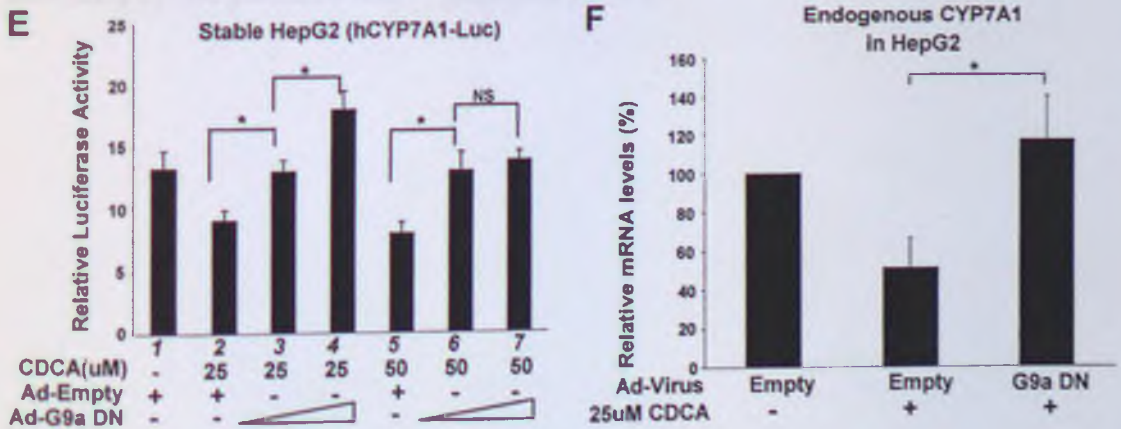
E
Stable HepG2 (hCYP7A1-Luc)
Relative Luciferase Activity
25
20
15
10
5
0
*
*
*
NS
1 2 3 4 5 6 7
CDCA(uM) - 25 25 25 50 50 50
Ad-Empty + + - - + - -
Ad-G9a DN - - - - - - -
F
Endogenous CYP7A1
In HepG2
Relative mRNA levels (%)
160
140
120
100
80
60
40
20
0
*
Ad-Virus Empty Empty G9a DN
25uM CDCA - + +

Fig. 3, cont.

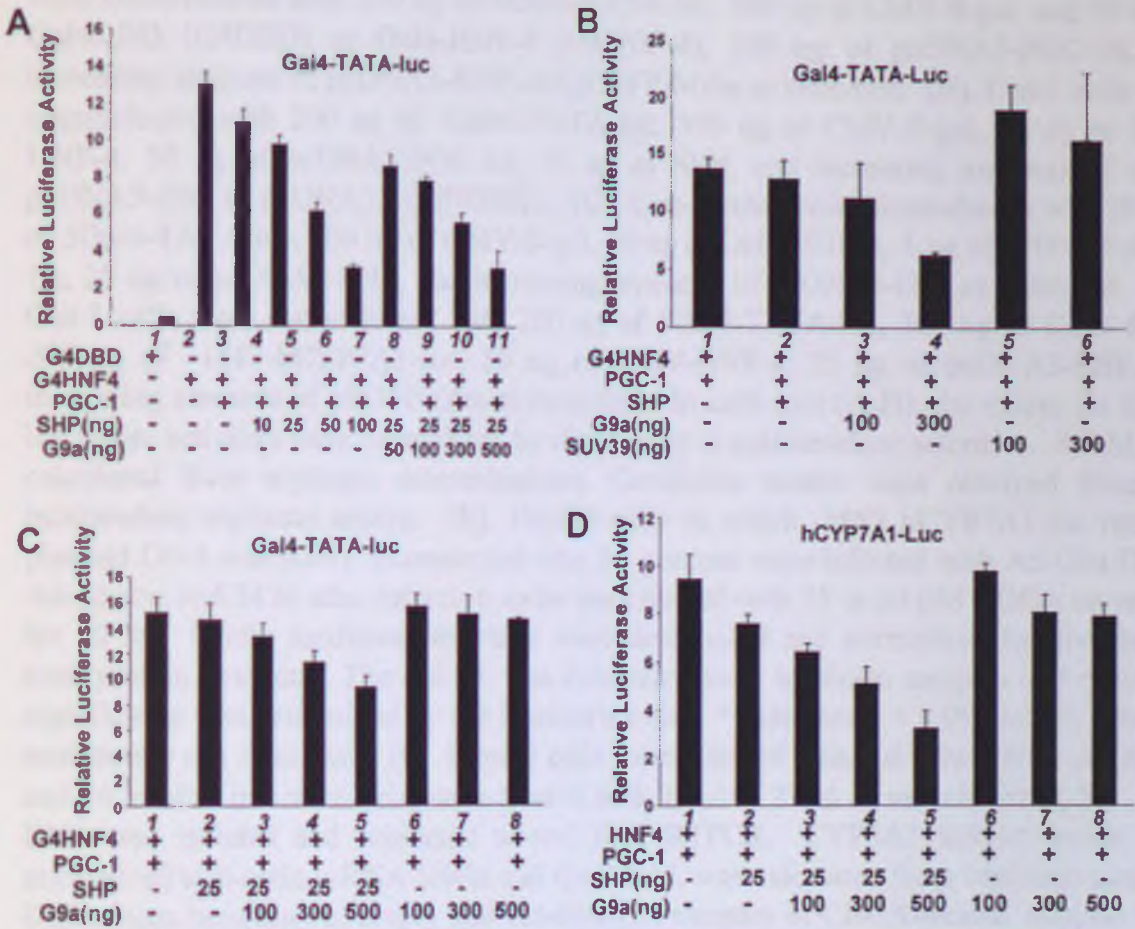
A
Gal4-TATA-luc
Relative Luciferase Activity
1 2 3 4 5 6 7 8 9 10 11
G4DBD + - - - - - - - - - -
G4HNF4 - + + + + + + + + + +
PGC-1 - - + + + + + + + + +
SHP(ng) - - - 10 25 50 100 25 25 25 25
G9a(ng) - - - - - - - 50 100 300 500
B
Gal4-TATA-Luc
Relative Luciferase Activity
1 2 3 4 5 6
G4HNF4 + + + + + +
PGC-1 + + + + + +
SHP - + + + + +
G9a(ng) - - 100 300 - -
SUV39(ng) - - - - 100 300
C
Gal4-TATA-luc
Relative Luciferase Activity
1 2 3 4 5 6 7 8
G4HNF4 + + + + + + + +
PGC-1 + + + + + + + +
SHP - 25 25 25 25 - - -
G9a(ng) - - 100 300 500 100 300 500
D
hCYP7A1-Luc
Relative Luciferase Activity
1 2 3 4 5 6 7 8
HNF4 + + + + + + + +
PGC-1 + + + + + + + +
SHP(ng) - 25 25 25 25 - - -
G9a(ng) - - 100 300 500 100 300 500

Fig. 3, cont. G9a enhances SHP inhibition of CYP7A1 transcription. (A). Cos-1 cells were cotransfected with 200 ng of 5Gal4-TATA-luc, 300 ng of CMV-ß-gal, and 50 ng of Gal4DBD (G4DBD) or Gal4-HNF-4 (G4HNF-4), 100 ng of pcDNA3-PGC-1α, and increasing amounts of pcDNA3-SHP and pEGFP-hG9a as indicated. (B). Cos-1 cells were cotransfected with 200 ng of 5Gal4-TATA-luc, 300 ng of CMV-ß-gal, 50 ng of Gal4-HNF-4, 50 ng of pcDNA3-PGC-1α, 25 ng of SHP, and increasing amounts of either pcDNA3-G9a or pcDNA3.1-SUV39H1. (C). Cos-1 cells were cotransfected with 200 ng of 5Gal4-TATA-luc, 300 ng of CMV-ß-gal, 10 ng of Gal4-HNF-4, 5 ng of pcDNA3-PGC-1α, 25 ng of pcDNA3-SHP, and increasing amounts of pcDNA3-G9a as indicated. (D). Cos-1 cells were cotransfected with 200 ng of 5Gal4-TATA-luc, 300 ng of CMV-ß-gal, 200 ng of –1887-hCYP7A1-luc, 50 ng of CMV-HNF-4, 25 ng of pcDNA3-SHP, and increasing amounts of pEGFP-G9a as indicated. In each case (A-D), the values for firefly luciferase activities were normalized by dividing by ß-galactosidase activities. S.E.M. was calculated from triplicate determinations. Consistent results were obtained from 2-4 independent triplicate assays. (E). HepG2 cells in which -1887 hCYP7A1-luc reporter plasmid DNA was stably incorporated into the genome were infected with Ad-G9a-DN or Ad-empty, and 24 hr after infection, cells were treated with 25 or 50 μM CDCA or vehicle for 10 hr. Firefly luciferase activities were determined and normalized by dividing by total protein amounts. The S.E.M. was calculated from triplicate samples and statistical significance was determined by the Student's t-test. * indicates $p < 0.05$ and NS refers to statistically not significant. (F). HepG2 cells were infected with Ad-G9a-DN or Ad-empty and 24 hr after infection, cells were treated with 25 μM CDCA or vehicle for 10 hr. Total RNA was isolated and subjected to real time RTPCR. CYP7A1 mRNA levels were normalized to ß-actin mRNA levels and the S.E.M. was calculated from triplicate samples. Differences between Ad-empty and Ad-G9a-DN samples in CDCA-treated samples were analyzed by the Student t-test. * indicates $p < 0.05$.

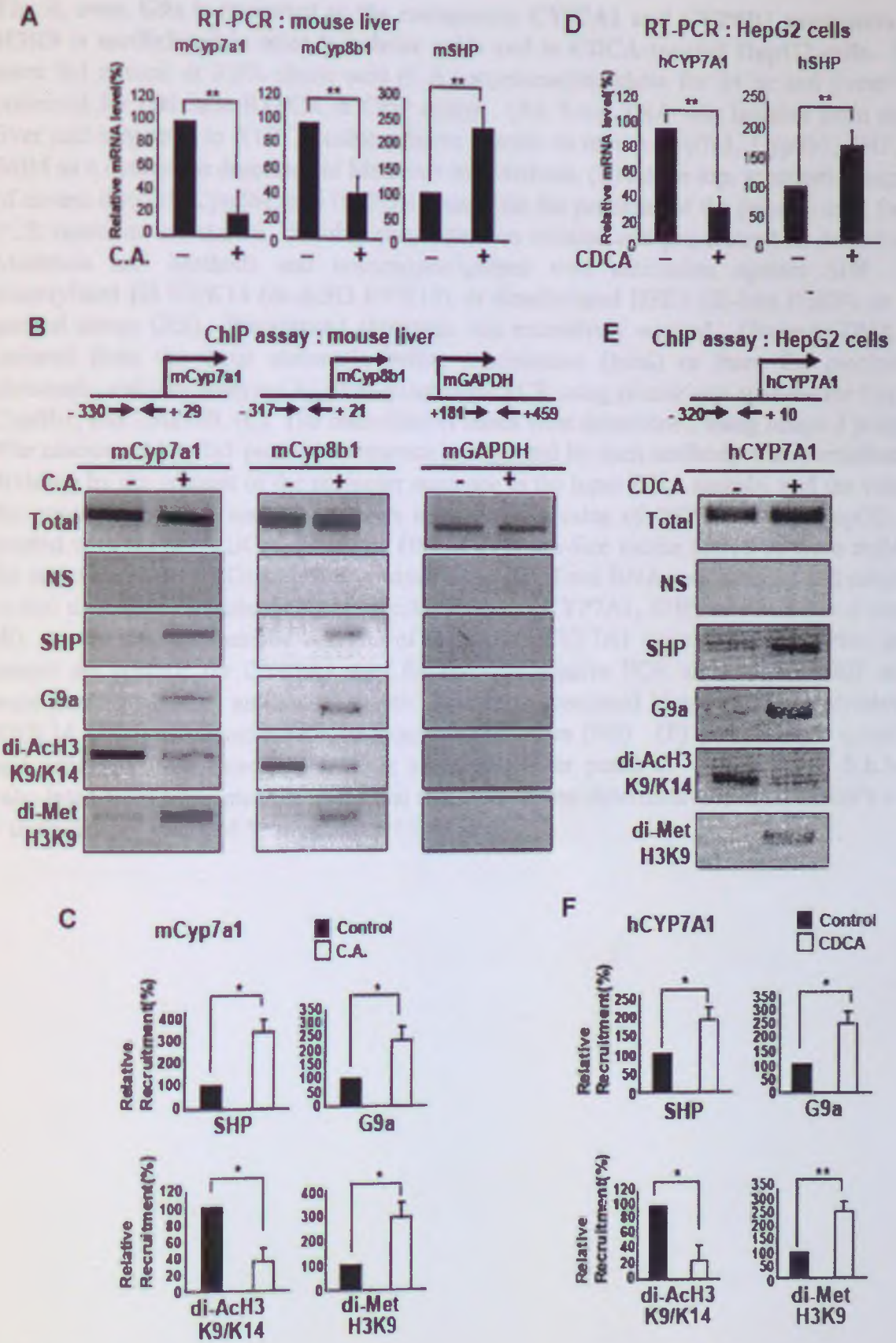
A
RT-PCR : mouse liver
mCyp7a1
mCyp8b1
mSHP
Relative mRNA level(%)
C.A.
D
RT-PCR : HepG2 cells
hCYP7A1
hSHP
CDCA
B
ChIP assay : mouse liver
mCyp7a1
mCyp8b1
mGAPDH
-330 +29
-317 +21
+181 +459
C.A.
Total
NS
SHP
G9a
di-AcH3 K9/K14
di-Met H3K9
E
ChIP assay : HepG2 cells
hCYP7A1
-320 +10
CDCA
C
Control
C.A.
Relative Recruitment(%)
SHP
G9a
di-AcH3 K9/K14
di-Met H3K9
F
Control
CDCA

Fig. 4, cont.

Fig. 4, cont. G9a is recruited to the endogenous CYP7A1 and CYP8B1 promoters and H3K9 is methylated in mice fed cholic acids and in CDCA-treated HepG2 cells. Mice were fed normal or 0.5% cholic acid (C.A.)-supplemented chow for 24 hr and livers were collected for real time RTPCR or ChIP assays. (A). Total RNA was isolated from mouse liver and subjected to RTPCR using primers specific to mouse Cyp7a1, Cyp8b1, SHP, and 36B4 as a control, as described in Materials and Methods. (B) At the top, schematic diagrams of mouse Cyp7a1, Cyp8b1, and GAPDH genes with the positions of the primers used for the PCR reactions are shown. Soluble chromatin was isolated and pre-cleared as described in Materials and Methods and immunoprecipitated with antibodies against SHP, G9a, diacetylated H3 K9/K14 (di-AcH3 K9/K14), or dimethylated H3K9 (di-Met H3K9), or with normal serum (NS). Precipitated chromatin was extensively washed. Genomic DNA was isolated from the input chromatin before precipitation (total) or from the precipitated chromatin and was analyzed by semi-quantitative PCR using primer sets specific for Cyp7a1, Cyp8b1, and GAPDH. (C) The intensities of bands were determined using Image J program. The amount of Cyp7a1 promoter sequence precipitated by each antibody was normalized by dividing by the amount of the promoter sequence in the input DNA sample, and the value in the control group for each factor were assigned as a value of 100%. (D-F). HepG2 cells treated with 50 μM CDCA or vehicle DMSO in serum-free media for 18 hr were collected for real time RTPCR (D) and ChIP assays (E,F). (D). Total RNA was isolated and subjected to real time RTPCR using primers specific to human CYP7A1, SHP, and 36B4 as a control. (E). At the top, a schematic diagram of the human CYP7A1 gene and the position of the primer set specific for CYP7A1 used for semi-quantitative PCR are shown. ChIP assays were performed using antibodies against SHP, G9a, acetylated histone H3, diacetylated H3 K9/K14, or dimethylated H3K9, or using normal serum (NS). (F) Results were quantified and analyzed from three experiments as described for panel C. (A-F). The S.E.M. is calculated from triplicates and statistical significance was determined by the Student's t-test. * indicates $p < 0.05$ and ** indicates $p < 0.01$.

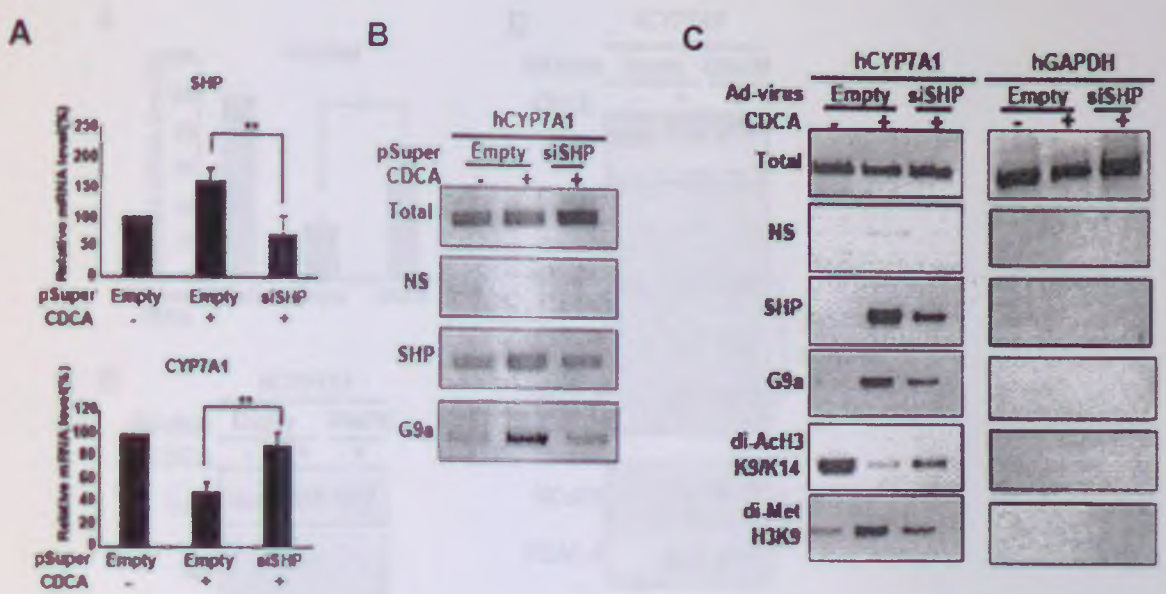

Fig. 5. G9a recruitment to the CYP7A1 promoter and subsequent H3K9 methylation after bile acid treatment is dependent on SHP expression. (A,B). HepG2 cells were transiently transfected with either pSUPER or pSUPER siSHP and treated with 50 μM CDCA for 18 hr. (A). Levels of mRNA were determined by real-time RTPCR relative to 36B4 mRNA levels. The S.E.M. was calculated from triplicate samples and statistical significance was determined by the Student's t-test. ** indicates $p < 0.01$. (B) ChIP assays were performed using antibodies against SHP and G9a. Precipitated chromatin was extensively washed and analyzed as described in the legend to Fig. 4E. (C). HepG2 cells were infected with Ad-empty or Ad-siSHP and treated with 50 μM CDCA or vehicle for 18 hr. Cells were then collected for ChIP assays using antibodies against SHP, G9a, diacetylated H3K9/K14, or dimethylated H3K9, or using normal serum (NS). Precipitated chromatin was extensively washed and analyzed as described in the legend to Fig. 4E.

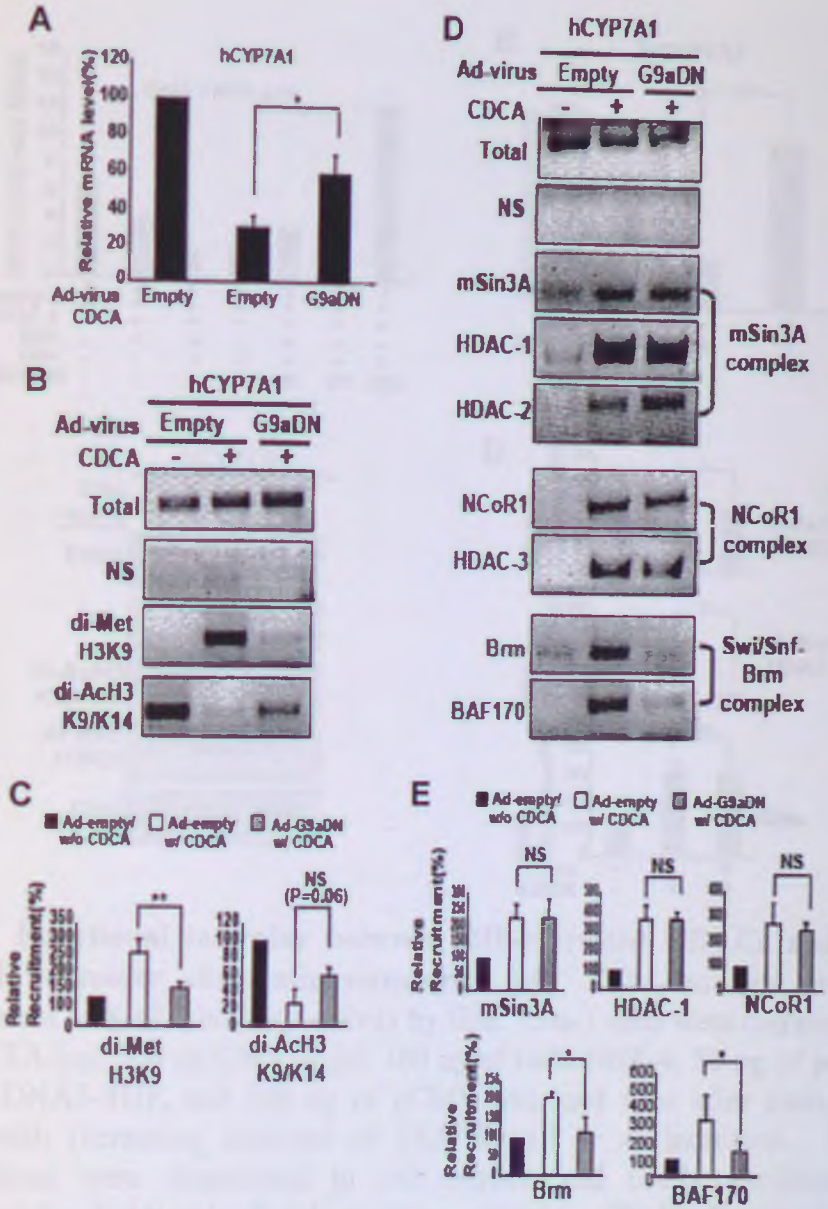

Fig. 6. Expression of the G9a-DN mutant inhibits H3K9 deacetylation as well as methylation and blocks recruitment of the Swi/Snf-Brm complex to the CYP7A1 promoter in CDCA-treated HepG2 cells. HepG2 cells were infected at a MOI of 10 with either Ad-G9a-DN or Ad-empty and 24 hr after infection, cells were treated with 50 μM CDCA or vehicle for 18 hr. (A). The mRNA levels of CYP7A1 were measured by real time PCR. (B, D) The infected cells were immunoprecipitated using antibodies against dimethylated H3K9, or diacetylated H3K9/K14, antibodies against Brm, BAF170, mSin3A, HDAC-1, HDAC-2, NcoR1, or HDAC-3 and normal serum (NS) as described in the legend to Fig 4E. Precipitated chromatin was extensively washed and isolated DNA was analyzed by semi-quantitative PCR using primer sets specific for human CYP7A1 as described in the legend to Fig 4E. (C, E) The intensities of bands in three independent experiments were determined using Image J program and analyzed as described in Fig 4C. (A-E). The S.E.M for triplicate determinations is shown and the statistical significance was determined by the Student's t-test. * indicates $p < 0.05$, ** indicates $p < 0.01$, and NS refers to statistically not significant.

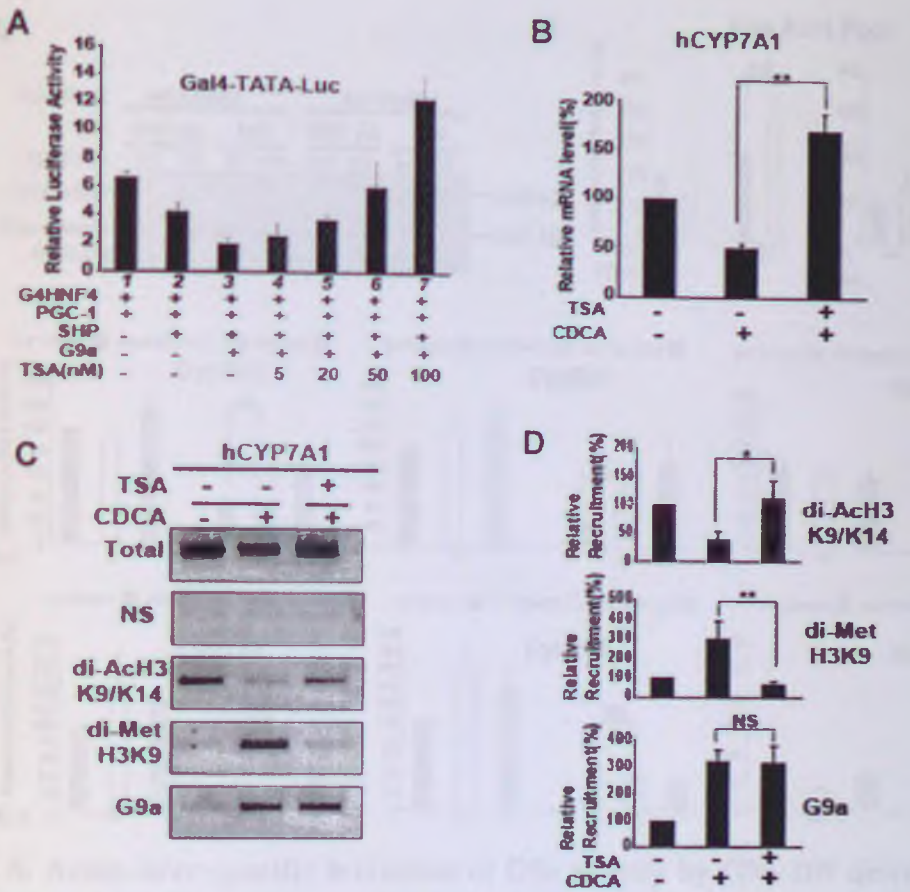

Fig. 7. Functional interplay between SHP-recruited HDACs and G9a in altering CYP7A1 promoter chromatin structure. (A). TSA treatment completely reversed enhancement of SHP inhibitory activity by G9a. Cos-1 cells were cotransfected with 200 ng Gal4-TATA-luc, 300 ng CMV-β-gal, 100 ng of Gal4-HNF-4, 50 ng of pcDNA3-PGC-1, 25 ng of pcDNA3-SHP, and 500 ng of pCMV-G9a, and 6 hr after transfection, cells were treated with increasing amounts of TSA for 16 hr as indicated. Luciferase and β-galactosidase were determined in cell extracts and firefly luciferase activities were normalized by dividing by β-galactosidase activities. (B, C). Deacetylation at H3K9 is a prerequisite for G9a-mediated methylation. HepG2 cells were pretreated with 100 nM of TSA and 1 hr later, cells were additionally treated with 25 μM CDCA or vehicle for 7 hr. (B). CYP7A1 mRNA levels were measured by real time RTPCR. (C). Cells were collected for ChIP assays using antibodies against diacetylated H3K9/K14, dimethylated H3K9, or G9a, or using normal serum (NS). (D) The intensities of bands were determined by Image J program and analyzed as described in Fig 4C. (B-D). The S.E.M. from triplicate determinations is shown and statistical significance was determined by the Student's t-test. * indicates $p < 0.05$ and ** indicates $p < 0.01$. NS indicates statistically not significant.

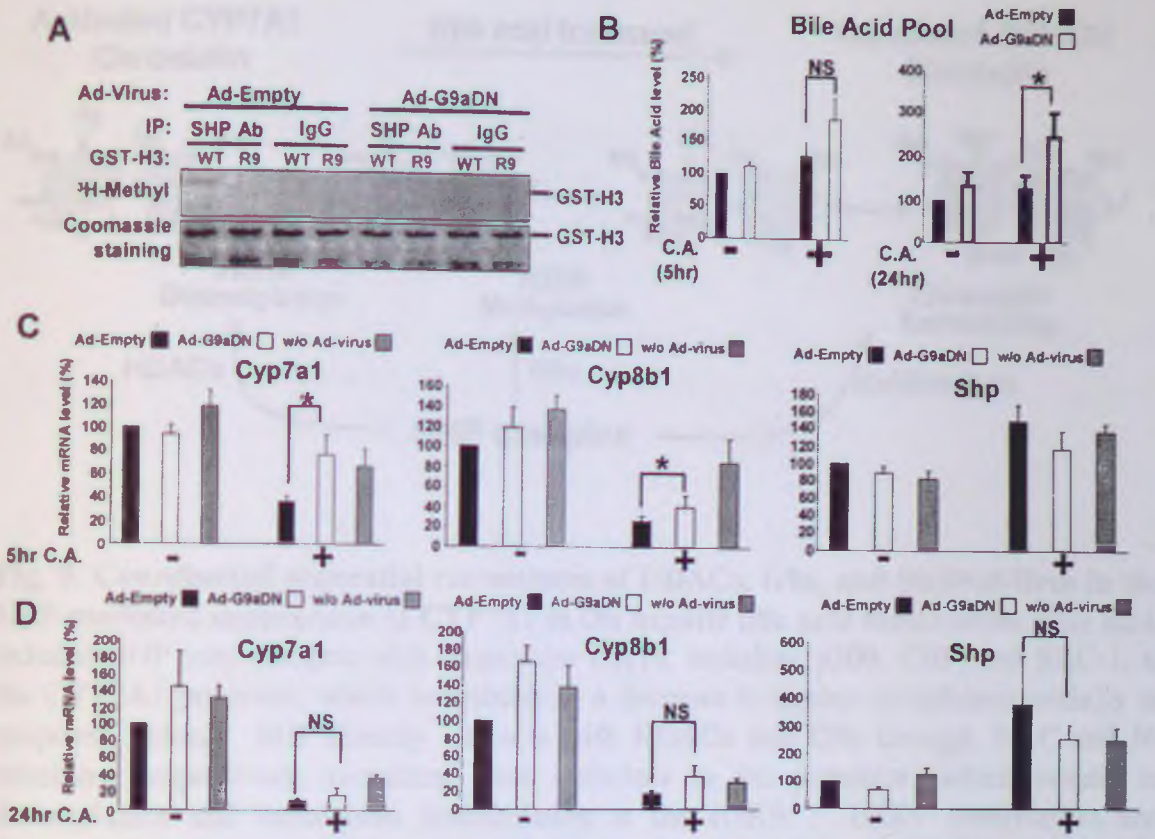

Fig. 8. Acute liver-specific inhibition of G9a activity by G9a-DN disrupted bile acid homeostasis and de-represses Cyp7a1 and Cyp8b1 in mice fed cholic acid. About 1 x 10^9 active viral particles (Ad-G9a-DN or Ad-empty) were injected into a mouse tail vein, and 3 days after infection, mice were fed normal or 0.5% cholic acid-containing chow for 5 hr or 24 hr. Liver, gall bladder, and small intestine were collected for further analyses. (A). Liver nuclear extracts were prepared from 3 mice for each group infected with Ad-empty or Ad-G9a-DN and immunoprecipitated with SHP antibody or control IgG. The immunopreciptates were used as the source of enzyme in in vitro HMT assays. GST-H3 (1-84) (WT) or GST-H3 mutant (H3R9) was used as histone substrates. The HMT reaction samples were analyzed as described in the legend to Fig. 2A. (B). Total bile acid pool size was measured from bile acid levels in gall bladder, liver, and the entire small intestine in mice fed normal or 0.5% cholic acid-supplemented chow for 5 hr or 24 hr. Total bile acid pool size was determined as described in Materials and Methods. The S.E.M. from samples from 3 mice are shown. * indicates $p < 0.05$ and NS refers to statistically not significant. (C, D). Mice were infected with either Ad-G9a-DN or Ad-empty and 3 days later, mice were fed normal or 0.5% cholic acid-containing chow for 5 hr (C) or 24 hr (D). As a control, normal uninfected mice were also analyzed in parallel. Total RNA was isolated from liver and subjected to quantitative real time RTPCR using primer sets specific for Cyp7a1, Cyp8b1, and SHP, and the amounts of PCR product was divided by the amount of 36B4 PCR product. The S.E.M. is shown for samples from 6 mice for 5 hr feeding and 3 mice for 24 hr feeding groups. Differences between Ad-empty and Ad-G9a-DN samples were analyzed by the Student t-test. * indicates $p < 0.05$ and N.S. refers to statistically not significant.

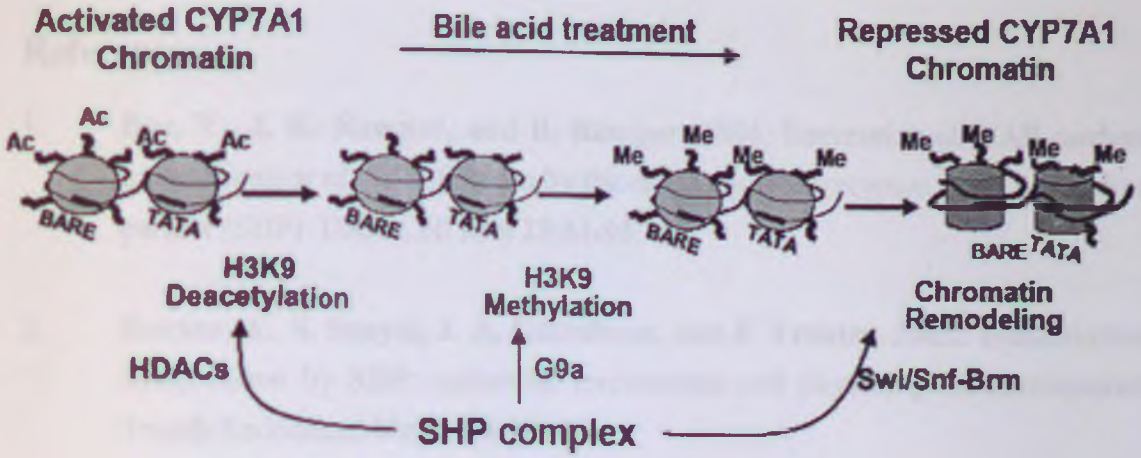

Fig. 9. Coordinated sequential recruitment of HDACs, G9a, and Swi/Snf-Brm in the SHP-mediated suppression of CYP7A1 in the hepatic bile acid metabolism. Bile acid-induced SHP may compete with coactivator HATs, including p300, CBP, and SRC-1, at the CYP7A1 promoter, which contributes to a decrease in histone acetylation initially as proposed before. SHP directly interacts with HDACs and G9a through its C-and N-terminus, respectively, recruiting these cofactors to the promoter, which results in deacetylation and subsequent dimethylation at the H3K9. H3K9 methylation and deacetylation create a binding surface for the recruitment of the Swi/Snf-Brm complex, which results in ATP-dependent chromatin remodeling and subsequent gene silencing of CYP7A1.

References

1. **Bae, Y., J. K. Kemper, and B. Kemper.** 2004. Repression of CAR-mediated transactivation of CYP2B genes by the orphan nuclear receptor, short heterodimer partner (SHP). DNA Cell Biol **23:**81-91.

2. **Bavner, A., S. Sanyal, J. A. Gustafsson, and E. Treuter.** 2005. Transcriptional corepression by SHP: molecular mechanisms and physiological consequences. Trends Endocrinol Metab **16:**478-88.

3. **Bhalla, S., C. Ozalp, S. Fang, L. Xiang, and J. K. Kemper.** 2004. Ligand-activated pregnane X receptor interferes with HNF-4 signaling by targeting a common coactivator PGC-1alpha. Functional implications in hepatic cholesterol and glucose metabolism. J Biol Chem **279:**45139-47.

4. **Borgius, L. J., K. R. Steffensen, J. A. Gustafsson, and E. Treuter.** 2002. Glucocorticoid signaling is perturbed by the atypical orphan receptor and corepressor SHP. J Biol Chem **277:**49761-6.

5. **Boulias, K., N. Katrakili, K. Bamberg, P. Underhill, A. Greenfield, and I. Talianidis.** 2005. Regulation of hepatic metabolic pathways by the orphan nuclear receptor SHP. Embo J **24:**2624-33.

6. **Boulias, K., and I. Talianidis.** 2004. Functional role of G9a-induced histone methylation in small heterodimer partner-mediated transcriptional repression. Nucleic Acids Res **32:**6096-103.

7. **Brendel, C., K. Schoonjans, O. A. Botrugno, E. Treuter, and J. Auwerx.** 2002. The small heterodimer partner interacts with the liver X receptor alpha and represses its transcriptional activity. Mol Endocrinol **16:**2065-76.

8. **Chiang, J. Y., R. Kimmel, C. Weinberger, and D. Stroup.** 2000. Farnesoid X receptor responds to bile acids and represses cholesterol 7alpha-hydroxylase gene (CYP7A1) transcription. J Biol Chem **275:**10918-24.

9. **De Fabiani, E., N. Mitro, F. Gilardi, D. Caruso, G. Galli, and M. Crestani.** 2003. Coordinated control of cholesterol catabolism to bile acids and of gluconeogenesis via a novel mechanism of transcription regulation linked to the fasted-to-fed cycle. J Biol Chem **278:**39124-32.

10. **del Castillo-Olivares, A., J. A. Campos, W. M. Pandak, and G. Gil.** 2004. The role of alpha1-fetoprotein transcription factor/LRH-1 in bile acid biosynthesis: a known nuclear receptor activator that can act as a suppressor of bile acid biosynthesis. J Biol Chem **279:**16813-21.

11. **Denson, L. A., E. Sturm, W. Echevarria, T. L. Zimmerman, M. Makishima, D. J. Mangelsdorf, and S. J. Karpen.** 2001. The orphan nuclear receptor, shp, mediates bile acid-induced inhibition of the rat bile acid transporter, ntcp. Gastroenterology **121:**140-7.

12. **Duan, Z., A. Zarebski, D. Montoya-Durango, H. L. Grimes, and M. Horwitz.** 2005. Gfi1 coordinates epigenetic repression of p21Cip/WAF1 by recruitment of histone lysine methyltransferase G9a and histone deacetylase 1. Mol Cell Biol **25:**10338-51.

13. **Eloranta, J. J., and G. A. Kullak-Ublick.** 2005. Coordinate transcriptional regulation of bile acid homeostasis and drug metabolism. Arch Biochem Biophys **433:**397-412.

14. **Gobinet, J., S. Carascossa, V. Cavailles, F. Vignon, J. C. Nicolas, and S. Jalaguier.** 2005. SHP represses transcriptional activity via recruitment of histone deacetylases. Biochemistry **44:**6312-20.

15. **Goodwin, B., S. A. Jones, R. R. Price, M. A. Watson, D. D. McKee, L. B. Moore, C. Galardi, J. G. Wilson, M. C. Lewis, M. E. Roth, P. R. Maloney, T. M. Willson, and S. A. Kliewer.** 2000. A regulatory cascade of the nuclear receptors FXR, SHP-1, and LRH-1 represses bile acid biosynthesis. Mol Cell **6:**517-26.

16. **Gyory, I., J. Wu, G. Fejer, E. Seto, and K. L. Wright.** 2004. PRDI-BF1 recruits the histone H3 methyltransferase G9a in transcriptional silencing. Nat Immunol **5**:299-308.

17. **Hake, S. B., A. Xiao, and C. D. Allis.** 2004. Linking the epigenetic 'language' of covalent histone modifications to cancer. Br J Cancer **90**:761-9.

18. **He, T. C., S. Zhou, L. T. da Costa, J. Yu, K. W. Kinzler, and B. Vogelstein.** 1998. A simplified system for generating recombinant adenoviruses. Proc Natl Acad Sci U S A **95**:2509-14.

19. **Jenuwein, T., and C. D. Allis.** 2001. Translating the histone code. Science **293**:1074-80.

20. **Johansson, L., A. Bavner, J. S. Thomsen, M. Farnegardh, J. A. Gustafsson, and E. Treuter.** 2000. The orphan nuclear receptor SHP utilizes conserved LXXLL-related motifs for interactions with ligand-activated estrogen receptors. Mol Cell Biol **20**:1124-33.

21. **Johansson, L., J. S. Thomsen, A. E. Damdimopoulos, G. Spyrou, J. A. Gustafsson, and E. Treuter.** 1999. The orphan nuclear receptor SHP inhibits agonist-dependent transcriptional activity of estrogen receptors ERalpha and ERbeta. J Biol Chem **274**:345-53.

22. **Kadam, S., and B. M. Emerson.** 2003. Transcriptional specificity of human SWI/SNF BRG1 and BRM chromatin remodeling complexes. Mol Cell **11**:377-89.

23. **Kadonaga, J. T.** 1998. Eukaryotic transcription: an interlaced network of transcription factors and chromatin-modifying machines. Cell **92**:307-13.

24. **Kemper, J. K., H. Kim, J. Miao, S. Bhalla, and Y. Bae.** 2004. Role of an mSin3A-Swi/Snf chromatin remodeling complex in the feedback repression of bile acid biosynthesis by SHP. Mol Cell Biol **24**:7707-19.

25. **Kerr, T. A., S. Saeki, M. Schneider, K. Schaefer, S. Berdy, T. Redder, B. Shan, D. W. Russell, and M. Schwarz.** 2002. Loss of nuclear receptor SHP impairs but does not eliminate negative feedback regulation of bile acid synthesis. Dev Cell **2:**713-20.

26. **Kornberg, R. D., and Y. Lorch.** 1999. Twenty-five years of the nucleosome, fundamental particle of the eukaryote chromosome. Cell **98:**285-94.

27. **Kouzarides, T.** 2002. Histone methylation in transcriptional control. Curr Opin Genet Dev **12:**198-209.

28. **Ktistaki, E., and I. Talianidis.** 1997. Modulation of hepatic gene expression by hepatocyte nuclear factor 1. Science **277:**109-12.

29. **Lee, Y. K., H. Dell, D. H. Dowhan, M. Hadzopoulou-Cladaras, and D. D. Moore.** 2000. The orphan nuclear receptor SHP inhibits hepatocyte nuclear factor 4 and retinoid X receptor transactivation: two mechanisms for repression. Mol Cell Biol **20:**187-95.

30. **Lee, Y. K., and D. D. Moore.** 2002. Dual mechanisms for repression of the monomeric orphan receptor liver receptor homologous protein-1 by the orphan small heterodimer partner. J Biol Chem **277:**2463-7.

31. **Lu, T. T., M. Makishima, J. J. Repa, K. Schoonjans, T. A. Kerr, J. Auwerx, and D. J. Mangelsdorf.** 2000. Molecular basis for feedback regulation of bile acid synthesis by nuclear receptors. Mol Cell **6:**507-15.

32. **Miao, J., S. Fang, Y. Bae, and J. K. Kemper.** 2006. Functional inhibitory cross-talk between constitutive androstane receptor and hepatic nuclear factor-4 in hepatic lipid/glucose metabolism is mediated by competition for binding to the DR1 motif and to the common coactivators, GRIP-1 and PGC-1alpha. J Biol Chem **281:**14537-46.

33. **Min, G., J. K. Kemper, and B. Kemper.** 2002. Glucocorticoid receptor-interacting protein 1 mediates ligand-independent nuclear translocation and activation of constitutive androstane receptor in vivo. J Biol Chem **277:**26356-63.

34. **Nielsen, S. J., R. Schneider, U. M. Bauer, A. J. Bannister, A. Morrison, D. O'Carroll, R. Firestein, M. Cleary, T. Jenuwein, R. E. Herrera, and T. Kouzarides.** 2001. Rb targets histone H3 methylation and HP1 to promoters. Nature **412:**561-5.

35. **Nishigori, H., H. Tomura, N. Tonooka, M. Kanamori, S. Yamada, K. Sho, I. Inoue, N. Kikuchi, K. Onigata, I. Kojima, T. Kohama, K. Yamagata, Q. Yang, Y. Matsuzawa, T. Miki, S. Seino, M. Y. Kim, H. S. Choi, Y. K. Lee, D. D. Moore, and J. Takeda.** 2001. Mutations in the small heterodimer partner gene are associated with mild obesity in Japanese subjects. Proc Natl Acad Sci U S A **98:**575-80.

36. **Nishio, H., and M. J. Walsh.** 2004. CCAAT displacement protein/cut homolog recruits G9a histone lysine methyltransferase to repress transcription. Proc Natl Acad Sci U S A **101:**11257-62.

37. **Ogawa, H., K. Ishiguro, S. Gaubatz, D. M. Livingston, and Y. Nakatani.** 2002. A complex with chromatin modifiers that occupies E2F- and Myc-responsive genes in G0 cells. Science **296:**1132-6.

38. **Rice, J. C., and C. D. Allis.** 2001. Histone methylation versus histone acetylation: new insights into epigenetic regulation. Curr Opin Cell Biol **13:**263-73.

39. **Sanyal, S., J. Y. Kim, H. J. Kim, J. Takeda, Y. K. Lee, D. D. Moore, and H. S. Choi.** 2002. Differential regulation of the orphan nuclear receptor small heterodimer partner (SHP) gene promoter by orphan nuclear receptor ERR isoforms. J Biol Chem **277:**1739-48.

40. **Seol, W., H. S. Choi, and D. D. Moore.** 1996. An orphan nuclear hormone receptor that lacks a DNA binding domain and heterodimerizes with other receptors. Science **272:**1336-9.

41. **Shi, Y., J. Sawada, G. Sui, B. Affar el, J. R. Whetstine, F. Lan, H. Ogawa, M. P. Luke, and Y. Nakatani.** 2003. Coordinated histone modifications mediated by a CtBP co-repressor complex. Nature **422:**735-8.

42. **Shin, D. J., J. A. Campos, G. Gil, and T. F. Osborne.** 2003. PGC-1alpha activates CYP7A1 and bile acid biosynthesis. J Biol Chem **278:**50047-52.

43. **Stewart, M. D., J. Li, and J. Wong.** 2005. Relationship between histone H3 lysine 9 methylation, transcription repression, and heterochromatin protein 1 recruitment. Mol Cell Biol **25:**2525-38.

44. **Strahl, B. D., and C. D. Allis.** 2000. The language of covalent histone modifications. Nature **403:**41-5.

45. **Tachibana, M., K. Sugimoto, T. Fukushima, and Y. Shinkai.** 2001. Set domain-containing protein, G9a, is a novel lysine-preferring mammalian histone methyltransferase with hyperactivity and specific selectivity to lysines 9 and 27 of histone H3. J Biol Chem **276:**25309-17.

46. **Tachibana, M., K. Sugimoto, M. Nozaki, J. Ueda, T. Ohta, M. Ohki, M. Fukuda, N. Takeda, H. Niida, H. Kato, and Y. Shinkai.** 2002. G9a histone methyltransferase plays a dominant role in euchromatic histone H3 lysine 9 methylation and is essential for early embryogenesis. Genes Dev **16:**1779-91.

47. **Wang, L., Y. Han, C. S. Kim, Y. K. Lee, and D. D. Moore.** 2003. Resistance of SHP-null mice to bile acid-induced liver damage. J Biol Chem **278:**44475-81.

48. **Wang, L., Y. K. Lee, D. Bundman, Y. Han, S. Thevananther, C. S. Kim, S. S. Chua, P. Wei, R. A. Heyman, M. Karin, and D. D. Moore.** 2002. Redundant pathways for negative feedback regulation of bile acid production. Dev Cell **2:**721-31.

49. **Watanabe, M., S. M. Houten, L. Wang, A. Moschetta, D. J. Mangelsdorf, R. A. Heyman, D. D. Moore, and J. Auwerx.** 2004. Bile acids lower triglyceride levels via a pathway involving FXR, SHP, and SREBP-1c. J Clin Invest **113:**1408-18.

50. **Workman, J. L., and R. E. Kingston.** 1998. Alteration of nucleosome structure as a mechanism of transcriptional regulation. Annu Rev Biochem **67:**545-79.

51. **Zhang, H. S., M. Gavin, A. Dahiya, A. A. Postigo, D. Ma, R. X. Luo, J. W. Harbour, and D. C. Dean.** 2000. Exit from G1 and S phase of the cell cycle is regulated by repressor complexes containing HDAC-Rb-hSWI/SNF and Rb-hSWI/SNF. Cell **101**:79-89.

Chapter Three

P300 is a critical metabolic regulator by coactivating the bile acid receptor FXR and its activity is constitutively elevated in ob/ob mice

Abstract

The bile acid receptor FXR controls lipid and glucose homeostasis by regulating expression of target genes, including an orphan receptor SHP, but how FXR activity is modulated remains unclear. Here, we report that the p300 acetylase coactivates FXR-mediated SHP induction *in vivo* by acetylating both FXR and histones at the SHP promoter but its activity is dysregulated in ob/ob mice. FXR/p300 interaction, their recruitment to the SHP promoter, and acetylation of FXR and histones were increased by FXR agonists. Down-regulation of p300 decreased acetylated FXR and histones and abolished SHP induction and also altered expression of other FXR target genes such that beneficial metabolic profiles would be expected. Strikingly, in ob/ob mice, FXR/p300 interaction and their recruitment to the SHP promoter and acetylated FXR and histones were constitutively increased, leading to constitutively elevated SHP expression. Inhibition of p300 activity may provide promising molecular targets for treating metabolic diseases.

Introduction

Farnesoid X receptor (FXR) is a member of the nuclear receptor superfamily (30) and a biosensor for endogenous bile acids (29, 48). Upon activated by physiological concentration of bile acids, FXR regulates expression of numerous metabolic target genes

in liver, kidney, and intestine (15). A number of studies utilizing synthetic FXR ligands and FXR-null mice have demonstrated that FXR plays a central role in maintaining whole body metabolic homeostasis (44, 52).

FXR regulates cholesterol and bile acid levels by induction of the orphan nuclear receptor and metabolic repressor, small heterodimeric partner (SHP) (7, 26). Induced SHP then represses the expression of cholesterol 7α-hydroxylase (CYP7A1), a key enzyme in bile acid biosynthesis (4, 13, 42). In addition to its role in cholesterol and bile acid homeostasis, functions of FXR have recently been extended to glucose and fatty acid metabolism, liver regeneration, and inhibition of intestinal bacterial growth (11, 12, 28, 51, 56). Although such critical roles of FXR in normal and disease states have now been established, the molecular mechanisms of the modulation of FXR activity *in vivo* are largely unknown.

Nuclear receptors, including FXR, collaborate with a number of transcriptional cofactors, coactivators and corepressors, to effectively modulate transcription of their target genes (21, 41). Potential FXR cofactors have been identified in mostly *in vitro* and cultured cell studies, including the histone arginine methyltransferases, CARM1 (1) and PRMT1 (39), a transcriptional mediator DRIP205 (36), and a versatile metabolic coactivator PGC-1α (55). Although potential cofactors of FXR have been described, whether these proteins actually regulate FXR activity *in vivo* remains largely unexplored.

The transcription cofactor p300 functions in diverse biological pathways, including differentiation, development, and proliferation (35, 53) and expression of p300 is altered in human gastric, colorectal, and prostate carcinomas (34). P300 is a histone acetyltransferase (HAT) that catalyzes the acetylation of lysine residues not only in

nucleosomal histones, but also in nuclear receptors, cofactors, and basal transcription factors, resulting in enhanced gene transcription in most cases (6, 19). Despite its role as a general transcription coactivator, the role of p300 *in vivo* in metabolic regulation under physiological and pathological states has not been reported.

The well known FXR target and metabolic repressor SHP is an unusual orphan receptor which lacks a DNA binding domain but contains a putative ligand binding domain (43). SHP interacts with and inhibits the activity of numerous nuclear receptors that are involved in regulation of diverse metabolic pathways (2, 16, 18, 22). We recently demonstrated that SHP inhibits transcription of target genes by coordinately recruiting chromatin modifying cofactors, such as mSin3A/HDACs, G9a histone lysine methyltransferase, and Swi/Snf-Brm remodeling complex to target gene promoters (5, 16). Marked alterations in cholesterol and bile acid levels in SHP-null mice have established a role for SHP in lipid homeostasis (17, 49). Interestingly, despite its crucial role in metabolic regulation, elevated SHP expression has been implicated in increased lipid levels in liver and serum. Prolonged liver-specific overexpression of SHP resulted in a depleted hepatic bile acid pool and the accumulation of hepatic lipids in transgenic mice (3). Furthermore, SHP expression is highly elevated in the leptin gene-deficient ob/ob mice, a mouse model of fatty liver disease, obesity, and type II diabetes (10). How bile acid-activated FXR induces expression of SHP and the molecular basis for the elevated SHP expression in ob/ob mice are unknown.

Here, we report for the first time that p300 is a critical *in vivo* metabolic regulator but its activity is constitutively elevated in ob/ob mice. P300 coactivates bile acid-activated FXR in SHP induction by acetylation of both FXR and histones at the SHP

promoter under normal physiological condition. Strikingly however, in ob/ob mice, despite reduced expression of FXR compared to normal mice, the p300/FXR activity is substantially elevated. Interaction of p300 with FXR and acetylation of both FXR and histones at the SHP promoter were constitutively elevated, concomitant with abnormally high constitutive SHP expression in ob/ob mice.

Materials and Methods

Cells

Human hepatoma HepG2 cells (ATCC HB8065) were grown in phenol red-free Dulbecco's modified Eagle's medium (DMEM)/F12 (1:1). Cos-1 cells were grown in DMEM media. Media were supplemented with 100 units/ml penicillin G-streptomycin sulfate and 10% heat inactivated fetal bovine serum.

Adenoviral experiments

An adenoviral vector expressing p300 siRNA (Ad-sip300) was kindly provided by Dr. P. Rotwein. Adenoviral vectors were amplified, purified, and titered as described (5, 37). For downregulation of p300, HepG2 cells were infected with 5-25 MOI of Ad-empty or Ad-sip300 and 2 days later, cells were transfected with reporter and expression plasmids as indicated in figure legends, and reporter assays were done. Consistent results were observed in at least 2 independent triplicate assays in each experiment.

Mouse *in vivo* experiments

Normal mice, ob/ob mice, and FXR null mice were maintained on a 12 hr light and 12 hr dark cycle. CA feeding was always started at 5:00 P.M. to reduce variability between experiments and food intake was monitored. For adenoviral experiments, mice were injected with about 0.5×10^9 active viral particles (Ad-empty, Ad-flag-FXR) in 200 μl of PBS via the tail vein, and 4-7 days after infection, the mice were fed normal chow or chow supplemented with 0.5% CA for 3 to 24 hr. All the animal use and adenoviral protocols were approved by the Institutional Animal Care and Use and Institutional Biosafety Committees at University of Illinois at Urbana-Champaign and were in accordance with National Institutes of Health guidelines.

Real time RTPCR

Total RNA was isolated using Trizol reagent and cDNA was synthesized and RTPCR was performed with an iCycler iQ (Biorad, Inc). The amount of PCR product for each mRNA was normalized by dividing by the amount of 36B4 PCR product. Sequences of the primers are available upon request.

Acetylation assays

For *in vitro* acetylation assays, histones were purified from HeLa cells and HATs from Sf9 insect cells infected with baculovirus encoding each of these proteins, as described (46). Purified GST, GST-FXR, or core histones were incubated with each of purified HATs in the presence of ^{3}H-acetyl-CoA. After incubation at 30°C for 1 hr, the proteins were separated by SDS-PAGE, proteins were detected coomassie blue staining, and

radioactivity by fluorography. In cell and *in vivo* acetylation studies were done as described (8, 31). For ligand experiments, HepG2 cells were infected with Ad-empty or Ad-flag-FXR and 24 hr later, cells were treated with CDCA, GW4064, or vehicle for 2.5 hr in the presence of TSA and Nam and CoIP acetylation assays were done. Flag-FXR was expressed in cells or mouse liver by infection with Ad-flag-FXR, and flag-FXR was immunoprecipitated with M2 antibody and acetylated flag-FXR was detected by western blotting using acetyl lysine antibody (Cell signaling, Inc) or vice versa. The same membrane was stripped and subjected to western blotting using M2 antibody (Sigma, Inc).

CoIP assays

CoIP assays were performed as described (5, 16, 37). Briefly, 1 mg of mouse liver nuclear extracts or 2.5 to 5 mg of liver extracts were incubated in lysis buffer (50 mM Tris-HCl, pH 8.0, 5 mM EDTA, 10% glycerol, 150 mM NaCl, 0.5% NP40, protease inhibitors, and 1 mM DTT) with 1 μg of antibodies and washed with lysis buffer (supplemented with NaCl up to 250 mM and 1% NP40) and proteins in the immunoprecipitates were detected by western blotting.

ChIP assays

ChIP assays were carried out essentially as described (5, 16, 33, 37). ChIP experiments in HepG2, normal mice, and ob/ob mice were repeated at least 3 times with reproducible results.

Results

Cholic acid (CA) feeding induces the interaction of FXR with p300 in mouse liver.

In initial biochemical studies, a protein of about 300 kd was detected in a protein complex associated with flag-FXR in human hepatoma HepG2 cells after treatment with GW4064, a synthetic FXR agonist (not shown). Therefore, to test if the transcriptional coactivator and histone acetyltransferase (HAT) p300 is involved in the regulation of FXR activity *in vivo*, we examined the interaction of p300 with FXR in mouse liver by CoIP assays. Mice were infected with Ad-flag-FXR or control Ad-empty and were fed normal chow or 0.5% CA-supplemented chow. Similar expression of flag-FXR was observed in the two groups (Supplemental Fig. S1). P300 was immunoprecipitated from liver nuclear extracts and flag-FXR in the immunoprecipitates was detected by western blotting. The levels of flag-FXR were similar in input samples, but substantially increased in the anti-p300 immunoprecipitates after CA feeding (Fig. 1A).

We confirmed these results with endogenous FXR without overexpressing flag-FXR in mouse liver. The amount of p300 in the anti-FXR immunoprecipitates was increased by CA feeding (Fig. 1B), while similar levels of endogenous p300 and FXR were detected in the input samples (Supplemental Fig. S2). These CoIP studies indicate that CA feeding increases the interaction of p300 with FXR in mouse liver, suggesting that p300 may be involved in bile acid-activated FXR signaling *in vivo*.

FXR transactivation is enhanced by p300 in a ligand-dependent manner.

To test if the p300/FXR interaction is functionally relevant, the effect of p300 on FXR transactivation was initially examined using cell-based reporter assays. Exogenous

expression of p300 enhanced FXR transactivation in a primary bile acid, chenodeoxycholic acid (CDCA)-dependent manner (Fig. 1C, lanes 4-6). In contrast to p300 wild type, a p300 HAT mutant did not enhance FXR transactivation but instead reduced the activity, presumably by acting as a dominant negative mutant (Fig. 1C, lanes, 4, 7, 8). These results suggest that HAT activity is required for p300-mediated coactivation of FXR.

Since the above experiments utilized overexpression of p300, we also tested the effects of down-regulation of endogenous p300 on FXR activity. Infection with Ad-sip300 decreased the p300 mRNA levels in HepG2 cells by 80% (Supplemental Fig. S3). Expression of FXR and RXR activated the FXRE reporter in the presence of GW4064 or CDCA, and infection with increasing amounts of Ad-sip300, but not of Ad-empty, progressively inhibited FXR transactivation (Fig. 1D). These results indicate that p300, at normal endogenous levels, functions as a coactivator of agonist-activated FXR. Since SHP is a direct FXR target, we also tested if p300 was a FXR coactivator for transactivation of the SHP promoter. Treatment with FXR agonists substantially increased FXR transactivation of the SHP promoter (Fig. 1E). Ad-sip300 markedly reduced the FXR activity in a dose-dependent manner, whereas Ad-empty had little effect. These results indicate that p300 functions as a coactivator for FXR transactivation of the SHP promoter.

CA feeding induces recruitment of p300 to the SHP promoter in mouse liver

We next examined whether CA feeding increased the association of endogenous p300 with the native Shp promoter in mouse liver using chromatin immunoprecipitation (ChIP)

assays. To first ensure that CA feeding effectively altered expression of Shp and Cyp7a1, a key enzyme in bile acid biosynthesis that is suppressed by Shp, mRNA levels of these genes were monitored. The Shp mRNA levels were increased by 3 hr, whereas Cyp7a1 mRNA levels were substantially and progressively decreased with time, after CA feeding (Fig. 2A). In ChIP assays, association of FXR and p300 was markedly increased after CA feeding (Fig. 2B). Consistent with p300 recruitment, acetylation of histone H3 at K9/K14 was increased and these effects were not observed for the control GAPDH sequence (Fig. 2B). In time courses, association of FXR was detected in livers of untreated mice and increased at 6 hr of CA feeding (Fig. 2C). P300 was recruited to the Shp promoter at 3 hr of CA feeding and reached a maximum at 6 hr. Consistent with p300 recruitment, acetylated histone H3 levels progressively increased from 3 to 24 hr after CA feeding (Fig. 2C).

To test if the p300 recruitment was dependent on FXR, ChIP assays were done in FXR-null mice. Association of FXR was not observed, as expected, and the association of p300, acetylated histones, and RNA polymerase II was also largely eliminated in these mice (Fig. 2D). In contrast, association of RXR was observed in wild type and FXR-null mice independent of CA feeding, suggesting that another nuclear receptor that could form a heterodimer with RXR was present at the promoter. These results suggest that p300 is recruited to the SHP promoter after CA feeding in a FXR-dependent manner.

Activated FXR signaling increases association of p300 and acetylated histones at the SHP promoter.

To delineate the mechanism of p300-mediated coactivation of FXR signaling in more detail, the effects of FXR agonists on the association of p300 and acetylated histones with the SHP promoter were studied in HepG2 cells. Acetylated histone H3 was detected in untreated cells and the levels were increased after CDCA treatment, most dramatically by GW4064 treatment, which is consistent with SHP induction (Fig. 2E). Interestingly, co-treatment with the FXR antagonist, guggulesterone (47), blocked the CDCA-mediated increase in histone H3 acetylation and reduced acetylation to lower than basal levels (Fig. 2E). These results suggest that ligand-regulated FXR signaling pathways are functional in HepG2 cells.

In HepG2 cells, FXR association with the SHP promoter and p300 recruitment were markedly increased after GW4064 or CDCA treatment (Fig. 2F, G). Consistent with the p300 recruitment, acetylation of histone H3 was also increased. An increase in the association of FXR and p300 was detected as early as 1 hr after CDCA treatment reaching a maximum at 3 to 6 hr (Fig. 2H).

To determine if p300 and FXR are simultaneously associated with the promoter, chromatin immunprecipitated with FXR antisera was reprecipitated with p300 antisera. SHP promoter sequences were detected in CDCA-treated samples reprecipitated by p300 antibody (Fig. 2I), suggesting that both p300 and FXR are associated with the same SHP promoter. These results show that p300 is recruited to the SHP promoter in a FXR ligand-dependent manner and provide further evidence that p300 is a FXR coactivator of SHP induction.

Down-regulation of p300 decreases FXR binding and histone acetylation at the SHP promoter.

To test if increased acetylation at the SHP promoter by FXR agonists is dependent on p300, endogenous p300 in HepG2 cells was down-regulated over 70% by infection with Ad-sip300. GW4064 treatment increased SHP mRNA levels about 3 fold and this increase was largely inhibited by p300siRNA (Fig. 3A). Acetylated histone H3 levels and association of FXR and RNA polymerase II with the promoter were increased by GW4064, and these increases were eliminated in cells infected with Ad-sip300 (Fig. 3B). Similar effects of p300 siRNA were observed with HepG2 cells treated with CDCA (Fig. 3C, D). These results demonstrate that increased histone H3 acetylation and FXR binding are dependent on p300, suggesting that p300 coactivates FXR-mediated SHP induction by increasing acetylation of promoter histones and FXR binding to the promoter.

FXR is acetylated by p300 *in vitro* and in cells.

Binding of transcriptional activators to promoter chromatin is increased not only by acetylation of histones but also by acetylation of the activators (27, 45). Since FXR binding to the SHP promoter was inhibited by down-regulation of p300 (Fig. 3), we further considered whether FXR can be acetylated by p300. To test this possibility, we first examined if p300 can directly interact with FXR and then if p300 can acetylate FXR. P300 was associated with GST-FXR *in vitro*, but in contrast to *in vivo* results (Fig. 1), the interaction was independent of treatment with CDCA (not shown) or GW4064 (Fig. 4A).

To test if FXR can be acetylated by p300, purified GST-FXR, GST, or core histones were incubated with HATs. Auto-acetylation of p300, CBP, pCAF was detected (Fig. 4B, asterisks). GST-FXR was acetylated by p300 and to a lesser extent by CBP, but not detectably by pCAF or GCN5. In contrast, histones were robustly acetylated by all these acetylases (Fig. 4C) and control GST was not acetylated (Supplemental Fig. S4). These studies indicate that FXR is acetylated by p300 *in vitro*.

To test if FXR is acetylated in cells, we first examined whether inhibition of deacetylation of proteins by the deacetylase inhibitors, trichostatin A (TSA) and nicotinamide (Nam), increased acetylated FXR levels. HEK293 cells were transfected with expression plasmids for flag-FXR and then treated with TSA and/or Nam. Acetylation of flag-FXR was detected by CoIP, immunoprecipitation with acetyl lysine antibody followed by detection of flag-FXR in the immunoprecipitates by western blotting as described (31). The levels of acetylated FXR were increased by either of the deacetylase inhibitors, indicating that FXR is normally acetylated in cells. Similar results were observed in HepG2 and Cos-1 cells (not shown).

Next, to determine if p300 acetylates FXR, cells were cotransfected with expression plasmids for flag-FXR and p300 wt or a p300 HAT mutant, and acetylated FXR levels were detected. Acetylation of flag-FXR was detected in cells expressing flag-FXR only and exogenous expression of p300 markedly increased the acetylation (Fig. 4D). In contrast, with the p300 HAT mutant, acetylated FXR levels were lower than basal levels. These results indicate that FXR can be acetylated by p300 in cells.

Acetylated FXR levels are increased after FXR agonist treatment

Since we observed that both the interaction of FXR with p300 and the association of FXR and p300 with the Shp promoter in mouse liver was increased after CA feeding (Fig. 1, 2), we postulated that FXR acetylation would be increased in cells by treatment with a FXR agonist. To test this possibility, the effects of CDCA or GW4064 on acetylated FXR levels were examined in HepG2 cells. Acetylated FXR levels were increased in cells treated with CDCA or GW4064 in the presence of HADC inhibitors (Fig. 4E, upper panel), whereas the amounts of flag-FXR were similar between groups (Fig. 4E, lower panel). These results indicate that acetylated FXR levels are increased after FXR agonist treatment.

Effects of down-regulation of p300 on the expression of FXR target

To further explore a general metabolic function of p300, we tested the effects of p300 siRNA on expression of FXR target genes in HepG2 cells. Injection of Ad-sip300 or the Ad-p300 HAT mutant was lethal in mice for unknown reasons so we could not conduct these experiments *in vivo*. In HepG2 cells, p300 mRNA levels were reduced by 70% by Ad-sip300 infection and were not altered by CDCA or GW 4064 treatment (Fig. 5A). The functions of representative FXR target genes that are examined in this study are briefly summarized in Fig. 5E. CDCA or GW4064 treatment reduced CYP7A1 mRNA levels about 70% as expected and while infection with Ad-sip300 reduced basal levels of CYP7A1, a further reduction was not observed with agonist treatment (Fig. 5B). Down-regulation of p300 resulted in substantial decreases in SHP mRNA levels and significant decreases in BSEP mRNA levels in cells treated with

vehicle or FXR agonists (Fig. 5B). In contrast, while the mRNA levels of ApoCII or ApoE were not changed by Ad-sip300 infection, PLTP and VLDLR mRNA levels were surprisingly increased (Fig. 5C). The mRNA levels of ApoAI were reduced by CDCA treatment and down-regulation of p300 reversed the inhibition of ApoAI expression (Fig. 5C). Interestingly, down-regulation of p300 substantially reduced mRNA levels of G-6-Pase and markedly reduced those of PEPCK (Fig. 5D).

These data indicate that down-regulation of p300 has differential effects on the expression of different FXR target genes. Interestingly, the changes in expression of genes involved in lipid metabolism are in directions that would lead to improved lipid profiles and those in glucose metabolism would lead to decreased serum glucose levels.

Constitutively elevated p300 activity in ob/ob mice

Prolonged expression of SHP in transgenic mice was associated with detrimental lipid profiles and development of fatty livers (3). Consistent with these results, SHP expression was abnormally elevated in ob/ob mice and knock-down of the SHP gene resulted in beneficial metabolic effects in these mice (10). Since p300/FXR activity is critical for SHP gene expression, we hypothesized that SHP expression might be abnormally elevated, at least in part, by defects in the p300/FXR pathway in ob/ob mice.

To test this possibility, we first compared mRNA levels of lipogenic factors, FXR, p300, and SHP in normal and ob/ob mice. The mRNA levels of lipogenic factors, SREBP-1c and PPARγ, were increased about 2-3 fold and their lipogenic target genes, such as FAS and SCD1, were dramatically increased in the ob/ob mice (Fig. 6A). While the mRNA levels of p300 were not significantly changed, FXR mRNA levels were

surprisingly reduced by 80% in ob/ob mice (Fig. 6B). SHP mRNA levels were elevated about 5 fold in the ob/ob mice, which is consistent with a recent report (10). The mRNA levels of BSEP, another well known FXR target and hepatic bile acid transporter, were modestly reduced in ob/ob mice but the decrease was not statistically significant.

In CoIP assays, the interaction of FXR with p300 was markedly and constitutively elevated in ob/ob mice compared to normal mice (Fig. 6C). Consistent with the increased interaction of FXR with p300 in ob/ob mice, acetylated FXR levels were dramatically elevated in these mice compared to normal mice (Fig. 6D). Acetylated FXR levels were not detected in control IgG-precipitated samples (Supplemental Fig. S5). Notably, the mobility of FXR was slightly reduced in samples from ob/ob mice, which may reflect increased post-translational modification of FXR in these mice. These results suggest that FXR is highly acetylated in ob/ob mice, which may be associated with increased SHP expression in these mice. These data provide a potential link between FXR hyperacetylation and metabolic dysfunction in these mice.

To further explore the molecular basis of dysregulation of the p300/FXR activity in ob/ob mice, we compared protein occupancy in normal and ob/ob mice at the SHP promoter and at the BSEP promoter, another FXR target gene, which responds similarly to CA feeding or CDCA treatment in normal mice and in HepG2 cells (Fig. 5B) (S. Fang and J. K. Kemper, unpublished data). In ChIP assays, association of FXR (in spite of its decreased expression, Fig. 6B), p300, and RNA polymerase II with the SHP promoter was increased in ob/ob mice compared to normal mice (Fig. 6 E, G). Acetylation at histone H3K9/K14, which is associated with gene activation (14), was markedly increased in ob/ob mice at the SHP promoter. Conversely, methylation of histone

H3K9, which is associated with gene suppression (5, 20), was decreased at the SHP promoter in ob/ob mouse liver. Interestingly, these changes at the SHP promoter were not detected at the BSEP promoter in ob/ob mice (Fig. 6 F, H). These results suggest that gene activation by FXR/p300 pathway is a gene-selective process in these mice. The mechanism underlying this gene selectivity is not clear from the present data. The changes in ob/ob mice are complex and regulation of SHP and BSEP genes is likely to be a combinatorial process involving multiple transcription factors and defects in upstream signaling pathways. Nevertheless, these data suggest that constitutively elevated p300 activity and highly elevated acetylation levels of FXR and histones at the SHP promoter may cause, at least in part, constitutive and abnormal elevation of SHP expression in these mice.

Discussion

From animal *in vivo* studies using normal mice, FXR null mice, and ob/ob mice, along with molecular mechanistic studies in HepG2 cells, we have obtained compelling evidence that p300 is a critical *in vivo* metabolic regulator in bile acid signaling. Coactivation of bile acid-activated FXR by p300 is critical for induction of the SHP gene, a well known FXR target and metabolic repressor, in normal mice. Surprisingly however, the p300 activity is constitutively elevated in ob/ob mice, a mouse model of fatty liver disease and diabetes, such that acetylation levels of both FXR and histones at the SHP promoter are constitutively and highly elevated.

Several lines of evidence indicate that p300 coactivates FXR induction via acetylation of both target gene histones and FXR. The most convincing evidence for

acetylation of histones by p300 is that p300 was recruited to the SHP promoter and histone acetylation was increased after CA feeding or treatment with FXR agonists but the increased histone acetylation was nearly completely blocked by down-regulation of p300 (Fig. 2). Further, the time-course of increased acetylation at the promoter after bile acid treatment correlated with that of p300 in both HepG2 cells and mouse liver *in vivo*. Finally, a mutation of p300 which eliminates HAT activity also eliminated coactivation by p300 of FXR transactivation of the SHP promoter. These results demonstrate that p300 enhances SHP induction, at least in part, by acetylation of chromatin histones.

Coactivator HATs, such as p300, can also directly acetylate nuclear receptors and modulate their activity. Acetylation of transcription factors, such as, ER, foxo-1,and AR, has been shown to alter their DNA binding ability, cofactor interaction, or protein stability (6, 19, 32). It was recently demonstrated that the activity of a transcriptional coactivator, PGC-1α, was substantially altered by its acetylation state which was dependent on GCN5 acetylase and SIRT1 deacetylase (23, 40). In the present studies, bile acid treatment increased interaction of FXR with p300 and the recruitment of FXR/p300 to the SHP promoter in mouse liver and in HepG2 cells. Consistent with these observations, acetylated FXR levels were increased by FXR agonists (Fig. 4E). Furthermore, acetylated FXR levels were increased by exogenous expression of p300, but were decreased by expression of a p300 HAT mutant. These studies strongly suggest that acetylation of FXR, in addition to histone acetylation, contributes to coactivation of FXR by p300.

We observed unexpected, intriguing results that down-regulation of p300 altered the expression of metabolic FXR target genes such that beneficial metabolic profiles would be expected (Fig. 5). The expected effects of the down-regulation are complex since direct targets of FXR/p300, like SHP, would be expected to be down-regulated and indirect targets of FXR via SHP induction would be expected to be up-regulated. Furthermore, if these metabolic genes are also regulated by other transcription factors that are coactivated by p300, decreased expression would be expected. Nevertheless, for the genes involved in lipoprotein metabolism, down-regulation of p300 resulted in a dramatic increase in the expression of the VLDL receptor gene which should increase the metabolism of triglyceride-rich lipoproteins and, therefore, decrease the levels of triglycerides, which is a beneficial result. Down-regulation of p300 also increased the basal levels of ApoCII, ApoE, and PLTP. While modest, these changes should result in increased synthesis of an HDL component, transfer of phospholipid to HDL, and increased metabolism of chylomicrons and VLDL. Each of these changes would result in improved lipid profiles that may reduce the probability of cardiovascular disease. For enzymes related to glucose metabolism, p300 reduced expression of G6Pase and PEPCK, both of which are involved in the production of glucose and would contribute to decreased serum glucose levels, a beneficial effect in diabetic states.

To examine the potential role of p300 in pathological states, we examined the regulation of the SHP gene by FXR/p300 activity in ob/ob mice. Abnormally elevated SHP expression has been observed in ob/ob mice and KKAy mice, mouse models for fatty liver and diabetes, suggesting that elevation of SHP expression may be associated with these metabolic diseases (10). Consistent with these studies, liver-specific

prolonged overexpression of SHP was shown to result in depleted hepatic bile acid pools and accumulation of hepatic lipids by indirectly promoting hepatic lipogenesis in transgenic mice (3). Also, SHP was a negative regulator of energy homeostasis, and decreased lipid levels and increased insulin sensitivity were detected SHP-null mice (50). Abnormal elevation of SHP expression, therefore, has been implicated as a key factor in disorders of lipid and glucose metabolism.

In ob/ob mice, while p300 mRNA levels were not significantly increased, surprisingly, FXR mRNA levels were dramatically reduced compared to normal animals. Remarkably, despite decreased FXR expression, interaction of FXR with p300 was substantially increased and FXR/p300 recruitment to the SHP promoter was also constitutively and highly increased in ob/ob mice compared to normal mice (Fig. 6). Consistent with these results, levels of acetylated FXR and histones at the SHP promoter were substantially elevated, concomitant with elevated SHP expression in ob/ob mice. These results suggest that the protein complex at the SHP promoter and modification of histones are similar in ob/ob mice fed normal chow and normal mice after CA feeding, except that the activation is exaggerated in ob/ob mice, with constitutively elevated FXR acetylation (Fig. 7). Our data, together with previous studies (3, 10), suggest that elevated p300 activity and subsequent elevated SHP expression may cause, at least in part, the pathogenesis observed in the ob/ob mice.

Interestingly, expression of a second FXR target and hepatic bile acid transporter, BSEP gene, was not elevated in the ob/ob mice. This result suggests that the activation of the FXR/p300 pathway is gene-selective in these mice. The mechanisms underlying this gene selectivity is not clear from the present data but

presumably is related to complex, combinatorial regulation of these genes. Additional research will be required to better understand the mechanism of the selective regulation of FXR target genes by p300.

P300 is a transcriptional coactivator critically involved in cell differentiation, development, and cell proliferation, and dysregulation of p300 activity has been detected in various human carcinomas (34). Our studies and previous studies suggest that expression and activity of critical coregulators, such as p300 and PGC-1α, must be tightly regulated to maintain normal metabolic homeostasis and that dysregulation of these cofactors leads to metabolic disease. For instance, the key metabolic regulator PGC-1α is critically involved in metabolic adaptation to fasting by stimulating entire program of hepatic gluconeogenesis and fatty acid β-oxidation (24, 38). These responses are lacking in PGC-1α null mice resulting in hypoglycemia and increased lipid levels in the liver (25). However, interestingly, constitutively elevated PGC-1α activity has been implicated in pathological states as well, resulting in elevated hepatic glucose production and subsequently elevated fasting glucose levels (9, 54). Analogous to these PGC-1α studies, our results demonstrate that p300 is a critical *in vivo* metabolic regulator in bile acid signaling but its activity is dysregulated and constitutively elevated in ob/ob mice. Reducing hepatic SHP expression by inhibiting the p300 activity, therefore, may have beneficial effects on metabolic diseases and inhibiting the p300 activity may be an attractive molecular target for treating metabolic disorders.

Acknowledgments

We are grateful to P. Rotwein for providing Ad-sip300, H. Lu for Ad-p300, R. Sato for Gal4-FXR and 3flag-FXR , P. Edwards for FXR deletion constructs, M. Stallcup for p300 wt and the DN mutant, M. Ananthanarayanan for FXRE-tk-luc, and P. Puigserver for GCN5 plasmids. We thank T. Willson for providing the GW4064 compound. We also thank to F. Gonzalez for permission to use FXR null mice. Special thank to B. Kemper for helpful discussions. This study was supported by grants CA103867 and CA124760 to C.M.C. and NIH DK062777 and AHA 0756028Z to J.K.K.

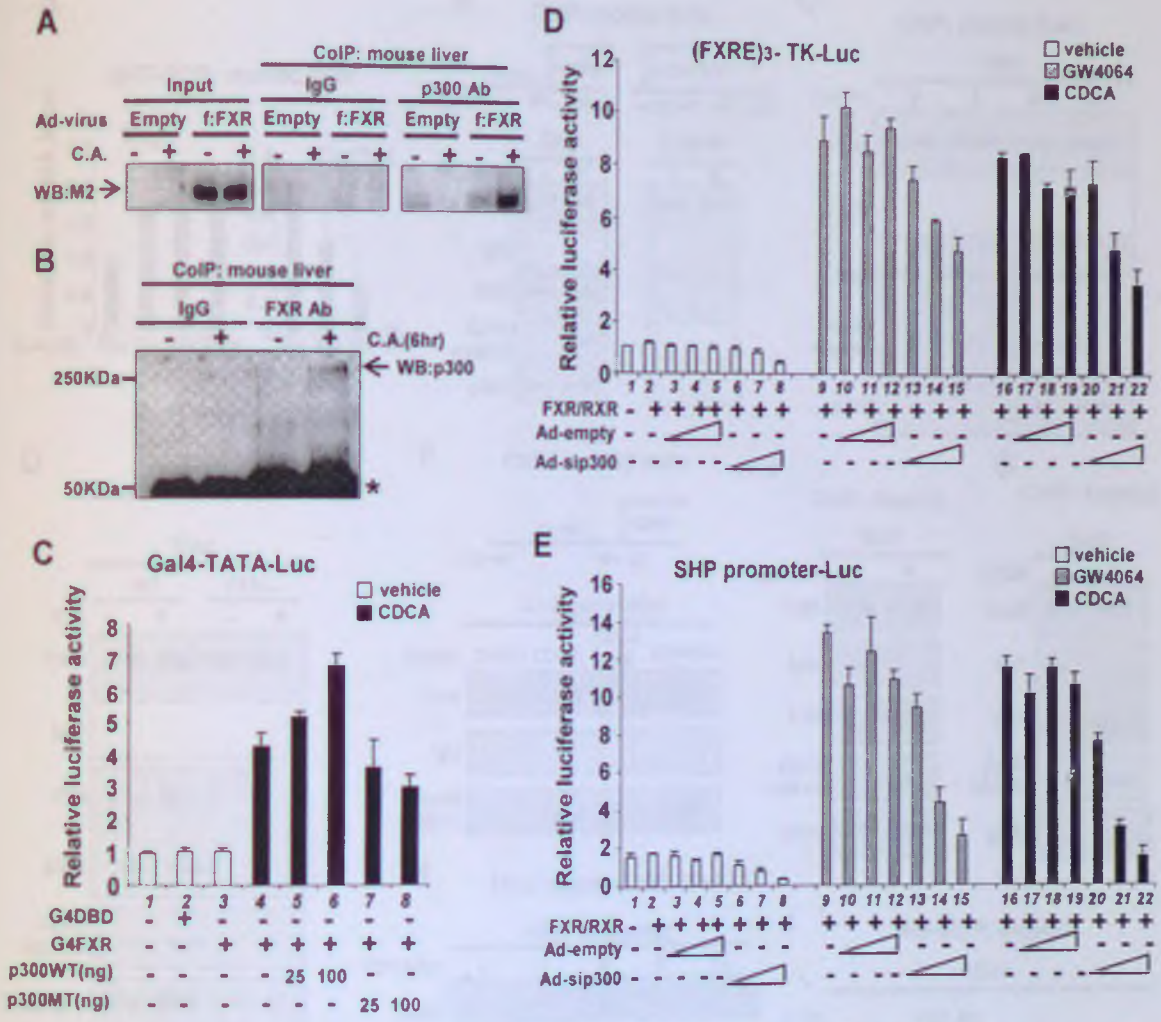

Fig. 1. P300 interacts with and coactivates FXR activity. (A) Mice were injected with Ad-flag-FXR or control Ad-empty and 5 days later, mice were fed normal or 0.5% CA chow for 6 hr, p300 was immunoprecipitated from liver nuclear extracts, and flag-FXR in the immunoprecipitates was detected by western blotting. (B) Uninfected mice were fed normal or 0.5% CA chow for 6 hr and liver nuclear extracts were subjected to CoIP assays. IgG heavy chains are indicated by an asterisk. (C) Cos-1 cells were cotransfected with 200 ng of Gal4-TATA-luc and 5 ng of Gal4-DBD or Gal4-FXR in the presence of p300 wild type or HAT mutant as indicated. Cells were treated with vehicle or CDCA overnight and harvested for reporter assays. (D, E) HepG2 cells were infected with 5-25 MOI of Ad-sip300 or Ad-empty and 2 days later, the cells were transfected with 200 ng of $(FXRE)_3$-luc (D) or SHP promoter-luc (E) vectors along with expression plasmids for FXR and RXR. Cells were treated with ligands overnight and harvested for reporter assays. The values for firefly luciferase activities were normalized by dividing by the β-galactosidase activities (n=3 for the SEM).

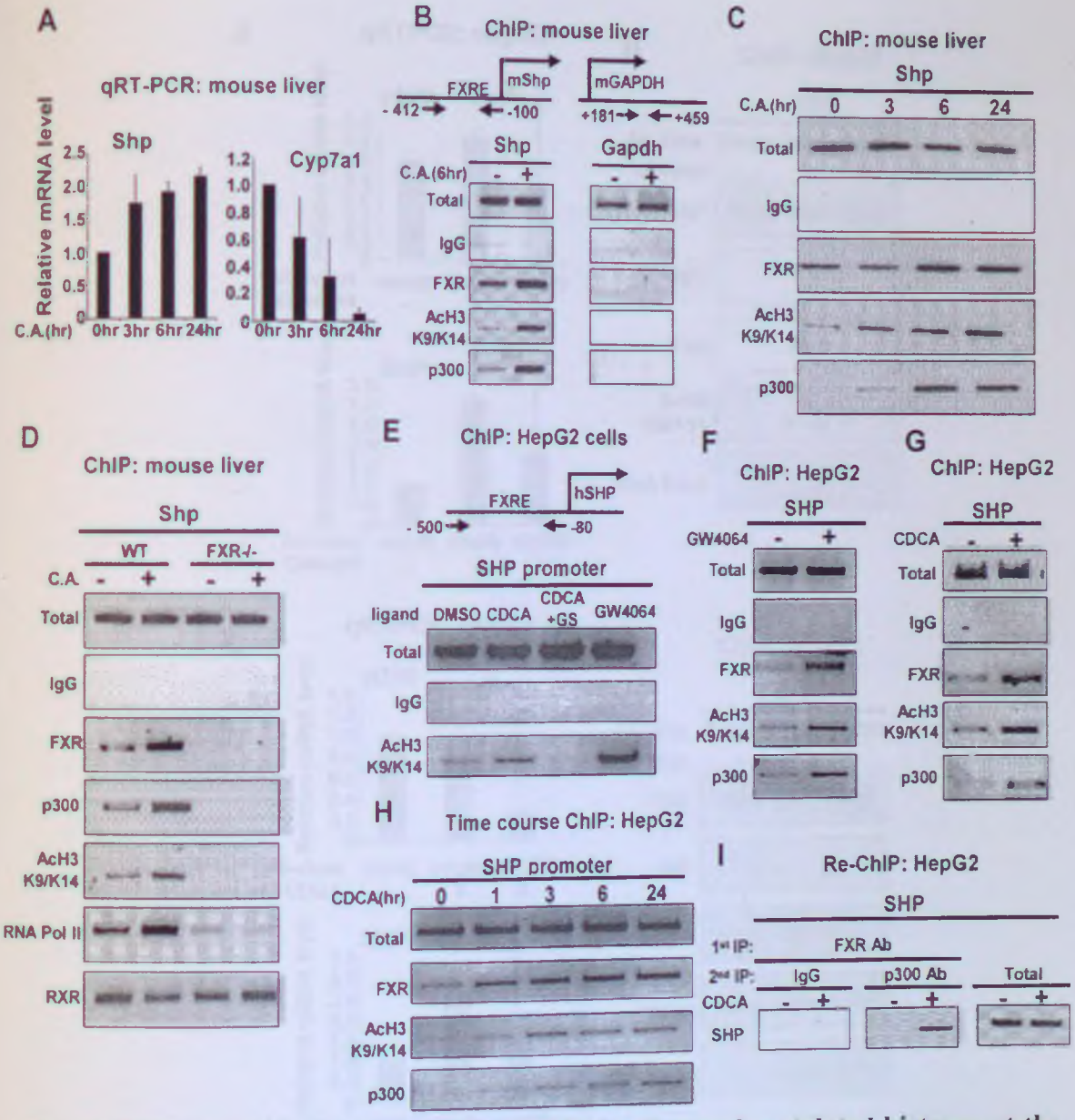

Fig. 2. FXR agonist treatment increases FXR binding and acetylated histones at the SHP promoter. Mice were fed normal or CA chow for the indicated times and livers were collected for analyses. (A) Levels of mRNA were determined by qRT-PCR and the mRNA levels were normalized to those of 36B4 (n=3). (B-D) Liver extracts were subjected to ChIP assays, and DNA in the immunoprecipitates was detected by PCR using primers specific to the SHP promoter or GAPDH gene control. Consistent results were obtained from 3 independent assays. (D) ChIP assays were done with FXR-null mice in parallel with normal mice. (E-I) Promoter occupancy was detected by ChIP assays in HepG2 cells. (E) HepG2 cells were treated with 1 μM GW4064, 50 μM CDCA in the presence or absence of 30 μM guggulesterone for 6 hr and cells were subjected to ChIP assays. (F-H) HepG2 cells were treated with GW4064 (F) or CDCA (G) for 3 hr. HepG2 cells were treated with CDCA for indicated times (H). (I) In re-ChIP assays, re-chromatin was first immunoprecipitated with antisera to FXR and then re-immunoprecipitated with IgG or p300 antibody. SHP promoter sequences in the second immunoprecipitates were detected by PCR.

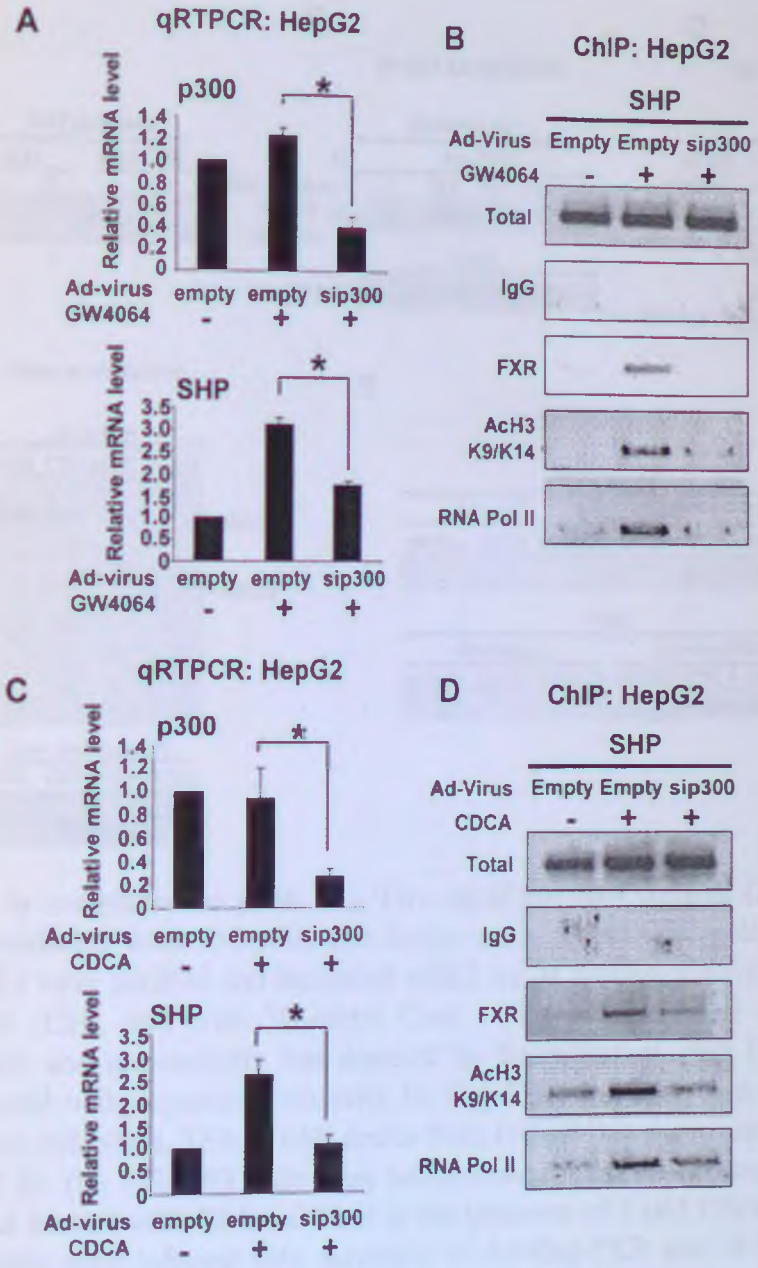

Fig. 3. Increased FXR binding and histone acetylation at the SHP promoter is p300 dependent. Two sets of HepG2 cells were infected with Ad-sip300 (sip300) or Ad-empty (empty) and 3 days later, cells were further treated with CDCA or GW4064. Cells were harvested for q-RTPCR (A, C) or ChIP assays (B, D). The SEM was determined for statistical significances as by Student's t test, * $p < 0.05$ (n=3).

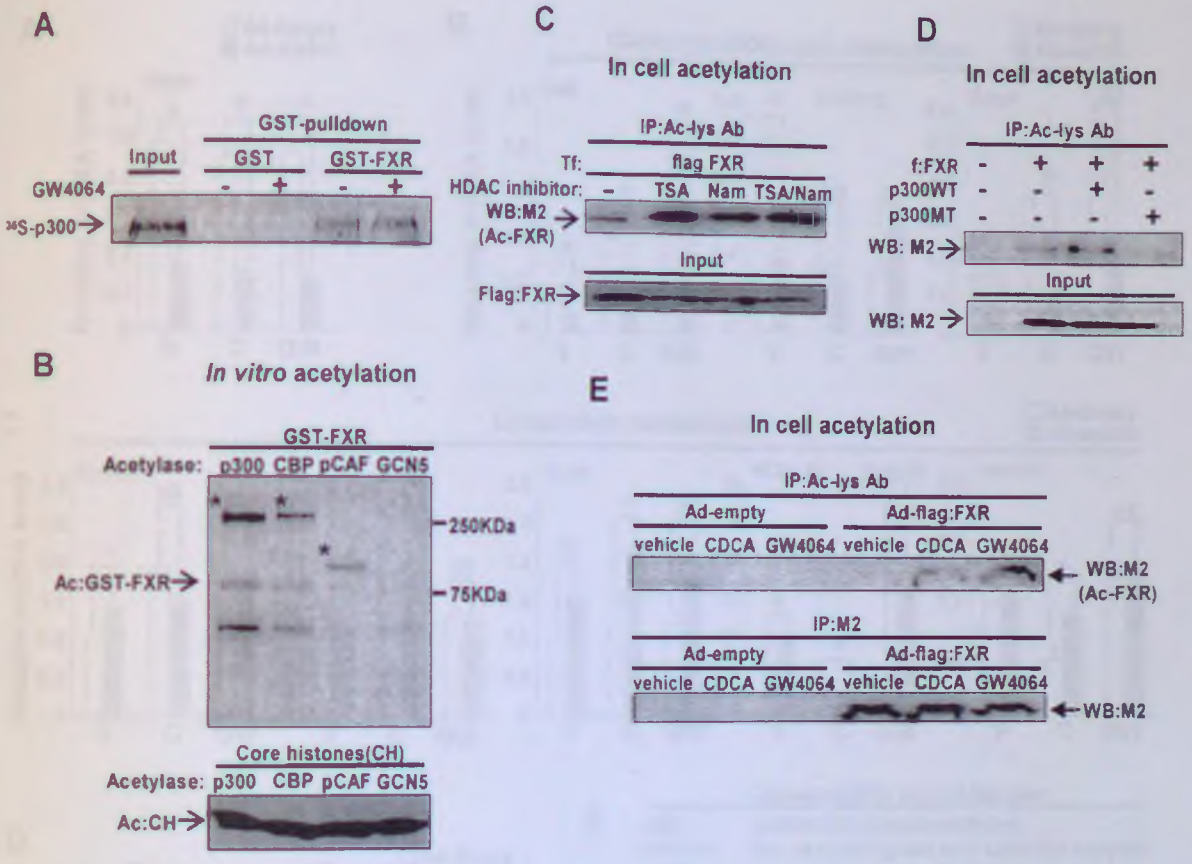

Fig. 4. FXR is acetylated by p300. (A). Two μg of purified control GST or GST-FXR was incubated with 35S-p300 and further subjected to GST pull down assay. (B) The HATs were purified and incubated with 2 μg of purified GST-FXR, GST, or core histones (CH), and with 3H-acetyl CoA. The proteins were separated by electrophoresis and radioactivity was detected by fluorography. (C) HEK293 cells were transfected with expression plasmids for flag-FXR and cells were treated with the deacetylase inhibitors, TSA (1 μM) and/or Nam (10 mM) in the presence of 25 μM CDCA for 6 hr. (D) HEK293 cells were cotransfected with expression plasmids as indicated, and treated with TSA and Nam in the presence of 1 μM GW4064 for 6 hr. (E) HepG2 cells were infected with Ad-empty or Ad-flag-FXR and 24 hr later, cells were treated with CDCA, GW4064 or vehicle in the presence of TSA and Nam for 2.5 hr and cells extracts were prepared. (C-E) Acetylated proteins were immunoprecipitated from cell extracts with acetyl lysine antibody and FXR in the immunoprecipitates and total FXR were detected with M2 antibody.

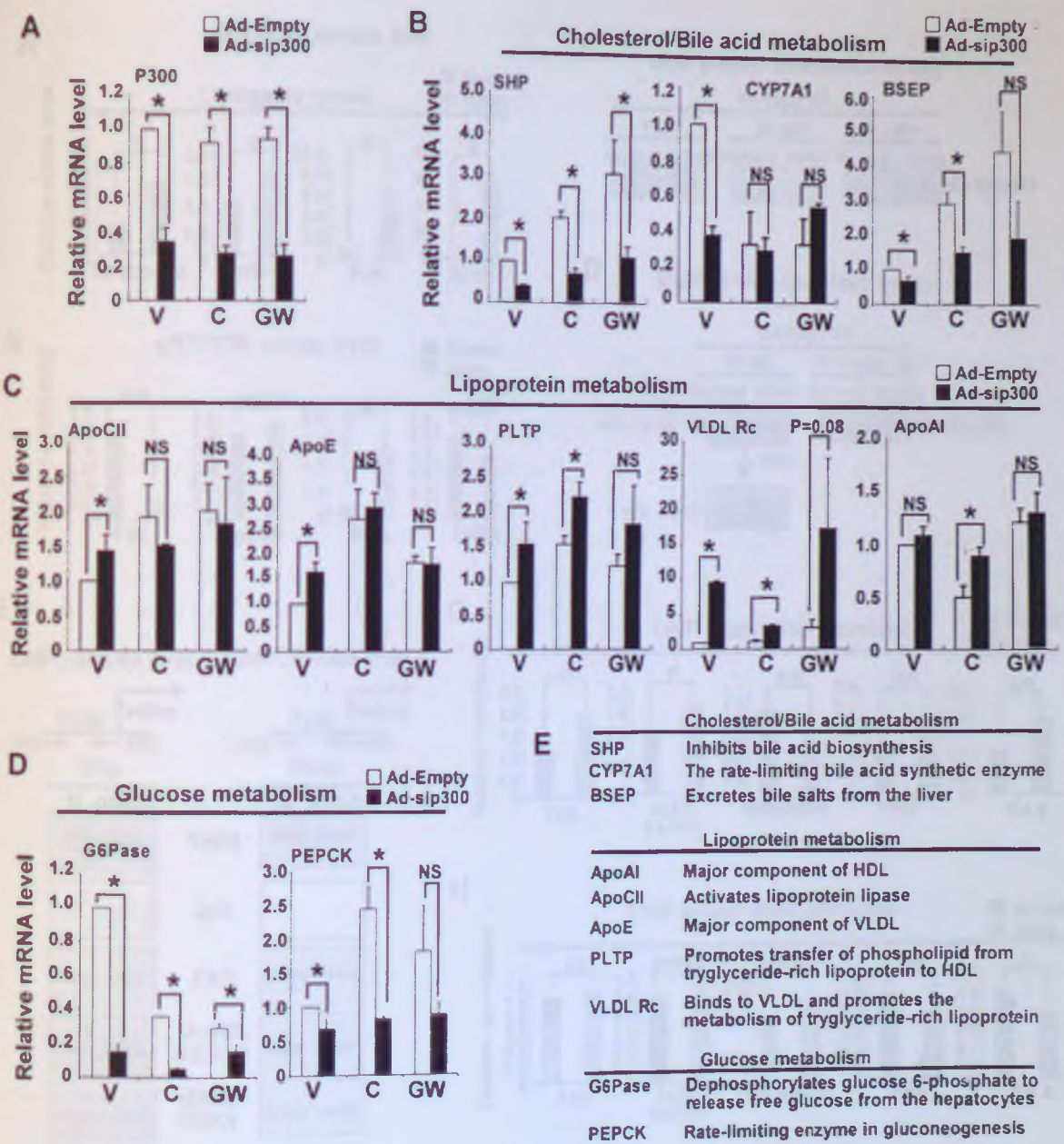

Fig. 5. Effects of p300 down-regulation on expression of metabolic FXR target genes (A-D) HepG2 cells were infected with Ad-sip300 or Ad-empty and 3 days later, cells were treated with ligands overnight and the mRNA levels of FXR target genes were determined by qRT-PCR. V, C, and GW indicate vehicle, 50 μM CDCA, and 100 nM GW4064, respectively. Statistical significance was determined by the Student t test, * $p < 0.05$, NS indicates not statistically significant (n=3). (E) FXR target genes examined in this study are listed with a brief description of the function of the gene product.

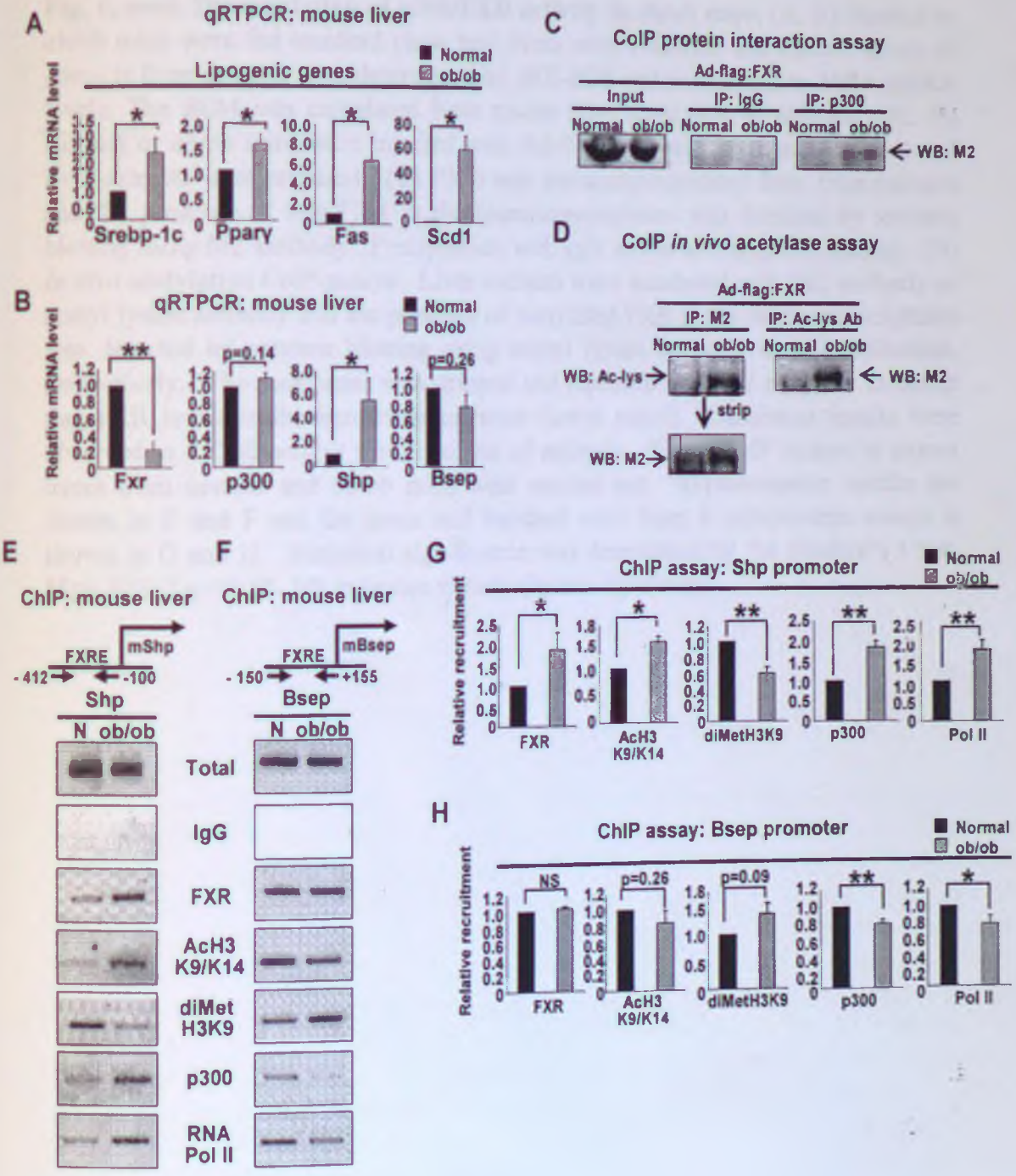
A
qRTPCR: mouse liver
Lipogenic genes
Normal
ob/ob
Relative mRNA level
Srebp-1c
Pparγ
Fas
Scd1
B
qRTPCR: mouse liver
Normal
ob/ob
Relative mRNA level
p=0.14
p=0.26
Fxr
p300
Shp
Bsep
C
CoIP protein interaction assay
Ad-flag:FXR
Input
IP: IgG
IP: p300
Normal ob/ob Normal ob/ob Normal ob/ob
WB: M2
D
CoIP in vivo acetylase assay
Ad-flag:FXR
IP: M2
IP: Ac-lys Ab
Normal ob/ob Normal ob/ob
WB: Ac-lys
WB: M2
strip
WB: M2
E
ChIP: mouse liver
FXRE
mShp
-412
-100
Shp
N ob/ob
F
ChIP: mouse liver
FXRE
mBsep
-150
+155
Bsep
N ob/ob
Total
IgG
FXR
AcH3 K9/K14
diMet H3K9
p300
RNA Pol II
G
ChIP assay: Shp promoter
Normal
ob/ob
Relative recruitment
FXR
AcH3 K9/K14
diMetH3K9
p300
Pol II
H
ChIP assay: Bsep promoter
Normal
ob/ob
Relative recruitment
NS
p=0.26
p=0.09
FXR
AcH3 K9/K14
diMetH3K9
p300
Pol II

Fig. 6, cont.

Fig. 6, cont. Dysregulation of p300/FXR activity in ob/ob mice. (A, B) Normal or ob/ob mice were fed standard chow and livers were collected and mRNA levels of genes in liver extracts were determined by qRT-PCR and normalized to 36B4 mRNA levels. The SEM was calculated from results from three sets of animals. (C, D) Normal or ob/ob mice were injected with Ad-flag-FXR and fed standard chow and liver extracts were prepared. (C) P300 was immunoprecipitated from liver extracts and the presence of flag-FXR in the immunoprecipitates was detected by western blotting using M2 antibody. Precipitation with IgG served as a negative control. (D) *In vivo* acetylation CoIP assays. Liver extracts were incubated with M2 antibody or acetyl lysine antibody and the presence of acetylated FXR in the immunoprecipitates was detected by western blotting using acetyl lysine antibody or M2 antibodies, respectively. The membrane was stripped and reprobed with M2 antibody to detect flag-FXR levels in the immunoprecipitates (lower panel). Consistent results were observed in 4 CoIP assays from two sets of animals. (E. H) ChIP assays in mouse livers from normal and ob/ob mice were carried out. Representative results are shown in E and F and the mean and standard error from 4 independent assays is shown in G and H. Statistical significance was determined by the Student's t test. $^{**}p< 0.01$ * $p < 0.05$, NS indicates statistically not significant.

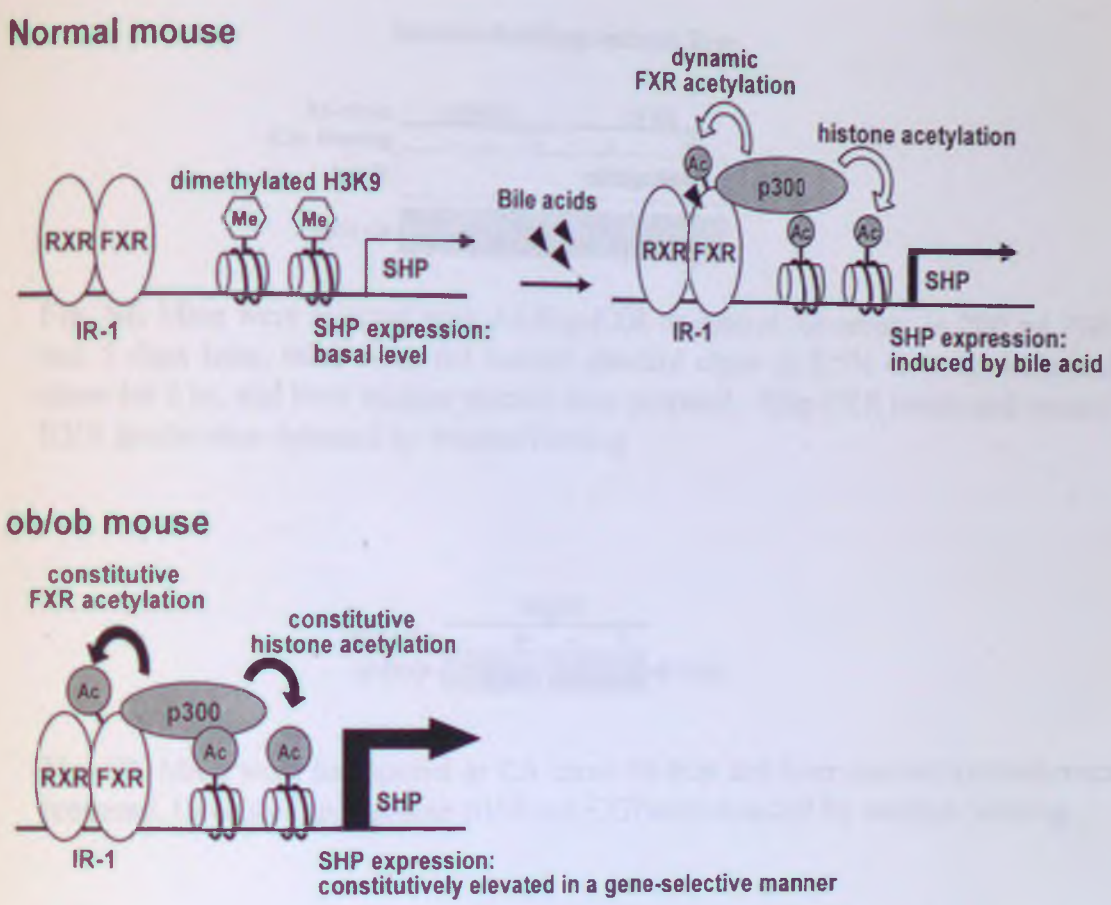

Fig. 7. Regulation of FXR activity by p300 in normal and ob/ob mice In normal mice, p300 is critical in FXR-mediated SHP expression in bile acid signaling. Unliganded FXR/RXR heterodimers are associated with the promoter and histones H3 are dimethylated at H3K9 (repressive histone mark), resulting in low basal levels of SHP expression. Activation of FXR signaling by CA feeding or FXR agonists increases the FXR interaction with p300 and recruits p300 to the SHP promoter, resulting in transient increases in both FXR acetylation and histone H3 acetylation at K9/14 (activated histone mark) with concomitant demethylation at K9. FXR binding to the promoter is also increased. These changes result in transient induction of the SHP gene in response to bile acids. In contrast, in ob/ob mice, the p300/FXR pathway is dysregulated. Despite surprisingly low expression of FXR, the interaction of p300 with FXR and recruitment of p300/FXR to the SHP promoter are highly elevated. Protein complex at the SHP promoter and modification of histones in ob/ob mice fed normal chow resemble those of normal mice after CA feeding, except that the expression of SHP is constitutively elevated in the ob/ob mice with constitutive acetylation of FXR and histones at the promoter. These effects are specific to the SHP gene because they were not detected at the BSEP promoter, another well known direct FXR target.

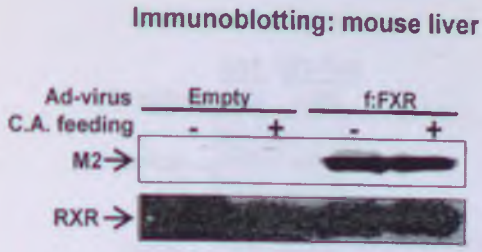

Fig. S1. Mice were injected with Ad-flag-FXR or control Ad-empty in 200 ml PBS and 5 days later, mice were fed normal standard chow or 0.5% CA-supplemented chow for 6 hr, and liver nuclear extracts were prepared. Flag-FXR levels and control RXR levels were detected by western blotting.

Fig. S2. Mice were fed normal or CA chow for 6 hr and liver nuclear extracts were prepared. Levels of endogenous p300 and FXR were detected by western blotting.

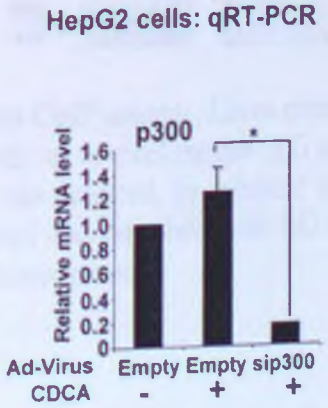

Fig. S3. HepG2 cells in 24 well plates were infected with 5-25 MOI of Ad-sip300 or Ad-empty and 2 days later, the cells were treated with 50 mM CDCA or vehicle overnight. Then, levels of p300 mRNA were determined by qRT-PCR and the mRNA levels were normalized to those of 36B4 (n=3).

Fig. S4. Two mg of purified GST or GST-FXR was incubated with purified p300 in the presence of ^{3}H-acetyl CoA. The proteins were separated by electrophoresis and radioactivity was detected by fluorography. Acetylated GST-FXR (about 85kd) is indicated by an arrow. Auto-acetylated p300 is indicated by an asterisk.

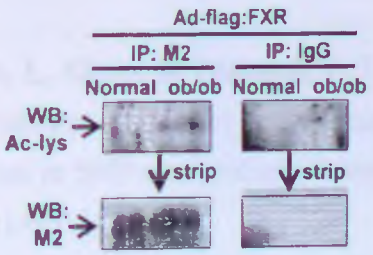

Fig. S5. *In vivo* acetylation CoIP assays. Liver extracts from normal or ob/ob mice were incubated with M2 antibody or control mouse IgG and the presence of acetylated FXR in the immunoprecipitates was detected by western blotting using acetyl lysine antibody. The membrane was stripped and reprobed with M2 antibody to detect flag-FXR levels in the immunoprecipitates (lower panel).

References

1. **Ananthanarayanan, M., S. Li, N. Balasubramaniyan, F. J. Suchy, and M. J. Walsh.** 2004. Ligand-dependent activation of the farnesoid X-receptor directs arginine methylation of histone H3 by CARM1. J Biol Chem **279:**54348-57.

2. **Bavner, A., S. Sanyal, J. A. Gustafsson, and E. Treuter.** 2005. Transcriptional corepression by SHP: molecular mechanisms and physiological consequences. Trends Endocrinol Metab **16:**478-88.

3. **Boulias, K., N. Katrakili, K. Bamberg, P. Underhill, A. Greenfield, and I. Talianidis.** 2005. Regulation of hepatic metabolic pathways by the orphan nuclear receptor SHP. Embo J **24:**2624-33.

4. **Chiang, J. Y. L.** 1998. Regulation of bile acid synthesis. Front. Biosci. **3:**D176-D193.

5. **Fang, S., J. Miao, L. Xiang, B. Ponugoti, E. Treuter, and J. K. Kemper.** 2007. Coordinated recruitment of histone methyltransferase G9a and other chromatin modifying enzymes in SHP-mediated regulation of hepatic bile acid metabolism. Mol Cell Biol **27:**1407-1424.

6. **Fu, M., M. Rao, C. Wang, T. Sakamaki, J. Wang, D. Di Vizio, X. Zhang, C. Albanese, S. Balk, C. Chang, S. Fan, E. Rosen, J. J. Palvimo, O. A. Janne, S. Muratoglu, M. L. Avantaggiati, and R. G. Pestell.** 2003. Acetylation of androgen receptor enhances coactivator binding and promotes prostate cancer cell growth. Mol Cell Biol **23:**8563-75.

7. **Goodwin, B., S. A. Jones, R. R. Price, M. A. Watson, D. D. McKee, L. B. Moore, C. Galardi, J. G. Wilson, M. C. Lewis, M. E. Roth, P. R. Maloney, T. M. Wilson, and S. A. Kliewer.** 2000. A regulatory cascade of the nuclear receptors FXR, SHP-1, and LRH-1 represses bile acid biosynthesis. Molecular Cell **6:**517-526.

8. **Gu, W., and R. G. Roeder.** 1997. Activation of p53 sequence-specific DNA binding by acetylation of the p53 C-terminal domain. Cell **90:**595-606.

9. **Herzig, S., F. Long, U. S. Jhala, S. Hedrick, R. Quinn, A. Bauer, D. Rudolph, G. Schutz, C. Yoon, P. Puigserver, B. Spiegelman, and M. Montminy.** 2001. CREB regulates hepatic gluconeogenesis through the coactivator PGC-1. Nature **413:**179-83.

10. **Huang, J., J. Iqbal, P. K. Saha, J. Liu, L. Chan, M. M. Hussain, D. D. Moore, and L. Wang.** 2007. Molecular characterization of the role of orphan receptor small heterodimer partner in development of fatty liver. Hepatology **46:**147-57.

11. **Huang, W., K. Ma, J. Zhang, M. Qatanani, J. Cuvillier, J. Liu, B. Dong, X. Huang, and D. D. Moore.** 2006. Nuclear receptor-dependent bile acid signaling is required for normal liver regeneration. Science **312:**233-6.

12. **Inagaki, T., A. Moschetta, Y. K. Lee, L. Peng, G. Zhao, M. Downes, R. T. Yu, J. M. Shelton, J. A. Richardson, J. J. Repa, D. J. Mangelsdorf, and S. A. Kliewer.** 2006. Regulation of antibacterial defense in the small intestine by the nuclear bile acid receptor. Proc Natl Acad Sci U S A **103:**3920-5.

13. **Jelinek, D. F., S. Andersson, C. A. Slaughter, and D. W. Russell.** 1990. Cloning and regulation of cholesterol 7alpha-hydroxylase, the rate-limiting enzyme in bile acid biosynthesis. Journal of Biological Chemistry **265:**8190-8197.

14. **Jenuwein, T., and C. D. Allis.** 2001. Translating the histone code. Science **293:**1074-80.

15. **Kalaany, N. Y., and D. J. Mangelsdorf.** 2006. LXRS and FXR: the yin and yang of cholesterol and fat metabolism. Annu Rev Physiol **68:**159-91.

16. **Kemper, J., H. Kim, J. Miao, S. Bhalla, and Y. Bae.** 2004. Role of a mSin3A-Swi/Snf chromatin remodeling complex in the feedback repression of bile acid biosynthesis by SHP. Mol Cell Biol **24:**7707-7719.

17. **Kerr, T. A., S. Saeki, M. Schneider, K. Schaefer, S. Berdy, T. Redder, B. Shan, D. W. Russell, and M. Schwarz.** 2002. Loss of nuclear receptor SHP impairs but does not eliminate negative feedback regulation of bile acid synthesis. Developmental Cell **2**:713-720.

18. **Kim, J. Y., H. J. Kim, K. T. Kim, Y. Y. Park, H. A. Seong, K. C. Park, I. K. Lee, H. Ha, M. Shong, S. C. Park, and H. S. Choi.** 2004. Orphan nuclear receptor small heterodimer partner represses hepatocyte nuclear factor 3/Foxa transactivation via inhibition of its DNA binding. Mol Endocrinol **18**:2880-94.

19. **Kim, M. Y., E. M. Woo, Y. T. Chong, D. R. Homenko, and W. L. Kraus.** 2006. Acetylation of estrogen receptor alpha by p300 at lysines 266 and 268 enhances the deoxyribonucleic acid binding and transactivation activities of the receptor. Mol Endocrinol **20**:1479-93.

20. **Kouzarides, T.** 2002. Histone methylation in transcriptional control. Curr Opin Genet Dev **12**:198-209.

21. **Lazar, M. A.** 2003. Nuclear receptor corepressors. Nucl Recept Signal **1**:e001.

22. **Lee, Y., and D. D. Moore.** 2002. Dual mechanism for repression of the monomeric orphan receptor liver receptor homologous protein-1 (LRH-1) by the orphan small heterodimer partner (SHP). Journal of Biological Chemistry **277**:2463-2467.

23. **Lerin, C., J. T. Rodgers, D. E. Kalume, S. H. Kim, A. Pandey, and P. Puigserver.** 2006. GCN5 acetyltransferase complex controls glucose metabolism through transcriptional repression of PGC-1alpha. Cell Metab **3**:429-38.

24. **Lin, J., C. Handschin, and B. M. Spiegelman.** 2005. Metabolic control through the PGC-1 family of transcription coactivators. Cell Metab **1**:361-70.

25. **Lin, J., P. H. Wu, P. T. Tarr, K. S. Lindenberg, J. St-Pierre, C. Y. Zhang, V. K. Mootha, S. Jager, C. R. Vianna, R. M. Reznick, L. Cui, M. Manieri, M. X. Donovan, Z. Wu, M. P. Cooper, M. C. Fan, L. M. Rohas, A. M. Zavacki, S. Cinti, G. I. Shulman, B. B. Lowell, D. Krainc, and B. M. Spiegelman.** 2004. Defects in adaptive energy metabolism with CNS-linked hyperactivity in PGC-1alpha null mice. Cell **119**:121-35.

26. **Lu, T. T., M. Makishima, J. J. Repa, K. Schoonjans, T. A. Kerr, J. Auwerx, and D. J. Mangelsdorf.** 2000. Molecular basis for feedback regulation of bile acid synthesis by nuclear receptors. Mol Cell **6**:507-15.

27. **Luo, J., M. Li, Y. Tang, M. Laszkowska, R. G. Roeder, and W. Gu.** 2004. Acetylation of p53 augments its site-specific DNA binding both in vitro and in vivo. Proc Natl Acad Sci U S A **101**:2259-64.

28. **Ma, K., P. K. Saha, L. Chan, and D. D. Moore.** 2006. Farnesoid X receptor is essential for normal glucose homeostasis. J Clin Invest **116**:1102-9.

29. **Makishima, M., A. Y. Okamoto, J. J. Repa, H. Tu, M. Learned, A. Luk, M. V. Hull, K. D. Lustig, D. J. Mangelsdorf, and B. Shan.** 1999. Identification of a nuclear receptor for bile acids. Science **284**:1362-1365.

30. **Mangelsdorf, D. J., and R. M. Evans.** 1995. The RXR heterodimers and orphan receptors. Cell **83**:841-850.

31. **Martinez-Balbas, M. A., U. M. Bauer, S. J. Nielsen, A. Brehm, and T. Kouzarides.** 2000. Regulation of E2F1 activity by acetylation. Embo J **19**:662-71.

32. **Matsuzaki, H., H. Daitoku, M. Hatta, H. Aoyama, K. Yoshimochi, and A. Fukamizu.** 2005. Acetylation of Foxo1 alters its DNA-binding ability and sensitivity to phosphorylation. Proc Natl Acad Sci U S A **102**:11278-83.

33. **Miao, J., S. Fang, Y. Bae, and J. K. Kemper.** 2006. Functional inhibitory cross-talk between car and HNF-4 in hepatic lipid/glucose metabolism is mediated by competition for binding to the DR1 motif and to the common coactivators, GRIP-1 and PGC-1alpha. J Biol Chem **281**:14537-46.

34. **Muraoka, M., M. Konishi, R. Kikuchi-Yanoshita, K. Tanaka, N. Shitara, J. M. Chong, T. Iwama, and M. Miyaki.** 1996. p300 gene alterations in colorectal and gastric carcinomas. Oncogene **12**:1565-9.

35. **Ogryzko, V. V., R. L. Schiltz, V. Russanova, B. H. Howard, and Y. Nakatani.** 1996. The transcriptional coactivators p300 and CBP are histone acetyltransferases. Cell **87**:953-959.

36. **Pineda Torra, I., L. P. Freedman, and M. J. Garabedian.** 2004. Identification of DRIP205 as a coactivator for the Farnesoid X receptor. J Biol Chem **279**:36184-91.

37. **Ponugoti, B., S. Fang, and J. K. Kemper.** 2007. Functional interaction of HNF-4 and PGC-1{alpha} in CYP7A1 regulation is inhibited by a key lipogenic activator, SREBP-1c. Mol Endocrinol.

38. **Puigserver, P., and B. M. Spiegelman.** 2003. Peroxisome proliferator-activated receptor-gamma coactivator 1 alpha (PGC-1 alpha): transcriptional coactivator and metabolic regulator. Endocr Rev **24**:78-90.

39. **Rizzo, G., B. Renga, E. Antonelli, D. Passeri, R. Pellicciari, and S. Fiorucci.** 2005. The methyl transferase PRMT1 functions as co-activator of farnesoid X receptor (FXR)/9-cis retinoid X receptor and regulates transcription of FXR responsive genes. Mol Pharmacol **68**:551-8.

40. **Rodgers, J. T., C. Lerin, W. Haas, S. P. Gygi, B. M. Spiegelman, and P. Puigserver.** 2005. Nutrient control of glucose homeostasis through a complex of PGC-1alpha and SIRT1. Nature **434**:113-8.

41. **Rosenfeld, M., and C. Glass.** 2001. Coregulator codes of transcriptional regulation by nuclear receptors. Journal of Biological Chemistry **276**:36865-36868.

42. **Russell, D. W.** 1999. Nuclear orphan receptors control cholesterol catabolism. Cell **97**:539-542.

43. **Seol, W., H. Choi, and D. D. Moore.** 1996. An orphan nuclear hormone receptor that lacks a DNA binding domain and heterodimerizes with other receptors. Science **272**:1336-1339.

44. **Sinal, C., M. Tohkin, M. Miyata, J. Ward, G. Lambert, and F. J. Gonzalez.** 2000. Targeted disruption of the nuclear receptor FXR/BAR impairs bile acid and lipid homeostasis. Cell **102**:731-744.

45. **Soutoglou, E., N. Katrakili, and I. Talianidis.** 2000. Acetylation regulates transcription factor activity at multiple levels. Mol Cell **5**:745-51.

46. **Thomas, M. C., and C. M. Chiang.** 2005. E6 oncoprotein represses p53-dependent gene activation via inhibition of protein acetylation independently of inducing p53 degradation. Mol Cell **17**:251-64.

47. **Urizar, N. L., A. B. Liverman, D. T. Dodds, F. V. Silva, P. Ordentlich, Y. Yan, F. J. Gonzalez, R. A. Heyman, D. J. Mangelsdorf, and D. D. Moore.** 2002. A natural product that lowers cholesterol as an antagonist ligand for FXR. Science **296**:1703-6.

48. **Wang, H., J. Chen, K. Hollister, L. Sowers, and B. M. Forman.** 1999. Endogenous bile acids are ligands for the nuclear receptor FXR/BAR. Molecular Cell **3**:543-553.

49. **Wang, L., Y. Lee, D. Bundman, Y. Han, S. Thevananther, C. Kim, S. Chua, P. Wei, R. Heyman, M. Karin, and D. Moore.** 2002. Redundant pathways for negative feedback regulation of bile acid production. Developmental Cell **2**:721-731.

50. **Wang, L., J. Liu, P. Saha, J. Huang, L. Chan, B. Spiegelman, and D. D. Moore.** 2005. The orphan nuclear receptor SHP regulates PGC-1alpha expression and energy production in brown adipocytes. Cell Metab **2**:227-38.

51. **Watanabe, M., S. M. Houten, L. Wang, A. Moschetta, D. J. Mangelsdorf, R. A. Heyman, D. D. Moore, and J. Auwerx.** 2004. Bile acids lower triglyceride levels via a pathway involving FXR, SHP, and SREBP-1c. Journal of Clinical Investigation **113**:1408-18.

52. **Willson, T. M., S. A. Jones, J. T. Moore, and S. A. Kliewer.** 2001. Chemical genomics: functional analysis of orphan nuclear receptors in the regulation of bile acid metabolism. Med Res Rev **21**:513-22.

53. **Yao, T. P., S. P. Oh, M. Fuchs, N. D. Zhou, L. E. Ch'ng, D. Newsome, R. T. Bronson, E. Li, D. M. Livingston, and R. Eckner.** 1998. Gene dosage-dependent embryonic development and proliferation defects in mice lacking the transcriptional integrator p300. Cell **93**:361-72.

54. **Yoon, J. C., P. Puigserver, G. Chen, J. Donovan, Z. Wu, J. Rhee, G. Adelmant, J. Stafford, C. R. Kahn, D. K. Granner, C. B. Newgard, and B. M. Spiegelman.** 2001. Control of hepatic gluconeogenesis through the transcriptional coactivator PGC-1. Nature **413**:131-8.

55. **Zhang, Y., L. W. Castellani, C. J. Sinal, F. J. Gonzalez, and P. A. Edwards.** 2004. Peroxisome proliferator-activated receptor-gamma coactivator 1alpha (PGC-1alpha) regulates triglyceride metabolism by activation of the nuclear receptor FXR. Genes Dev **18**:157-69.

56. **Zhang, Y., F. Y. Lee, G. Barrera, H. Lee, C. Vales, F. J. Gonzalez, T. M. Willson, and P. A. Edwards.** 2006. Activation of the nuclear receptor FXR improves hyperglycemia and hyperlipidemia in diabetic mice. Proc Natl Acad Sci U S A **103**:1006-11.

Chapter Four

Preliminary additional studies

LSD-1 is a potential cofactor in SHP-mediated CYP7A1 inhibition

Post-translational modifications of histones control gene expression by altering chromatin structure or by serving as platforms to recruit other cofactors. Among histone modifications, methylation was thought to be an irreversible modification until a demethylase was recently identified for the first time. In 2004, it was found that lysine specific demethylase (LSD-1) is a bona fide histone lysine demethylase (12).

LSD-1, a nuclear amine oxidase homolog, contains the C-terminal amine oxidase domain and a central SWIRM (SWI3p, Rsc8p and Moira) domain. SWIRM domains have been found in many chromatin-associated proteins and might serve as DNA binding motifs (1, 4). The oxidation reaction by LSD-1 reverses methylated lysines to unmodified lysines in a FAD-dependent manner. LSD-1 specifically demethylates mono- and di-methylated H3K4 whereas demethylation of tri-methylated H3K4 is prevented in the absence of protonated nitrogen which is required for oxidation reaction (12). In general, methylation of H3K4 is likely related to gene activation, and in contrast, its demethylation accompanies gene repression. Thus, the role of LSD-1 to remove the gene activation mark on H3K4 contributes to suppression of gene transcription. Recently, it was reported that LSD-1 is present in a ligand-activated androgen receptor complex and is able to demethylate mono- and dimethylated H3K9 to induce gene expression (9), suggesting that LSD-1 may serve as both a coactivator and a corepressor to regulate gene expression.

Previously, I reported that SHP represses CYP7A1 gene transcription by interacting with histone methyltransferase G9a which methylates H3K9 at the promoter of CYP7A1. Since histone modifications do not occur independently but affect each other to modulate gene transcription, I have further examined whether LSD-1 is involved in SHP-mediated CYP7A1 repression through demethylation of H3K4 in bile acid signaling.

First, I examined if LSD-1 directly interacts with SHP *in vitro*. GST fusions with SHP or fragments of SHP (Fig.1A) that had been bound to glutathione-Sepharose were incubated with ^{35}S-labeled LSD-1. LSD-1 bound to SHP or SHP mutants containing the N-terminal domain (1-92 amino acids), whereas no binding was detected with SHP mutants lacking this region (Fig.1A). Consistent with this result, ^{35}S-labeled SHP bound to GST fusioned LSD-1 protein (Fig.1B), suggesting that LSD-1 directly interacts with SHP *in vitro*. To test if LSD-1 associates with SHP in mouse hepatocytes *in vivo*, the interaction between SHP and LSD-1 in mouse hepatocytes was examined by co-immunoprecipitation. SHP was detected in the anti-LSD-1 immunoprecipitates and conversely, LSD-1 was detected in the anti-SHP immunopreciptiates (data not shown). These results indicate that SHP directly interacts with LSD-1 in hepatic cells.

To examine whether exogenously expressed LSD-1 increases the inhibitory activity of SHP, transient reporter assays were performed. Transfection of increasing amounts LSD-1 expression plasmid with a constant amount of SHP plasmid increased inhibition of the HNF-4/ PGC-1α activation in a dose-dependent manner (Fig.2A). To test if LSD-1 inhibition of HNF-4/PGC-1α activation is dependent on SHP, LSD-1 was expressed in transfected Cos-1 cells with or without expression of SHP. In the absence

of SHP, LSD-1 had little effect on the inhibition of HNF-4/PGC-1α transactivation (Fig.2B), suggesting that SHP is required for the inhibitory effect of LSD-1. To evaluate the role of LSD-1 in the inhibitory activity of SHP, exogenous plasmids expressing siRNA against LSD-1 were co-transfected with reporter genes. Transient knock-down of LSD-1 completely reversed the combinatorial inhibitory activity of SHP and LSD-1 using Gal4 reporter system in Cos-1 cells (Fig.2C) and CYP7A1 promoter-luciferase system in HepG2 cells (Fig.2D). Transient knock-down of endogenous LSD-1 by siRNA completely reversed the bile acid-mediated repression of the CYP7A1 gene expression (Fig.2E,F), suggesting that LSD-1 is involved in SHP-mediated suppression of CYP7A1 expression.

If the interaction of LSD-1 with SHP is physiologically relevant for bile acid metabolism, then LSD-1 should be recruited to the transcriptionally suppressed promoters of CYP7A1, the well-known SHP target gene, in mice fed cholic acid. To examine whether endogenous LSD-1 is recruited to the CYP7A1 promoter in response to cholic acid, ChIP assays were performed in normal-fed or cholic acid-fed mouse. My ChIP assay data showed that recruitment of SHP and LSD-1 and the levels of di-methylated H3K9 were increased whereas the levels of acetylated H3K9/K14 and di-methylated H3K4, the specific substrate of LSD-1, and recruitment of RNA polymerase II were decreased at the promoter of CYP7A1 gene with bile acid treatment *in vivo* (Fig.3).

Thus, my preliminary data suggest that LSD-1 is a potential corepressor which enhances the inhibitory activity of SHP by demethylation of H3K4 to suppress CYP7A1 transcription in response to bile acid signaling.

SIRT1 antagonizes the p300 mediated-FXR transactivation by deacetylation of FXR

SIRT1, also known as silent mating type information regulation 2 homolog, is an enzyme that deacetylates proteins to regulate cellular processes, such as gene silencing, metabolism and aging (5). Recently, it has been revealed that SIRT1 removes acetyl groups from modified lysines in both histones and regulatory proteins, such as PGC-1α, LXR, and p53 in a NAD^+-dependent manner (2, 8, 10, 11, 14). SIRT1 deacetylase and GCN5 acetylase have been shown to modulate the activity of a coactivator PGC-1α in the regulation of hepatic glucose. While GCN5 decreased PGC-1α activity by altering the intra-nuclear distribution of PGC-1α, SIRT1 increased its activity by deacetylating PGC-1α (7, 11). In addition to its role in deacetylation of transcriptional factors, SIRT1 has been shown to deacetylate histones in chromatin of target genes (6, 13). SIRT1 was shown to be recruited to the promoters of SIRT1 target genes such as PPARγ, a key factor for adipogenesis, and suppressed the expression of this gene by further recruiting the corepressors, NcoR1 and SMRT (10). SIRT1 was also recruited to the promoter of UCP2 gene and inhibited transcription, resulting in increased ATP production and insulin secretion in pancreatic β cells (3).

My recent findings showed that p300 acetylates FXR, as well as histones, to initiate gene transcription. Interestingly, the FXR acetylation was markedly increased by treatment with nicotine amide (NAM), a specific SIRT1 inhibitor, indicating that SIRT1 may be involved in the modulation of FXR activity by FXR deacetylation. Thus, I have examined if SIRT1 has a potential role in the regulation of FXR activity.

To test if SIRT1 is associated with FXR, I examined the interaction of SIRT1 with FXR by coimmunoprecipitation assay. Mice were infected with Ad-flag-FXR or

control Ad-empty and were fed normal chow or 0.5% CA-supplemented chow. Flag-FXR was immunoprecipitated from liver nuclear extracts by M2 and endogenous SIRT1 in the immunoprecipitates was detected by western blotting. The levels of flag-FXR were similar in input samples (data not shown). The interaction of SIRT1 with FXR substantially decreased in the M2 immunoprecipitates after CA feeding (Fig.4A). A similar result was observed in an endogenous experimental setting without expression of flag-FXR. The amount of SIRT1 in the anti-FXR immunoprecipitates was decreased by CA feeding (Fig. 4B), while similar levels of endogenous SIRT1 were detected in the input samples. These CoIP studies indicate that CA feeding decreases the interaction of SIRT1 with FXR in mouse liver, suggesting that SIRT1 may be involved in unliganded-FXR signaling *in vivo*.

Recent studies have shown that SIRT1 deacetylates a number of transcriptional factors. Thus, I tested whether SIRT1 can deacetylate FXR that was acetylated by p300 *in vitro*. GST or GST-FXR proteins were acetylated by p300 *in vitro*. After *in vitro* acetylation assay, samples were subjected to deacetylation assay with SIRT1 in the presence or absence of NAD^+, the SIRT1 cofactor. SIRT1 deacetylated FXR that had been acetylated by p300 in a NAD^+-dependent manner (Fig.5A). To test the functional role of SIRT1 in FXR transactivation, transient reporter assays were performed. My preliminary data showed that SIRT1 antagonizes p300-mediated FXR transactivation (Fig.5B). Consistent with reporter assays, my ChIP data showed that SIRT1 is associated at the native promoter of SHP gene and is dissociated from the promoter of SHP gene by bile acid treatment (Fig.5C), suggesting that SIRT1 functions as a corepressor to suppresses FXR target gene transcription.

Recently, I found that the association of p300 with FXR is markedly increased in obese mice compared to normal mice. Interestingly, my preliminary coimmunoprecipitation data showed that the association of SIRT1 with FXR is markedly decreased in obese mice compared to normal mice (Fig.6A). In addition, SIRT1 is not associated with the SHP native promoter without bile acid feeding in obese mice (Fig.6B), suggesting that the control of FXR transactivation by SIRT1 is dysregulated in disease states, resulting in constitutively elevated SHP gene expression in obese mice.

Thus, my preliminary data suggest that SIRT1 also plays a key role as a deacetylase to control FXR activity and modulate transcription of the FXR target genes in response to bile acid signaling.

Fig. 1. LSD-1 associates with SHP *in vitro*. (A) Schematic diagrams of SHP and full length (FL) GST-SHP, and GST-SHP deletion mutants. RID and RD refer to receptor interacting and intrinsic repression domains, respectively. ^{35}S-LSD-1 was synthesized in vitro, and GST pull down assays were performed. The input represents 10% of the ^{35}S-labeled LSD-1 used in the binding reactions. The position of LSD-1 is indicated. (B). A schematic diagram of the GST-LSD-1. ^{35}S-SHP was synthesized and GST pull down assays were performed. The input represents 10% of the ^{35}S-labeled SHP used in the reactions.

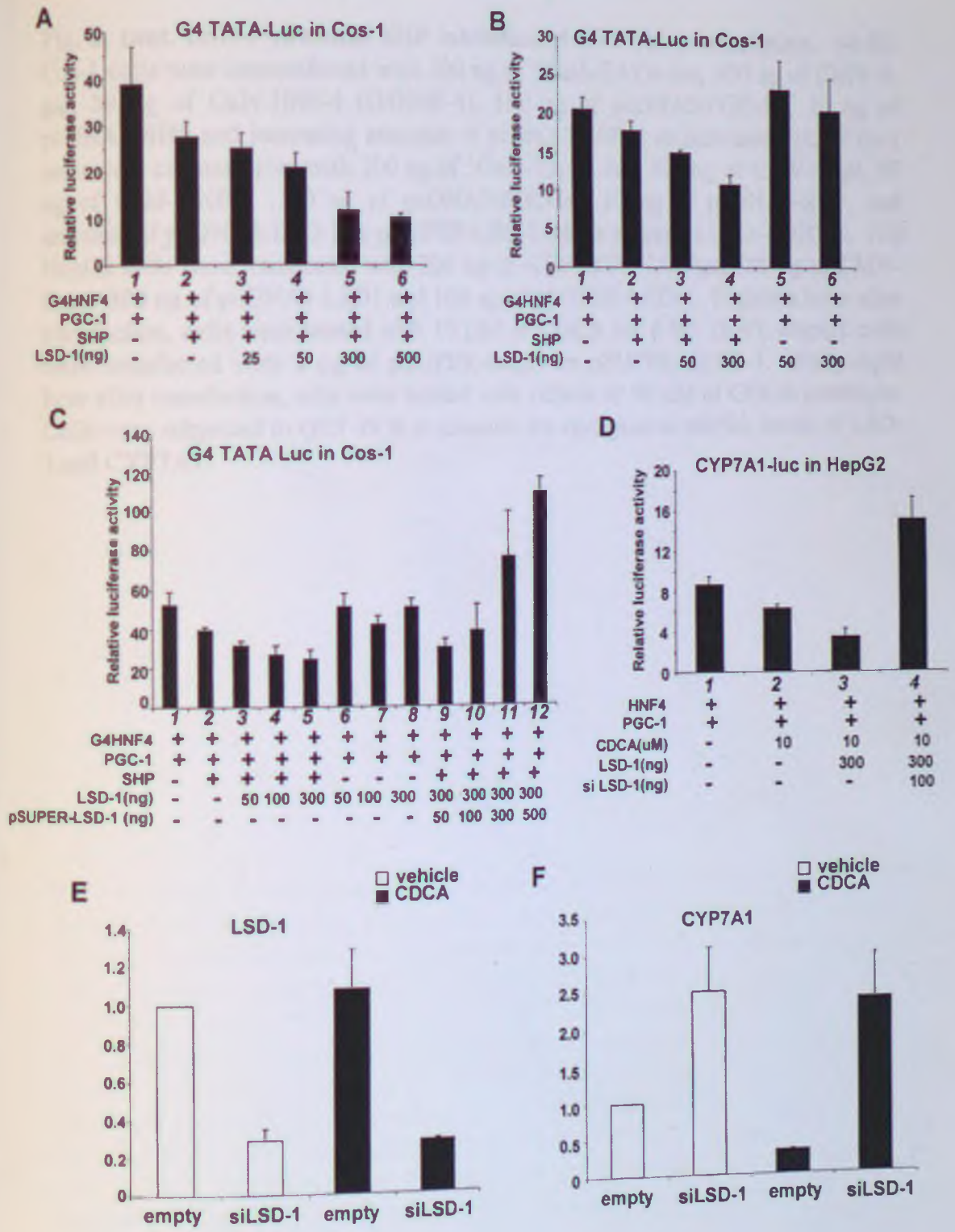
A
G4 TATA-Luc in Cos-1
Relative luciferase activity
G4HNF4
PGC-1
SHP
LSD-1(ng)
B
G4 TATA-Luc in Cos-1
Relative luciferase activity
G4HNF4
PGC-1
SHP
LSD-1(ng)
C
G4 TATA Luc in Cos-1
Relative luciferase activity
G4HNF4
PGC-1
SHP
LSD-1(ng)
pSUPER-LSD-1 (ng)
D
CYP7A1-luc in HepG2
Relative luciferase activity
HNF4
PGC-1
CDCA(uM)
LSD-1(ng)
si LSD-1(ng)
E
vehicle
CDCA
LSD-1
empty
siLSD-1
empty
siLSD-1
F
vehicle
CDCA
CYP7A1
empty
siLSD-1
empty
siLSD-1

Fig. 2, cont.

Fig. 2, cont. LSD-1 enhances SHP inhibition of CYP7A1 transcription. (A-B). Cos-1 cells were cotransfected with 200 ng of 5Gal4-TATA-luc, 300 ng of CMV-ß-gal, 50 ng of Gal4-HNF-4 (G4HNF-4), 100 ng of pcDNA3-PGC-1α, 10 ng of pcDNA3-SHP and increasing amounts of pcDNA3-LSD-1 as indicated. (C). Cos-1 cells were cotransfected with 200 ng of 5Gal4-TATA-luc, 300 ng of CMV-ß-gal, 50 ng of Gal4-HNF-4 , 50 ng of pcDNA3-PGC-1α, 10 ng of pcDNA3-SHP, and amounts of pcDNA3-LSD-1 or pSUPER-LSD-1 which expresses LSD-1 siRNA. (D). HepG2 cells were transfected with 200 ng of -1887 hCYP7A1-luc, 300 ng of CMV-ß-gal, 300 ng of pcDNA3-LSD1 and 100 ng of pSUPER-LSD-1. Eighteen hour after transfection, cells were treated with 10 μM of CDCA for 6 hr. (E-F). HepG2 cells were transfected with 3 μg of pSUPER-empty or pSUPER-siLSD-1. Forty-eight hour after transfection, cells were treated with vehicle or 50 μM of CDCA overnight. Cells were subjected to QRT-PCR to measure the endogenous mRNA levels of LSD-1 and CYP7A1.

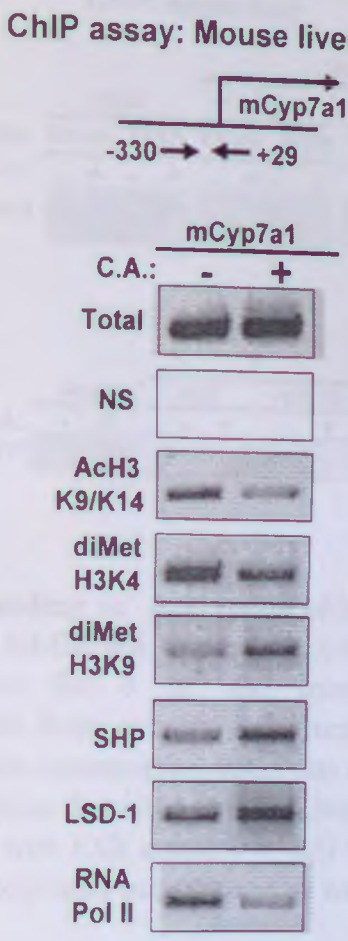

Fig. 3. LSD-1 is recruited to the endogenous CYP7A1 promoter and H3K4 is demethylated in mice fed cholic acid. Mice were fed normal or 0.5% cholic acid (C.A.)-supplemented chow for 24 hr and livers were collected for ChIP assays. At the top, a schematic diagram of the mouse Cyp7a1 promoter with the positions of the primers used for the PCR reactions is shown. Soluble chromatin was isolated and pre-cleared as described in Materials and Methods and immunoprecipitated with antibodies against SHP, LSD-1, diacetylated H3 K9/K14 (di-AcH3 K9/K14), or dimethylated H3K9 (di-Met H3K9), dimethylated H3K4 (di-Met H3K4), RNA polymerase II or normal serum (NS). Precipitated chromatin was extensively washed. Genomic DNA was isolated from the input chromatin before precipitation (total) or from the precipitated chromatin and was analyzed by semi-quantitative PCR using primer sets specific for Cyp7a1.

Fig. 4. Effects of CA feeding on interaction of FXR with SIRT1 in mouse liver (A) Mice infected with Ad-flag-FXR or control Ad-empty were fed normal or 0.5% CA-supplemented chow for 6 hr and livers were collected for CoIP. Immunoprecipitates from liver extracts were incubated with control IgG or M2 antibody and SIRT1 in the immunoprecipitates was detected by western blotting. (B) Uninfected mice were fed as described in (A). Liver extracts were subjected to CoIP and immunoprecipitates with FXR antibody or IgG were isolated and the presence of SIRT1 in the immunoprecipitates was detected by western blotting.

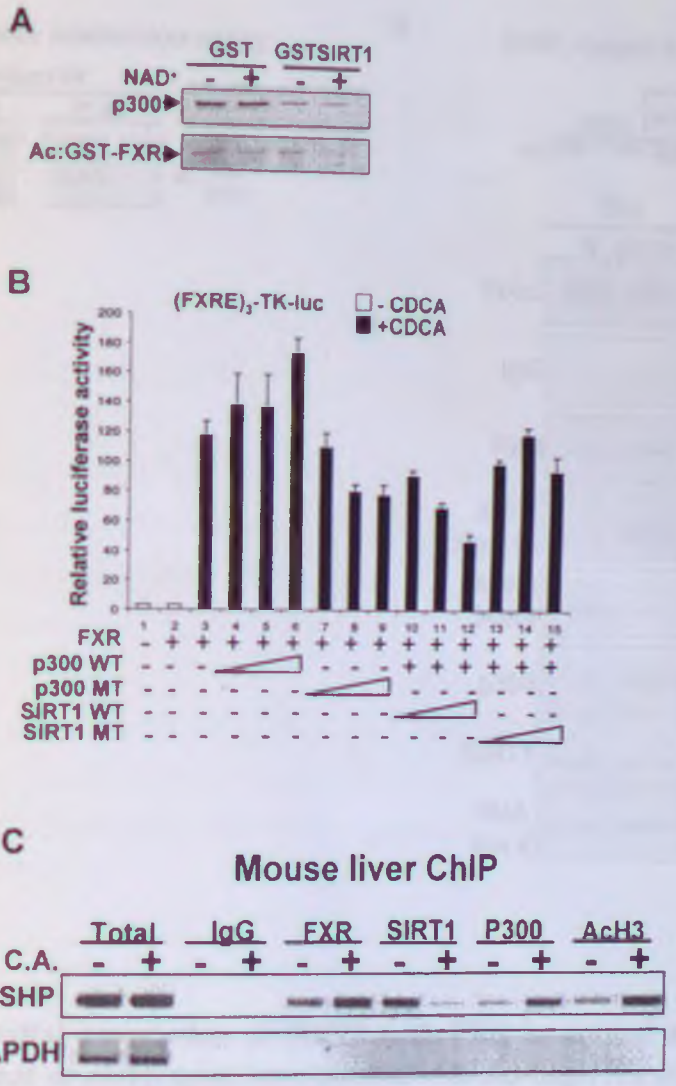

Fig. 5. SIRT1 antagonizes FXR transactivation. (A). Two mg of GST-FXR acetylated by p300 was incubated with 1 mg of GST or GST-SIRT1 in the presence or absence of 200 mM NAD^+ and analyzed by fluorography. (B). HEK293 cells were cotransfected with 200 ng of $(FXRE)_3$tk-luc, 5 ng of CMV-FXR, and increasing amounts (25, 50, 100 ng) of expression plasmids for wild type (WT) or catalytically inactive (MT) p300 or SIRT1. (C) Mice were fed normal or 0.5 % CA chow for 6 hr and ChIP assays were done using the indicated antisera.

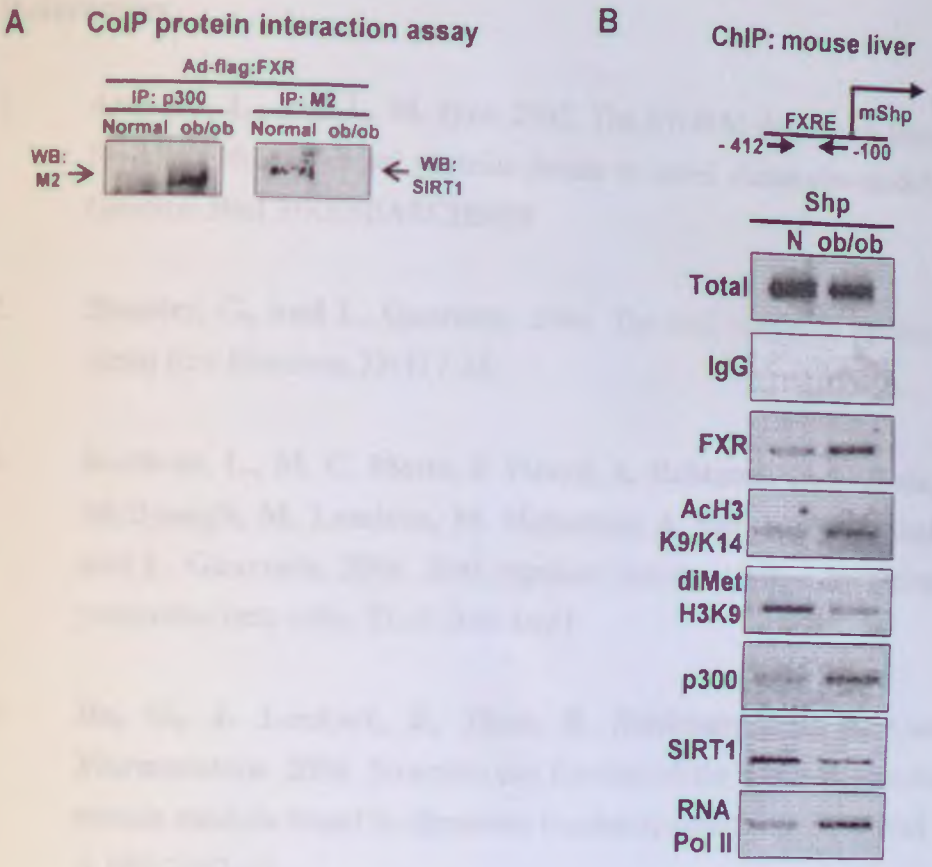

Fig. 6. Differential association of SIRT1 with FXR in normal and ob/ob mouse liver (A). Normal or ob/ob mice were infected with Ad-flag-FXR or Ad-empty and 5 days later, liver extracts were immunoprecipitated and the presence of flag-FXR in the anti-p300 immunoprecipitates and the presence of SIRT1 in the M2 immunoprecipitates were determined by western blotting. (B). ChIP assays were done in livers from normal and ob/ob mice fed normal chow using the indicated antibodies.

References

1. **Aravind, L., and L. M. Iyer.** 2002. The SWIRM domain: a conserved module found in chromosomal proteins points to novel chromatin-modifying activities. Genome Biol **3**:RESEARCH0039.

2. **Blander, G., and L. Guarente.** 2004. The Sir2 family of protein deacetylases. Annu Rev Biochem **73**:417-35.

3. **Bordone, L., M. C. Motta, F. Picard, A. Robinson, U. S. Jhala, J. Apfeld, T. McDonagh, M. Lemieux, M. McBurney, A. Szilvasi, E. J. Easlon, S. J. Lin, and L. Guarente.** 2006. Sirt1 regulates insulin secretion by repressing UCP2 in pancreatic beta cells. PLoS Biol **4**:e31.

4. **Da, G., J. Lenkart, K. Zhao, R. Shiekhattar, B. R. Cairns, and R. Marmorstein.** 2006. Structure and function of the SWIRM domain, a conserved protein module found in chromatin regulatory complexes. Proc Natl Acad Sci U S A **103**:2057-62.

5. **Guarente, L.** 2000. Sir2 links chromatin silencing, metabolism, and aging. Genes Dev **14**:1021-6.

6. **Imai, S., C. M. Armstrong, M. Kaeberlein, and L. Guarente.** 2000. Transcriptional silencing and longevity protein Sir2 is an NAD-dependent histone deacetylase. Nature **403**:795-800.

7. **Lerin, C., J. T. Rodgers, D. E. Kalume, S. H. Kim, A. Pandey, and P. Puigserver.** 2006. GCN5 acetyltransferase complex controls glucose metabolism through transcriptional repression of PGC-1alpha. Cell Metab **3**:429-38.

8. **Li, X., S. Zhang, G. Blander, J. G. Tse, M. Krieger, and L. Guarente.** 2007. SIRT1 deacetylates and positively regulates the nuclear receptor LXR. Mol Cell **28**:91-106.

9. **Metzger, E., M. Wissmann, N. Yin, J. M. Muller, R. Schneider, A. H. Peters, T. Gunther, R. Buettner, and R. Schule.** 2005. LSD1 demethylates repressive histone marks to promote androgen-receptor-dependent transcription. Nature **437**:436-9.

10. **Picard, F., M. Kurtev, N. Chung, A. Topark-Ngarm, T. Senawong, R. Machado De Oliveira, M. Leid, M. W. McBurney, and L. Guarente.** 2004. Sirt1 promotes fat mobilization in white adipocytes by repressing PPAR-gamma. Nature **429**:771-6.

11. **Rodgers, J. T., C. Lerin, W. Haas, S. P. Gygi, B. M. Spiegelman, and P. Puigserver.** 2005. Nutrient control of glucose homeostasis through a complex of PGC-1alpha and SIRT1. Nature **434**:113-8.

12. **Shi, Y., F. Lan, C. Matson, P. Mulligan, J. R. Whetstine, P. A. Cole, and R. A. Casero.** 2004. Histone demethylation mediated by the nuclear amine oxidase homolog LSD1. Cell **119**:941-53.

13. **Vaquero, A., M. B. Scher, D. H. Lee, A. Sutton, H. L. Cheng, F. W. Alt, L. Serrano, R. Sternglanz, and D. Reinberg.** 2006. SirT2 is a histone deacetylase with preference for histone H4 Lys 16 during mitosis. Genes Dev **20**:1256-61.

14. **Vaziri, H., S. K. Dessain, E. Ng Eaton, S. I. Imai, R. A. Frye, T. K. Pandita, L. Guarente, and R. A. Weinberg.** 2001. hSIR2(SIRT1) functions as an NAD-dependent p53 deacetylase. Cell **107**:149-59.

Chapter Five

Conclusion

The main purpose of this study is to address the functional roles of the orphan nuclear receptors, SHP and FXR, and their cofactors in bile acid signaling that regulates expression of genes involved in a number of metabolic pathways. My major findings to support the roles of SHP and FXR in bile acid signaling are as follows: 1) p300 and SIRT1 are critical *in vivo* FXR cofactors for modulation of FXR transactivation by acetylation or deacetylation of both histones and FXR. 2) In the absence of bile acid, unliganded FXR/RXR heterodimers recruit a corepressor complex including SIRT1 to the SHP promoter. SIRT1 is associated with FXR to inhibit FXR transactivation by deacetylation. Histones H3 are dimethylated at K9, a repressive marker, resulting in a low basal level of SHP expression. 3) In the presence of bile acids, SIRT1 is dissociated from FXR whereas p300 interaction with FXR increases resulting in a transient increase of acetylation levels of both FXR and histones which correlates with initiation of transcription of SHP gene. 4) In obese mice, FXR and histones are constitutively and highly acetylated and p300/FXR activity is elevated in the absence of bile acid. 5) Bile acid-induced SHP directly interacts with and recruits G9a and LSD-1 to the native CYP7A1 promoter and promotes to methylation of H3K9 and demthylation of H3K4, respectively, which correlates with suppression of transcription of the CYP7A1 gene. 6) Interestingly, SHP sequentially recruits its cofactors, including HDAC, Brm-based Swi/Snf chromatin remodeling complex and G9a. First, SHP recruits HDAC to deacetylate core histones, and then recruits G9a to methylates H3K9. Finally, SHP

recruits Brm-based Swi/Snf chromatin remodeling complex and changes the chromatin structure which is associated with gene repression (Fig.1). These findings delineate the molecular mechanisms of bile acid signaling which regulate cholesterol/bile acid homeostasis in the liver.

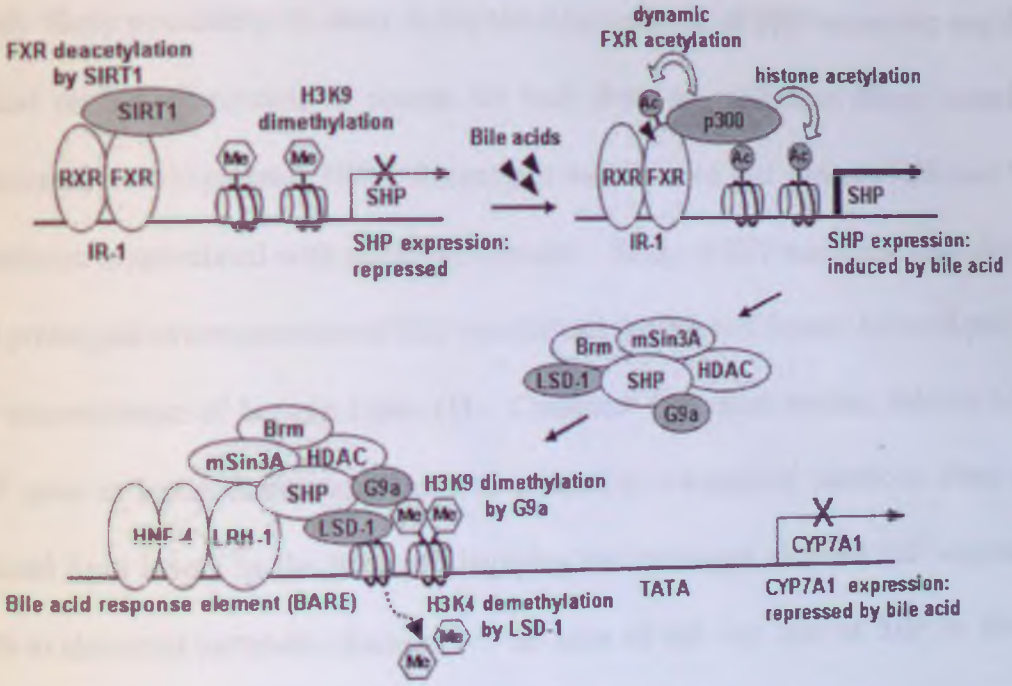

Figure 1. Roles of orphan nuclear receptors, SHP and FXR, and their cofactors in bile acid signaling

My preliminary data showed that SHP mRNA levels reached almost maximum levels (a little over 2-fold) as early as 3 hr after bile acid treatment and were not further increased at longer times, implying the existence of an autoregulation for SHP expression which prevents prolonged increases in expression in normal metabolic physiology. The mechanism of autoregulation for SHP expression still remains unknown, but several previous studies implied that SHP itself may regulate its own expression via a negative regulatory loop. It has been shown that SHP strongly interacts with LRH-1 in both mammalian two-hybrid assay and *in vitro* pulldown assay and efficiently suppresses the

transactivation of LRH-1 (2). Notably, a LRH-1-responsive element was also identified at the SHP promoter (6), thus, SHP is likely to bind to LRH1 at its promoter and negatively regulate its own gene expression.

Why the expression of SHP is autoreagulated has not been determined. One highly likely possibility of many is that the autoregulation of SHP expression may be a critical regulatory process to protect the body from the malignant effects caused by abnormally overexpressed SHP. Recently, it was reported that abnormal elevated SHP expression is associated with metabolic diseases. Study of SHP-transgenic mice showed that prolonged overexpression of SHP resulted in a depletion of hepatic bile acid pool and the accumulation of hepatic lipids (1). Consistent with these studies, deletion of the SHP gene in leptin-deficient obese mice resulted in a beneficial metabolic effect with reduced lipid levels in the liver (4), implying that prolonged elevated SHP expression leads to abnormal metabolic diseases. In spite of the key role of SHP in diverse hepatic metabolic regulations, the mechanisms of regulation of SHP expression remain largely unknown.

Recent study showed that the SHP expression is abnormally elevated in obese mice compared to normal mice (4). My recent work revealed that SHP expression is abnormally elevated in obese mice, at least in part, as a result of dysregulated p300/FXR activity. P300 was constitutively associated with the SHP promoter and with high acetylation of histones as well as FXR, which correlates with abnormal elevated SHP expression in obese mice. In contrast, SIRT1 interaction with FXR was marked decreased in obese mice compared to normal mice. SIRT1 was able to deacetylate FXR *in vitro*, thus, dissociation of SIRT1 from FXR in obese mice may result in constitutive

FXR acetylation, which abnormally enhances SHP gene expression in obese mice. These results provide a correlation between dysregulated functions of transcriptional factors to modulate FXR activity and abnormal elevated SHP expression in metabolic disorders.

In my preliminary data, SIRT1 was shown to deacetylate FXR in vitro and decrease p300-mediated FXR transactivation, thus, increasing SIRT1 activity would be a novel therapeutic method to restore the dysregulated FXR acetylation in hepatic metabolic diseases. Previous study reported that treatment with resveratrol, a polyphenol found in red wine, stimulated SIRT1 activity, resulting in increasing DNA stability and expanding lifespan in yeast (3). Recently, it was found that resveratrol also impacts mitochondrial function and metabolic homeostasis. Treatment of mice with resveratrol increased consumption of oxygen in muscle fiber and protected mice against diet-induced obesity and insulin resistance by stimulating the activity of SIRT1 (5). Interestingly, I found that resveratrol treatment decreased the levels of FXR acetylation in obese mice (data not shown). This finding suggested that resveratrol is likely to modulate FXR activity by stimulating SIRT1 activity to deacetylate FXR, which may result in decreasing FXR activity to reduce SHP gene expression in obese mice.

SHP and FXR function as pleiotropic regulators of diverse biological functions by regulating numerous genes in multiple pathways. Their transcriptional activities, regulated by interactions with cofactors, are tightly controlled to maintain metabolic homeostasis in normal physiology. If their functional activities are dysresgulated, it may cause metabolic diseases. My recent findings showed that the functional balance between p300 and SIRT1 is critical to modulate FXR activity and maintain adequate

levels of SHP expression in the body. Thus, restoring the functional balance between p300 and SIRT1 to modulate FXR activity normally may be an attractive strategy to reduce abnormal elevated SHP expression which is associated with some hepatic metabolic disorders. However, the mechanisms underlying functional balance between transcriptional factors, including p300 and SIRT1, are largely unknown. Therefore, my studies to define the function and mechanism of the p300 and SIRT1 in the regulation of FXR activity and SHP expression may facilitate the design of novel therapeutic methods for treating metabolic diseases, such as, fatty liver, hypercholesterolemia, diabetes, and obesity.

References

1. **Boulias, K., N. Katrakili, K. Bamberg, P. Underhill, A. Greenfield, and I. Talianidis.** 2005. Regulation of hepatic metabolic pathways by the orphan nuclear receptor SHP. Embo J **24**:2624-33.

2. **Goodwin, B., S. A. Jones, R. R. Price, M. A. Watson, D. D. McKee, L. B. Moore, C. Galardi, J. G. Wilson, M. C. Lewis, M. E. Roth, P. R. Maloney, T. M. Willson, and S. A. Kliewer.** 2000. A regulatory cascade of the nuclear receptors FXR, SHP-1, and LRH-1 represses bile acid biosynthesis. Mol Cell **6**:517-26.

3. **Howitz, K. T., K. J. Bitterman, H. Y. Cohen, D. W. Lamming, S. Lavu, J. G. Wood, R. E. Zipkin, P. Chung, A. Kisielewski, L. L. Zhang, B. Scherer, and D. A. Sinclair.** 2003. Small molecule activators of sirtuins extend Saccharomyces cerevisiae lifespan. Nature **425**:191-6.

4. **Huang, J., J. Iqbal, P. K. Saha, J. Liu, L. Chan, M. M. Hussain, D. D. Moore, and L. Wang.** 2007. Molecular characterization of the role of orphan receptor small heterodimer partner in development of fatty liver. Hepatology **46**:147-57.

5. **Lagouge, M., C. Argmann, Z. Gerhart-Hines, H. Meziane, C. Lerin, F. Daussin, N. Messadeq, J. Milne, P. Lambert, P. Elliott, B. Geny, M. Laakso, P. Puigserver, and J. Auwerx.** 2006. Resveratrol improves mitochondrial function and protects against metabolic disease by activating SIRT1 and PGC-1alpha. Cell **127**:1109-22.

6. **Lee, Y. K., K. L. Parker, H. S. Choi, and D. D. Moore.** 1999. Activation of the promoter of the orphan receptor SHP by orphan receptors that bind DNA as monomers. J Biol Chem **274**:20869-73.

Curriculum Vitae

Sungsoon Fang

EDUCATION

University of Illinois at Urbana-Champaign

Ph.D. Dept. of Molecular and Integrative Physiology, May 2008

Dissertation Advisor: Dr. Kim Jongsook Kemper

Dissertation title: "The roles of orphan nuclear receptors, SHP and FXR, and their cofactors in bile acid signaling"

Seoul National University, Seoul, Korea

B.S., Dept. of Molecular Biology, Feb 1999

WORK & RESEARCH EXPERIENCE

University of Illinois at Urbana-Champaign, Illinois

Dept. of Molecular and Integrative Physiology

Research Assistant Jan 2006-May 2008

• Investigating role of p300/SIRT1 in the regulation of FXR transcriptional activity in bile acid signaling

Teaching Assistant Jan 2006-Dec 2006

• MCB103, Introduction of Human Physiology

• MCB151, Molecular & Cellular Basis of Life Laboratory

Research Assistant Jan 2004-Dec 2005

• Role of histone methyltransferase, G9a in bile acid homeostasis via SHP-dependent pathway

Fellow of the School of Molecular and Cellular Biology Aug 2003-Dec 2003

SK Pharma Co. Ltd. May 2002-Aug 2002

• Internship as a Research Assistant

Defense Security Command, Republic of Korea May 1999-Jul 2001

Secretary of Commanding General

• Sergeant, Military Service

PUBLICATIONS

• **Fang, S.**, Tsang, S., Jones, R., Yoon, H., Wu, S., Chiang, M., and Kemper, J.K. (2008) The p300 histone acetyltransferase is a critical in vivo regulator in bile acid signaling. ***In manuscript.***

• Ponugoti, B., **Fang, S.**, and Kemper, J.K. (2007)
Functional Interaction of HNF-4 and PGC-1α in CYP7A1 Regulation Is Inhibited by a Key Lipogenic Activator, SREBP-1c. ***Mol Endocrinol.*** Nov;21(11):2698-712.

• **Fang, S.**, Miao, J., Xiang, L., Ponugoti, B., Treuter, E., and Kemper, J.K. (2007)
Coordinated recruitment of histone methyltransferase G9a and other chromatin-modifying enzymes in SHP-mediated regulation of hepatic bile acid metabolism. ***Mol. Cell. Biol.*** Feb;27(4):1407-24.

• Miao, J., **Fang, S.**, Bae, Y., and Kemper, J.K. (2006)
Functional inhibitory cross-talk between CAR and HNF-4 in hepatic lipid/glucose metabolism is mediated by competition for the binding to DR1 motif and to the common coactivators, GRIP-1 and PGC-1α. ***J. Biol Chem.***, 281(21): 14537-46

• Bhalla, S., Ozalp, C., **Fang, S.**, Xiang, L., and Kemper, J.K. (2004)
Ligand-activated PXR interferes with HNF-4 signaling by targeting a common coactivator PGC-1a: Functional implication in hepatic cholesterol and glucose metabolism. ***J. Biol. Chem.***, 279, 45139-47